BRAIN MICRO- AND MACRO-STRUCTURAL CHARACTERISTICS INVESTIGATION IN FIBROMYALGIA USING MULTI-MODAL MAGNETIC RESONANCE IMAGING

Estephan Jose Moana-Filho

A dissertation submitted to the faculty at the University of North Carolina at Chapel Hill in partial fulfillment of the requirements for the degree of Doctor of Philosophy in the Curriculum in Oral Biology (Concentration in Pain Neurobiology) in the School of Dentistry.

Chapel Hill
2014

Approved by:

Richard H. Gracely

Gregory K. Essick

William Maixner

J. Douglas Mann

Mark Tommerdahl

ABSTRACT

Estephan Jose Moana-Filho: Brain Micro- and Macro-Structural Characteristics Investigation in Fibromyalgia Using Multi-Modal Magnetic Resonance Imaging
(Under the direction of Richard H. Gracely)

Fibromyalgia (FM) is a chronic widespread pain condition that deeply impacts the lives of patients. Multiple symptoms such as fatigue, impaired cognition, and sleep disturbances among others are commonly described. Despite intensive research effort, no disease-specific mechanism uniquely explains the clinical presentation of FM. Nonetheless, current evidence points to a major role of the central nervous system for the main feature of this condition: pain and sensory augmentation. Neuroimaging techniques provide a window into the brain mechanisms that may play a role in FM. Several studies using functional magnetic resonance imaging (MRI) show abnormalities in pain processing in the brain of FM patients. Likewise, structural abnormalities are found using anatomical MRI however the findings are less consistent. The main goal of this dissertation was to comprehensively assess brain structural features of FM patients and matched controls at both micro- (cellular-level structures such as membranes, myelin as well as axonal density) and macro-structural (gross anatomical) levels as measured by diffusion-weighted and high-resolution anatomical MRI respectively.

The results from diffusion MRI show evidence of widespread micro-structural white matter (WM) abnormalities in the brains of FM patients compared to controls, and also within relevant pain-related brain regions. These findings give support to the view

that alterations in the brain of patients potentially contribute to the symptoms experienced by them. Conversely, macro-structural brain features showed little difference between patients and controls regarding gray matter (GM) characteristics. Between-group differences were only found for increased volume in the amygdalae and WM adjacent to the anterior cingulate cortex and left insula for FM patients relative to controls.

Taken together these findings may indicate that structural abnormalities in the brain of FM patients are more widespread in the micro-structural level, while regional differences limited to subcortical structures and WM adjacent to pain-related cortical areas are more typical at the macro-structural level with no measurable impact to GM morphological characteristics.

To my mother, who dedicated her life to her family and provided me the environment and conditions so I could be my best. I will never forget all your love, dedication, affection, and support for me to experience all the good things in life. May God bless you and keep you close to Him.

To my father, I appreciate and recognize all your effort to provide me the best resources to grow as a person and as a professional. Your support for my decisions about my professional life was fundamental for me to achieve my goals.

To my sisters, who helped me organize my endeavors in Brazil while I was living abroad. All the visits to see you in our home country were always filled with fun and joy!

To my nephew Pedro and niece Maria Isadora, I am sorry to have missed your growth during my studying abroad. I hope we made the best of our time together during my visits to Brazil, and we will plan for you to visit me more frequently wherever I may be in the future.

To my former advisor Don Nixdorf, who has been a career mentor and a friend ever since we started working together, even after I moved to the next step of my career. I appreciate all your support and guidance during all this time, and look forward to continue working with you.

To all my friends who supported me in one way or another. A special thanks to **Sandro**, my childhood friend who always kept in touch and never let the friendship die even with all the physical distance between us. I am looking forward for more fun in the years ahead!

To my wife Karla. No other person – none! – knows better than you all the sacrifice, countless hours of study and work, and time away from family and friends that was needed for me to achieve this goal.
This Doctorate of Philosophy is as much mine as it is yours, and I cannot think of anybody else who could be a better spouse and partner than you. This is my public recognition of the love, support, dedication, and self-sacrifice you offered me during all these years. I will continue doing all within my reach to provide you the same in return.

“Life is not for amateurs!”

ACKNOWLEDGEMENTS

This dissertation resulted not only from my personal effort, but also from many other people who helped me throughout this research project:

My mentor and advisor Richard Gracely, who gave all his support to develop this neuroimaging effort beyond the original research project. I appreciate your guidance and the freedom you provided me so I could learn my own way through research;

To Inna Tchivileva, our study coordinator who put much effort in taking this project off the ground and helped expedite data collection so I could graduate in time. I appreciate our discussions on academic and life matters;

To Mike Young and Ollie Monbureau, your help on technical aspects of our project was fundamental to have it started and going on smoothly;

To Cindy Blake, who take good care of her Oral Biology students;

To Patrick Flood, who always had his students' best interest and was always available to us;

To all Oral Biology faculty, in guiding us students during our learning years;

To all past and present fellow Oral Biology PhD students, your support and companionship during these years was much needed and welcomed;

To the Biomedical Research Imaging Center staff, who were always helpful in accommodating this project needs and were fun to work with (much of what I know about North Carolina leisure destinations I learned form you!).

TABLE OF CONTENTS

LIST OF TABLES

LIST OF FIGURES

LIST OF ABBREVIATIONS

ACR	American College of Rheumatology
AD	Axial diffusivity
CNS	Central nervous system
CSF	Cerebral spinal fluid
DTI	Diffusion tensor imaging
DWI	Diffusion weighted imaging
FA	Fractional anisotropy
FM	Fibromyalgia
fMRI	Functional magnetic resonance imaging
FSS	Functional somatic syndrome
GM	Gray matter
MD	Mean diffusivity
MNI	Montreal Neurological Institute
MO	Mode of anisotropy
MRI	Magnetic resonance imaging
NRS	Numerical rating scale
RD	Radial diffusivity
SS	Symptom severity scale
VBM	Voxel-based morphometry
WM	White matter

CHAPTER 1: INTRODUCTION, METHODS OVERVIEW AND SUBJECT SAMPLE DESCRIPTION

Introduction

When one ponders on the meaning of the word “pain”, some possibilities arise. It could refer to the conscious experience related to bodily injury or disease processes, which is probably one of the most common interpretations. Another possible meaning would be the discomfort associated with unpleasant feelings, such as the separation from a spouse or the mourning of a loved one. This dichotomous view on pain is present for millennia, dating from the times of the ancient Greek philosophers such as Aristotle (Perl, 2007; Cervero, 2009). In the last centuries, competing pain theories developed describing distinct features: i. Following a noxious stimulus in peripheral tissues (e.g., skin), dedicated pain receptors in the periphery detect and transmit the noxious input through pain specific pathways to the brain (specificity theory); ii. Peripheral stimulus intensity as transduced by unspecialized afferent fibers would dictate a non-painful (innocuous stimulus) or painful (intense stimulus) perception according to the level of neuronal discharge (intensity theory); or iii. Peripheral receptors, irrespective of sensory input modality, following an intense stimulation would trigger a sequence of impulses in peripheral and central neurons in particular spatial and temporal patterns such as to convey a pain percept (pattern theory) (Perl, 2007). In the last 50 years, several lines of evidence showed that neither theory alone could explain all pain-related mechanisms and that likely both specificity and pattern concepts must

be considered to some extent in different scenarios of clinical and experimental pain (Prescott et al., 2014).

The complexity of the pain phenomenon is well recognized currently, where the view of it as a dedicated “alarm system” that serves solely a protective function for survival and well being is not sufficient. Pain is now considered a multi-dimensional experience, that includes sensory-discriminative, affective-motivational and cognitive-evaluative components (Treede et al., 1999). This multidimensionality is embedded within the definition of pain provided by the International Association of Pain (IASP) (Merskey and Bogduk, 1994):

> *“An unpleasant sensory and emotional experience associated with actual or potential tissue damage, or described in terms of such damage.”*

This definition includes distinct aspects related to pain: it is a subjective (i.e., personal and individualized) experience that encompasses both sensory and emotional components, and tissue damage does not necessarily have to take place. Given this inherent intricacy, it is not a surprise that several types of pain exist such as nociceptive, inflammatory or neuropathic (Cervero and Laird, 1991; Cervero, 2009). The first two types of pain are considered physiological and serve to protect an individual from harm. Neuropathic pain however, where even innocuous peripheral stimuli can evoke pain, can be considered a neurological disease secondary to damage or dysfunction of the peripheral and/or central nervous systems.

Another important distinction related to the pain experience is between acute and chronic. The former usually has a known causal factor and is expected to reduce over time as the healing process ensues; the later is present beyond the expected tissue healing time (e.g., over 3 months), appears to have no useful purpose to an individual

and can be seen as a pathological process (Davis, 2013), with ample evidence of associated functional, structural and neurochemical brain changes (Tracey and Bushnell, 2009). The processes related to the transition from acute to chronic pain are not completely understood (Mifflin and Kerr, 2014), nonetheless predictors of this transition are under investigation (Apkarian et al., 2013).

The aforementioned complexity of pain is well represented in puzzling clinical conditions considered together under the term “functional somatic syndrome”. It refers to related syndromes where symptoms, suffering and disability better characterize the clinical presentation than disease-specific structural or functional abnormalities (Barsky and Borus, 1999). Functional somatic syndromes (FSS) usually are not present in isolation but rather with one or more comorbid pain conditions (Wessely et al., 1999; Aaron and Buchwald, 2001), and previous diagnosis of a FSS is a strong risk factor for other FSSs (Warren et al., 2013). These associations of comorbid pain conditions likely represent underlying common pathophysiological mechanisms (Yunus, 2007), and studies based on mechanism-driven hypotheses might help understand each condition’s peculiarity beyond those shared general mechanisms (Croft et al., 2007).

Most reports describing FSSs, if not all, include fibromyalgia. Fibromyalgia (FM) can be considered a prototypical FSS (Ablin et al., 2012), that is mainly characterized by chronic widespread body pain and associated symptoms that includes fatigue, sleep disturbances and cognitive dysfunction with no measurable organic cause sufficient to explain those symptoms (Clauw, 2009). Concerted research efforts to elucidate the pathophysiology of FM took place in the past decades, and several concepts proposed for this condition have been reformulated or abandoned based on the recent evidence

gathered. What follows is a brief description of the history and current accepted knowledge of FM.

Fibromyalgia: an overview

Early studies of fibromyalgia

Initial reports of a condition with similar clinical presentation as FM can be traced back to the beginning of the 20th century. Sir William Gowers provided a comprehensive description of what was known then about this condition and proposed naming it "fibrositis", as it was believed to be some form of "inflammation of the fibrous tissue of the muscles" (Gowers, 1904). Almost fifty years later, Graham described the controversy surrounding "fibrositis" within the rheumatology specialty and how it became a "depot for many varieties of non-articular rheumatism" (Graham, 1953). Of note, he mentions the lack of evidence for an inflammatory etiology for this condition and therefore questioning the propriety of that term ("-itis" = inflammation).

Moldofsky and colleagues provided interesting insights in systematically investigating sleep disturbances using electroencephalography (EEG) in FM patients and in healthy controls following sleep deprivation (Moldofsky et al., 1975). They reported a disruption in the EEG sleep pattern in FM patients named "alpha-delta" sleep, and that a 3-night sleep deprivation during the non rapid eye movement (REM) stages elicited musculoskeletal and mood symptoms in healthy controls similar to those seen in FM patients. Following recovering nights with undisrupted sleep, healthy controls experienced remission of those symptoms (Moldofsky et al., 1975). In a later study it was shown that while disruption during non-REM sleep could evoke FM-like symptoms in healthy controls, REM sleep disruptions could not (Moldofsky and Scarisbrick, 1976).

Following these observations, Smythe and Moldofsky proposed criteria for the diagnosis of “fibrositis”, that could differentiate FM patients from patients suffering from other diffuse pain syndromes, malingering or neuroticism (Smythe and Moldofsky, 1977). Many consider this seminal work the birth of the modern concept of FM (Clauw, 2009; Wolfe and Hauser, 2011). A comprehensive clinical description of 50 FM patients and 50 age-, sex- and race-matched healthy controls was offered by Yunus and collaborators, where they also proposed using “fibromyalgia” as opposed to “fibrositis” given the lack of evidence for inflammation as a etiological factor for the so-called primary FM (i.e., “when no known cause or associated contributory disorder is present”) (Yunus et al., 1981). Additional early studies have shown no specific personality profile for FM patients, and that pharmacological (antidepressants, non-steroidal anti-inflammatory drugs, chlorpromazine) and non-pharmacological (strenuous physical exercise) treatment modalities provided significant improvements in FM symptoms (McCain and Scudds, 1988).

Fibromyalgia classification and diagnostic criteria

A major advancement for FM research took place in 1990, when the American College of Rheumatology (ACR) criteria for the classification of fibromyalgia was published (Wolfe et al., 1990). It required a history of at least 3 months of widespread body pain and pain on digital palpation in 11 or more out of 18 tender point sites for an individual to be classified as having FM. These criteria allowed standardization of inclusion requirements for FM subjects in research studies, which provides more homogenous subject samples thus improving the comparability of findings across studies; however, they were not considered suitable for use in clinical practice as they

might exclude patients that present several but not all signs and symptoms to meet the ACR 1990 FM classification criteria (Clauw, 2009).

Partly to overcome this limitation and to address objections from different parties to the ACR 1990 FM classification criteria, new diagnostic criteria for FM were offered in 2010 (Wolfe et al., 2010). The most significant change was removing the requirement for tender point examination and count. In addition, two metrics were developed: 1. Widespread pain index (WPI), where the investigator notes how many body areas (out of 19) the patient had pain in the last week; and 2. Symptom severity (SS) scale, that considers the severity of fatigue, waking unrefreshed and cognitive symptoms plus the extent of somatic symptoms in general (score range: 0-12). To satisfy the ACR 2010 FM diagnostic criteria a patient must meet three conditions: i. Either a WPI ≥ 7 and SS ≥ 5, or WPI 3-6 and SS ≥ 9; ii. Symptoms must be present at similar levels for at least 3 months; and iii. No presence of other disorder that could explain the pain (Wolfe et al., 2010). The authors stressed that these diagnostic criteria were not meant to replace the ACR 1990 criteria, but rather offer an alternative method of diagnosis.

With the goal of developing criteria that allowed self-administration thus eliminating the need for an interviewer, a modification of the ACR 2010 diagnostic criteria was proposed (Wolfe et al., 2011). To achieve that goal, the SS scale was modified in a way that, instead of having a somatic symptoms list to check, patients respond “yes” or “no” to the presence of headaches, pain / cramps in the lower abdomen of depression symptoms in the last 6 months. Its score range was unchanged (0-12) though, as well the WPI was also virtually unchanged – except that now it is self-administered. A new scale named FM symptom scale (FS) was proposed, which is

simply the sum of the WPI and the modified SS with a score range of 0-31; a score of ≥ 13 was shown to have good sensitivity and specificity for identifying FM (Wolfe et al., 2011). Given the self-administering feature of this modified criteria, the authors provided a cautionary note that this instrument does not serve as a self-diagnosis tool or substitutes a physician's diagnosis.

These recent criteria were received with mixed opinions, and several researchers argued about the added value they brought beyond that offered by the accepted ACR 1990 FM classification criteria (Wolfe and Hauser, 2011; Abbi and Natelson, 2013; Hannonen, 2013). Nonetheless, these criteria are recognized as valuable instruments in designing studies that will help elucidate etiological factors, identify more homogenous subgroups of patients and develop targeted treatments (McBeth and Mulvey, 2012).

A supplementary issue to the classification of FM is the recognition (or the lack thereof) of it as a valid clinical entity (Ablin et al., 2012). On one side are those who defend that FM is no more than a collection of symptoms, i.e., "aches and pain that all people often have" at some point in life (Ehrlich, 2003). On the opposite side are investigators who, although acknowledging the limitations in the available FM criteria and that those affected by this condition may be at "end of the bell-shaped curve", understand that FM arises from altered pain processing mechanisms as shown by several studies (Harris and Clauw, 2006). In an article named "Fibromyalgia wars", Wolfe explores the myriad of interests of different agents pro and against having FM as a legitimate diagnosis: patients, some specialty physicians vs. the majority of physicians, pharmaceutical companies, professional organizations, patients' support groups, governmental agencies, and attorneys (Wolfe, 2009). When reading the available

literature on this topic, it becomes clear that FM is a controversial subject in the scientific and medical field, and that it impacts not only the affected patients but also the society at large.

Etiology, pathophysiology and treatment of fibromyalgia

Several studies have investigated the pathophysiology of FM, trying to determine etiological (i.e., causative) factors and pathophysiological (i.e., functional changes associated with a condition) mechanisms of this syndrome. Different investigational approaches brought some light on putative etiological factors in FM, even though some early studies tended to have relatively small samples that make interpretation of its results difficult.

Genetic factors seem to play an important role in FM, given the familial aggregation found where having a relative with FM increased the odds of other relatives presenting it (Buskila and Neumann, 2005), with one study showing odds ratio of 8.5 when compared to families with one member affected by rheumatoid arthritis (Ablin et al., 2006). Family members of FM patients are more sensitive to pain than controls, and they also have higher rates of comorbid conditions including irritable bowel syndrome (IBS), temporomandibular disorders (TMD), headaches or other regional pain syndromes (Clauw, 2009). Genetic polymorphisms were found in higher frequencies in FM patients for genes encoding the serotonin transporter (5-HTT), the serotonin 5-HT2A receptor, cathecol-O-methyl transferase (COMT), the dopamine D4 receptor and the substance P receptor NK1 (Ablin et al., 2006). Recently a systematic review and meta-analysis of candidate genes in FM showed that polymorphism in the serotonin 2A receptor had significant association with FM susceptibility (overall odds ratio = 1.33),

while no associations were found for 5-HTT and COMT (Lee et al., 2012). Given the evidence for genetic factors in FM, some environmental triggers associated with FM have been described. Among those are physical trauma, some infections (mostly viral), and emotional stress (Clauw, 2009).

Impairment of the stress responses and dysfunction of the hypothalamic-pituitary-adrenal (HPA) axis are linked to FM, however the abnormalities found varies across studies (Clauw, 2009). Disturbances in the autonomic nervous system are described in FM including postural orthostatic tachycardia (Staud, 2008), hyperactivity at rest / hyporeactivity during stress (Martinez-Lavin, 2007), and abnormalities in heart rate variability (Staud, 2008; Lerma et al., 2011). Proinflammatory cytokines were found to be mildly increased in FM patients compared to controls, however the methodological quality of those studies was considered low thus preventing a better understanding on the role of cytokines in FM pathophysiology (Uceyler et al., 2011).

Mood disorders like anxiety and depression are commonly reported in FM patients, but this could be attributed at least partly to sampling bias by selecting patients from tertiary care centers (Clauw, 2009). Sleep disturbances are part of the core symptoms of FM, and several recent studies provide additional support for the role of sleep based on questionnaires (Osorio et al., 2006; Munguia-Izquierdo and Legaz-Arrese, 2011) and polysomnography (Shah et al., 2006) data. However, sleep measures determined by 24-hour actigraph use and sleep diary for 14 days failed to predict clinical pain levels (Anderson et al., 2012).

Both peripheral and central sensitization have been implicated in the pathophysiology of FM pain, as reviewed by Staud and Rodriguez (Staud and

Rodriguez, 2006). An interesting finding was abnormalities related to the temporal summation of pain or “wind-up”, which is the increased pain sensation that arises when identically intense stimuli are presented repeatedly; it has been shown to result from central mechanisms that involve the N-methyl-D-aspartate (NMDA) receptor system. FM patients exhibit wind-up following experimental stimuli (mechanical, thermal, electrical) at lower frequencies and lower stimulus intensities than controls, and after sensations are more intense, longer-lasting and are more painful in patients (Staud, 2006).

In fact, augmented sensory and pain processing in FM is well supported by evidence. Using sophisticated psychophysical methodology in which stimuli presentation was done in a random fashion, Petzke and colleagues demonstrated that FM patients are more sensitive to pressure and heat than healthy controls (Petzke et al., 2003) however the increased pain sensitivity is dissociated from pain unpleasantness ratings (Petzke et al., 2005). Sensitivity to other stimulus modalities such as cold and electrical are not different between FM patients and controls, however patients do exhibit lower thresholds to noxious auditory tones (Clauw, 2009). One potential explanation for the augmented pain processing in FM is a deficiency in endogenous analgesics system such as the diffuse noxious inhibitory controls (DNIC) (McBeth and Mulvey, 2012), and this might be related to impaired serotonergic and noradrenergic activity but not opioidergic activity - since the latter was found to be normal or even increased in FM (Clauw, 2009).

Recently other factors have been investigated for their role in FM. Obesity is frequently observed in FM patients (Ursini et al., 2011), and it was found to reduce their

quality of life (Timmerman et al., 2013). Peripheral factors as part of FM etiology have been investigated before but the evidence provided was considered weak (Abeles et al., 2007), however small nerve pathology got some attention in 2013 when two studies reporting this were published a few months apart. In the first study published by a German group (Uceyler et al., 2013), they used three methods (quantitative sensory testing, pain-related evoked potentials, and skin punch biopsies) that converged in supporting impaired small nerve fiber function in FM patients. The second study used standard tests for clinical diagnostic criteria of small-fiber polyneuropathy (distal-leg skin biopsy and autonomic function testing) in FM patients and matched controls (Oaklander et al., 2013), and showed that over 50% of FM patients exhibited evidence of small-fiber polyneuropathy compared to 17.2% of controls. The fact that two different groups found reproducible findings is promising, even though they are not in agreement of the specific pathology affecting small nerve fibers (Uceyler and Sommer, 2013).

Neuroimaging studies have provided much new information about FM pathophysiology, and they will be addressed separately in a later section of this chapter.

Treatment options for FM are numerous, since the above discussed mechanisms may play a role for the expression of FM symptoms in each patient in different degrees thus an individualized treatment plan is of utmost importance (Staud, 2007). Non-pharmacological options include physical therapy modalities (thermal, electrical stimulation, massage, laser, acupuncture), cognitive behavioral therapy, complementary and alternative therapies (body-mind techniques, dietary supplementation, physical manipulation), and physical exercise (Casale et al., 2008). The latter has a good level of evidence in reducing FM symptoms like pain and fatigue and improving the quality of life

(Busch et al., 2011). The pharmacotherapy for FM reported in the literature is broad, including several categories such as analgesics, muscle relaxants, antidepressants, anticonvulsants, sedative-hypnotic drugs, among others; the evidence for benefit is equally diverse ranging from no efficiency to those showing strong evidence of benefit (Clauw, 2009). Three drugs are currently approved by the U.S Food and Drug Administration (FDA) for treatment of FM: pregabalin (an alpha2-delta calcium channel ligand), duloxetine and minalcipran (both are serotonin-norepinephrine reuptake inhibitors) (Hsu, 2011). Despite the numerous options for treatment, prognosis of FM is in general somber with limited improvements over periods of up to 10 years (McBeth and Mulvey, 2012). A study that followed 1,555 FM patients semi-annually with questionnaires for up to 11 years showed no clinically meaningful symptomatic improvement, however 25% had at least moderate improvement of pain over time (Walitt et al., 2011). It has been suggested that the prognosis might depend on where a particular FM patient falls within the disease severity spectrum (Clauw, 2009), and this must be taken into account when developing a treatment plan for each individual.

Epidemiology and health care cost of fibromyalgia

Several investigators have assessed epidemiology of FM in the past decades. Wolfe and collaborators reported a prevalence of 2% in the general population, with 3.4% and 0.5% figures for women and men respectively (Wolfe et al., 1995). McBeth and Mulvey in their review report an estimate of patients with symptoms fitting FM criteria ranging between 2-22% for clinical populations, while prevalence estimates in the general population fall within 1-11% (McBeth and Mulvey, 2012). A recent review of the worldwide epidemiology of FM described several studies in different settings and

countries spanning four continents (Africa, the Americas, Asia and Europe) (Queiroz, 2013). The estimated global mean prevalence of FM was 2.7% (range = 0.4 – 9.3%), with a mean prevalence for women of 4.2% and for men 1.4% (female:male ratio = 3:1). Incidence of FM was estimated in two studies only, with one reporting an incidence of 5.83 new cases per 1,000 persons-years for females only while the other described numbers of new FM cases per 1,000 person-years as 11.28 for females and 6.88 for males (Queiroz, 2013).

Health care costs associated with FM are higher when compared to non-FM patients. Using a U.S. health insurance database to determine characteristics and health care costs within a 12-month period, FM patients had three-fold higher mean cost and four times more doctor office visits when compared to non-FM patients (Berger et al., 2007). More recently, a retrospective study from the Quebec provincial health plans reported that the annual number of visits for FM patients was 25.1 with an associate cost of $ 4,065, while non-FM patients had a mean of 14.8 visits and costs of $ 2,766 (Lachaine et al., 2010).

Brain characteristics in fibromyalgia assessed by neuroimaging techniques

Pain research in humans has benefited from recent advancements in neuroimaging, since it allows probing brain functional and structural characteristics *in vivo* with minimal to no invasiveness. Numerous neuroimaging technologies have been used for the study of pain including magnetic resonance imaging (MRI), positron-emission tomography, magnetoencephalography, and EEG among others (Davis, 2011). These techniques are being used to unravel novel information on the brain plasticity secondary to chronic pain states (Lee and Tracey, 2013), and may also help parse out

complex genetic relationships through the concept of endophenotypes, i.e., a measurable component (such as neuroimaging measurements) of a clinical condition that has a more direct link to the underlying genetics than the condition itself (Tracey, 2011).

Diverse neuroimaging techniques have been used to investigate brain characteristics of FM patients, as the numerous reviews on the subject describe (Williams and Gracely, 2006; Cook et al., 2007; Nebel and Gracely, 2009; Gracely and Ambrose, 2011; Staud, 2011; Jorge and Amaro, 2012). Here the focus will be on MRI-based modalities, as this dissertation uses only this technique.

MRI generates images of the body through the use of strong magnetic fields and radiofrequency pulses. The well studied properties of hydrogen nuclei (which are abundant in the human body in water molecules) when placed within a strong magnetic field allows investigators to manipulate several variables in order to generate brain images with different characteristics. In a very crude description, MRI modalities can generate brain images through exploring distinct magnetic properties of brain tissues, e.g.,: i. In high-resolution structural imaging, the gray and white matter and cerebral spinal fluid (CSF) can be distinguished according to their unique magnetic relaxation time (T_1); ii. Functional MRI (fMRI) can detect the levels of blood oxygenation across the brain to indirectly infer neuronal activity in real time with reasonable spatial resolution; and iii. Diffusion weighted imaging (DWI) can assess the micro-structure of brain tissues by measuring the diffusion of water molecules within it. Thus the broadest division of MRI modalities for the study of the brain is between functional and structural. Functional

MRI is sensitive to changes over time of neuronal activity, while structural MRI measures biophysical properties of local brain tissue (Smith et al., 2004).

Stimulus-evoked fMRI studies in FM are abundant. The first such study was developed by Gracely and collaborators in 2002, using blunt pressure to the thumb nail as stimulus (Gracely et al., 2002). They used a pressure level able to evoke pain in 16 FM patients, and used two pressure levels in 16 controls: higher pressure level in order to elicit comparable subjective pain ratings or a lower pressure level that matches that used for the FM patients. Brain activations were similar for both groups only when matched for subjective pain ratings (using much greater pressure for controls), while no common activations were found following matched pressure level stimuli in both groups. These results were replicated when painful heat was used as stimulus (Cook et al., 2004). Other notable findings using fMRI following noxious thumb pressure stimulation in FM patients were association of depression (Giesecke et al., 2005) and catastrophizing (Gracely et al., 2004) scores to brain activations that failed to be reproduced in subsequent studies (Jensen et al., 2010; Burgmer et al., 2011), and also reduced activation in rostral anterior cingulate cortex compared to controls (Jensen et al., 2009). Other types of stimuli and cognitive tasks have been also used in fMRI studies with FM patients, along with resting-state BOLD studies where the functional connectivity of the brain is investigated and magnetic resonance spectroscopy to measure neurochemical metabolites to infer brain properties related to pathology and pharmacological manipulation (Gracely and Ambrose, 2011).

Structural MRI studies in FM patients are fewer. Most used voxel-based morphometry (VBM) to assess gray matter density / volume (Kuchinad et al., 2007;

Schmidt-Wilcke et al., 2007; Luerding et al., 2008; Burgmer et al., 2009; Hsu et al., 2009; Robinson et al., 2011) or VBM with another MRI modality such as diffusion weighted imaging (Lutz et al., 2008) or imaging technique like positron emission tomography (Wood et al., 2009). Diffusion weighted imaging was used alone in an early study (Sundgren et al., 2007) and recently a cortical thickness analysis was done in conjunction with functional connectivity of stimulus-evoked BOLD measurements (Jensen et al., 2013) as well as a multi-modal MRI using both functional and structural imaging in FM patients (Ceko et al., 2013). These studies will be described in more details in the respective chapters on diffusion weighted (chapter 2) and high-resolution anatomical imaging (chapter 3).

Rationale for investigating brain structural characteristics of fibromyalgia

As described above, structural brain characteristics in FM patients have been explored mostly via VBM assessment of gray matter volume / density measurements. These measurements are capable of showing brain structural differences between chronic pain patients and controls, as shown in a recent meta-analysis (Smallwood et al., 2013). Neuroplasticity has long been associated with chronic pain, however it was unknown if brain structural changes were a cause or consequence of it (May, 2008). Longitudinal studies reporting pre- and post-treatment data of patients suffering from chronic pain secondary to osteoarthritis (Rodriguez-Raecke et al., 2009; Gwilym et al., 2010) and low back pain (Seminowicz et al., 2011) showed that most of the brain structural abnormalities detected were reversible. This finding is supported by a study that compared older non-clinical subjects divided into 3 groups: controls, ongoing pain and past pain (stopped > 12 months) (Ruscheweyh et al., 2011). The ongoing pain

group showed gray matter decreases compared to controls, while the past pain group did not. Other interesting recent findings in healthy controls were that lack of habituation to noxious stimuli is associated with gray matter reductions (Stankewitz et al., 2013) and a negative association between pain ratings and gray matter density (Emerson et al., 2014). These studies show that other variables besides patient status might explain gray matter morphometric differences, and those must be taken into account when interpreting results from clinical samples.

Diffusion MRI can probe tissue micro-structure in a non-invasive manner, providing unique brain information on the microscopic scale in both health and disease states (Le Bihan, 2003). Two early studies reported DWI data from FM patients (Sundgren et al., 2007; Lutz et al., 2008). These pioneering studies, while valuable, were limited by the available technology, i.e., use of 1.5 Tesla MR scanners, low number of encoding directions, manually drawn ROIs, and focus on only 2 diffusion metrics (apparent diffusion coefficient and fractional anisotropy). Current MR technology and software packages for neuroimaging analyses allow a more extensive approach to DWI, for both data acquisition (higher signal-to-noise ratio from higher magnetic fields, greater number of diffusion-encoding directions, cardiac-gate acquisition, brain probabilistic atlases for region of interest selection among others) and processing (several available software packages for DWI data analysis) (Hasan et al., 2011; Soares et al., 2013).

From the aforementioned, it seems possible that the brain structural characteristics in FM have been underexplored. In order to address this gap of knowledge, this dissertation project aimed at developing a comprehensive assessment

of brain micro- and macro-structural characteristics in FM patients using reference data from healthy, painfree control subjects.

Objectives

The objectives of this dissertation were:

- To recruit a relatively large sample of FM patients and age- and sex-matched controls and perform a detailed characterization based on demographic attributes, clinical measures and psychosocial instruments;
- To determine global and regional micro-structural brain tissue characteristics using diffusion weighted imaging for those subjects; and
- To do a comprehensive assessment of brain macro-structural features for both FM and control subjects using high-resolution anatomical imaging, which includes brain volume estimation, gray matter assessment, subcortical structures segmentation and volumetric analysis, and measurement of brain cortical and subcortical characteristics.

Methods overview

In this section, an overview of the methods used in this dissertation will be provided. All subjects recruited as described below participated in the studies reported in subsequent chapters, and their data (demographic characteristics, clinical measures, questionnaires scores) were used accordingly where appropriate for particular analyses as outlined in each chapter.

Subjects

Study participants consisted of 30 female FM patients and 30 age-matched healthy females. Participants were recruited by referrals from local rheumatologists and

through advertisements in the local community. A calibrated examiner assessed all subjects using the 1990 ACR classification criteria (Wolfe et al., 1990). Additionally, FM patients were also assessed using the ACR 2010 diagnostic criteria (Wolfe et al., 2010). Inclusion criteria for FM patients were: 1) female patients with age between 18 and 64 years; and 2) fulfillment of the ACR 1990 FM classification criteria. Exclusion criteria for all subjects were: 1) significant hearing loss (determined by self-report and hearing screening) or the use of hearing aid; 2) medical conditions capable of worsening physical functional status independent of FM (e.g., morbid obesity, cardiopulmonary disorders, uncontrolled hypertension, uncontrolled endocrine or allergic disorders, disorders of vestibular system, renal disorders, seizures, psychiatric disorders requiring hospitalization ≤ 6 months, cancer within the last 2 years or current chemotherapy / radiation treatment); 3) current substance abuse; 4) pregnancy; or 5) any typical MRI contraindication, including claustrophobia. Patients taking opioid medications on a regular basis were also excluded. Participants were allowed to continue with their regular medication regimen; however, they were asked to avoid any analgesic medication 24 hours prior to the MRI session. Healthy controls reported no current chronic pain condition at the time of enrollment. Informed consent was obtained from all study participants for procedures approved by the Institutional Review Board at the University of North Carolina (UNC) at Chapel Hill.

Data collected for this dissertation were part of a larger project that included psychophysical and behavioral testing done for all subjects in separate visits, in addition to a single MRI scanning session where multi-modal MRI data were collected (stimulus-

evoked BOLD, resting-state BOLD, resting-state arterial spin labeling) in addition to the herein reported diffusion weighted and high-resolution T1-weighted anatomical imaging.

Demographic characteristics and clinical measures

Age, weight and height were collected from all subjects by self-report. We assessed handedness by using the scale proposed by Chapman and Chapman (Chapman and Chapman, 1987). It consists of 13 items that describes several specific activities where the participant must answer, “which hand you ordinarily use for each activity” (1-right, 2-either, 3-left). It yields a summed score that can range from 13 (completely right-handed) to 39 (completely left-handed). We used the cut-off ranges suggested by those authors: right-handed = 13-17, left-handed = 33-39, ambilateral = 18-32.

FM patients reported the average pain level in the past 2 weeks using a 0-100 numerical rating scale (NRS; anchors: 0 = No pain, 100 = Most intense pain imaginable). They were also asked to report the time in years since the onset of their widespread pain. At the day of the MRI scanning, all participants were asked to rate their current pain level using the 0-100 NRS, and they also rated separately their current pain intensity and pain unpleasantness using the 0-20 Gracely’s box scales (Gracely et al., 1978).

Questionnaires

Measures of affective distress

Depressive symptoms were measured using the Beck Depression Inventory (BDI) (Beck et al., 1961). The BDI is a 21-item questionnaire that measures symptoms and attitudes related to depression by rating their intensity between 0-3, and it has been

extensively validated (Beck et al., 1988). The sum of all items gives the total score, which ranges between 0-63.

Level of trait anxiety was measured using the State-Trait Anxiety Inventory (STAI Y2) (Spielberger et al., 1983). Participants rated how they generally feel by answering each of the 20 items using a 4-category scale (1 = Almost Never; 2 = Sometimes; 3 = Often; 4 = Almost Always). The total score is the sum of all items scores, ranging from 20 to 80.

Measure of psychosocial stress

The perceived stress scale (PSS) is 10-item scale that assesses the perception of stress (Cohen et al., 1983). Participants indicate for each item how they felt or thought in the previous month using a 5-category scale (Never, Almost Never, Sometimes, Fairly Often, Very Often). The total perceived stress score is the sum of the weights of all items (0-4), ranging from 0 to 40.

Measure of coping

The Coping Strategies Questionnaire-Revised (CSQ-R) is a revised version of the originally proposed CSQ (Rosenstiel and Keefe, 1983), and it is composed of 27 items that are related to the strategies used by individuals to cope with pain. For each item, the participants indicate how frequent they engaged in a particular coping strategy using a 7-category numerical scale (anchors: 0 = Never do that; 6 = Always do that). Six subscales measuring different strategies used by the individual are derived: catastrophizing (range for the subscale items sum = 0-36), distraction (0-30), ignoring pain (0-30), distancing from pain (0-24), coping self-statements (0-24), and praying (0-18).

Measure of somatic awareness

Somatic awareness, or the general tendency to endorse physical symptoms, can be estimated through the Pennebaker Inventory of Limbic Languidness (PILL) (Pennebaker, 1982). This questionnaire is composed of 54 items that describes physical symptoms and the participant answers how often each occur in a 5-category scale (Never or almost never have, Less than 3 or 4 times per year, Every month or so, Every week or so, More than once every week). The PILL summary score was derived by summing the scores for each of the 54 items.

Additional questionnaires (pain descriptors, sleep quality)

The short-form McGill pain questionnaire (SF-MPQ) provides information on the dimensions of clinical pain (Melzack, 1987). The version used in the present study includes the 15 pain descriptors that the participant must rate the intensity in a 4-category scale (None, Mild, Moderate, Severe). The pain descriptors can be divided in sensory or affective, and by summing the respective items two scores are formed (range for sensory score = 0-33; affective score = 0-12).

Sleep quality was assessed by the Pittsburgh Sleep Quality Index (PSQI) (Buysse et al., 1989), which has 19 questions where the participant reports different aspects of their sleep in the last month. These 19 items are then combined in 7 component scores (Subjective sleep quality, Sleep latency, Sleep duration, Habitual sleep efficiency, Sleep disturbances, Use of sleep medication, Daytime dysfunction) where each ranges from 0 (no difficulty) to 3 (severe difficulty). A global PSQI score can be derived by summing all components, ranging from 0 to 21 according to the degree of severity in each area as described by the components' scores.

MRI scanning session

All participants underwent a single MRI scanning session at the Biomedical Research Imaging Center at UNC-Chapel Hill, using its 3-Tesla Trio Siemens MR scanner with a 12-channel head coil. Prior to entering the scanner room participants filled the 0-100 NRS for current pain and the Gracely's box scales for pain intensity and unpleasantness, and they were instructed on what to expect during the scanning (high level of noises and vibrations, avoidance of head motion during imaging acquisition, ability to communicate with investigators at any time if needed). Once in the scanner room, participants were fitted comfortably on the scanner bed with a leg support pillow. Their head was padded with foam pads to minimize movements and ear muffs were used for hearing protection. A vitamin E capsule was attached to the right temple of the participants' head to avoid right-left ambiguities during imaging data processing and analysis. Physiological monitoring was done by fitting a peripheral pulse oximeter to the participant's left index finger and a respiration belt. Communication with participants was established via intercom in between imaging runs. After all imaging data were acquired, participants were removed from the scanner and debriefed for any discomfort or problems during the scanning.

Details for diffusion weighted and high-resolution anatomical imaging acquisition parameters will be offered in the respective chapters.

Statistical analysis

Results are reported in the format of mean ± SD, unless otherwise stated. Data distribution was checked via histograms and tested using the Kolmogorov-Smirnov test. Data fitting the normal distribution were tested for between-group comparisons using

the independent samples t-test (2-tailed). Non-normally distributed data were tested using the independent samples Mann-Whitney U test (2-tailed). All statistical tests were considered significant at $p < 0.05$.

Results

Demographic characteristics and clinical measures

Subjects' demographic characteristics and clinical measures details are offered in Table 1.1. We used the ACR 1990 FM classification criteria as the inclusion criterion for the patient group, and found discordance in 3 patients that met the classification but did not fit the ACR 2010 FM diagnostic criteria. As a result of the matching procedure, the participants' age did not significantly differ between groups (FM patients mean age ± SD: 42.9 ± 12.2 years; controls: 44.2 ± 11.7 years; $p = 0.675$), with a wide range observed (FM patients minimal and maximum age: 23 - 63; controls: 23 - 61). Body mass index (BMI) was calculated for all subjects in units of kg/m^2 and it was significantly different between groups, with FM patients and controls mean BMI at the opposite ends of the range for the "overweight" category (FM: 29 ± 6.8; controls: 25.6 ± 5.5; $p = 0.037$) (http://www.nhlbi.nih.gov/health/public/heart/obesity/lose_wt/risk.htm). Handedness was similar between groups, with the major difference being in the "right" and "ambilateral" categories. As noted by its proponents, the cut-off ranges are "necessarily arbitrary" (Chapman and Chapman, 1987). Using the individuals' scores and assigning right-handedness to a range of 13-25 and left-handedness to 26-39, FM patients and controls included 27 and 28 right-handed participants respectively which was not significantly different ($p = 0.285$).

The duration of widespread pain for FM patients was 11.4 years (± 9.3) on average, with a range of 1 to 40 years. Average pain in the last 2 weeks was a minimum of 25 and a maximum of 85 using the 0-100 NRS (mean ± SD: 57.1 ± 16.3). At the day of MRI scanning, FM patients rated their current pain (0-100 NRS: 47.8 ± 19), current pain unpleasantness (0-20: 8.2 ± 2.9) and intensity (0-20: 9.7 ± 3.4) significantly different than controls ($p < 0.0001$) as expected.

Questionnaires

Measures of affective distress, psychosocial stress, coping, and somatic awareness were markedly higher for FM patients compared to controls (Table 1.2). Depressive symptoms and trait anxiety as measured by BDI and STAI Y2, respectively, were significantly greater for the patient group ($p < 0.0001$). Psychosocial distress as perceived by participants was highly significantly different between groups (FM patients: 18.8 ± 8.3; controls: 9.7 ± 6; $p < 0.0001$). From the coping strategies measured by the CSQ-R, only catastrophizing ($p < 0.0001$) and ignoring pain ($p < 0.017$) reached statistical significance for group differences. Somatic awareness, derived from PILL scores, was significantly greater for FM patients (153.8 ± 36.7) compared to controls (84.9 ± 20.8) ($p < 0.0001$).

As expected, scores for sensory and affective pain descriptors were much greater for the patient group ($p < 0.0001$ for both). Finally, moderately reduced sleep quality was present for the FM patients according to the PSQI global score (10.9 ± 3.4) but not for controls (3.2 ± 2) ($p < 0.0001$).

Discussion

The present subject sample was well characterized using several demographic characteristics and clinical measures, with results reported here consistent with previous literature including BMI (Ursini et al., 2011; Timmerman et al., 2013). Many of the psychosocial measures described have been used in neuroimaging studies of FM patients (Schmidt-Wilcke et al., 2007; Jensen et al., 2010; Burgmer et al., 2011; Jensen et al., 2013). Assessment of sleep quality in FM using the PSQI has been performed previously, with similar results (Osorio et al., 2006; Munguia-Izquierdo and Legaz-Arrese, 2011). Given the use of validated classification criteria for FM, the characterization of our subjects using different dimensions of clinical and psychosocial measures and also the relatively large sample size, the results reported here and subsequent chapters are likely representative of the FM patient population.

Tables

Table 1.1. Demographic characteristics and clinical measures.

	FM	HC	p-value
Age (years)	42.9 (± 12.2)	44.2 (± 11.7)	0.675†
BMI (kg/m^2)	29.0 (± 6.8)	25.6 (± 5.5)	0.037†
Handedness: Right	21	25	-
Ambilateral	7	3	-
Left	2	2	-
Pain duration (years)	11.4 (± 9.3)	-	-
Fibromyalgia tender points (0-18)	16.5 (± 1.9)	1.3 (± 1.6)	< 0.0001††
Average pain in last 2 weeks (0-100)	57.1 (± 16.3)	-	-
Current pain (0-100)	47.8 (± 19.0)	1.0 (± 3.8)	< 0.0001††
Current pain unpleasantness (0-20)	8.2 (± 2.9)	0.3 (± 1.1)	< 0.0001††
Current pain intensity (0-20)	9.7 (± 3.4)	0.5 (± 1.7)	< 0.0001††

Mean (± SD). FM = fibromyalgia; HC = healthy controls.
Handedness count based on scores as measured by the scale from Chapman & Chapman (1987).
BMI = Body Mass Index.

† = Independent samples t-test. †† = Independent samples Mann-Whitney U test.

Table 1.2. Questionnaires scores.

	FM	HC	p-value†
BDI (0-63)	18.3 (± 12.3)	3.1 (± 4.2)	< 0.0001
STAI Y2 (20-80)	46.5 (± 14.0)	29.6 (± 6.9)	< 0.0001
PSS (0-40)	18.8 (± 8.3)	9.7 (± 6.0)	< 0.0001
CSQ-R Catastrophizing (0-36)	10.9 (± 6.8)	2.8 (± 3.8)	< 0.0001
CSQ-R Distraction (0-30)	14.9 (± 5.5)	16.1 (± 9.1)	0.539
CSQ-R Ignoring Pain (0-30)	11.6 (± 6.6)	16.6 (± 8.2)	0.017
CSQ-R Distancing from Pain (0-24)	5.8 (± 6.5)	7.3 (± 6.1)	0.260
CSQ-R Coping (0-24)	15.3 (± 4.9)	16.3 (± 4.9)	0.419
CSQ-R Praying (0-18)	9.7 (± 6.0)	7.5 (± 6.3)	0.162
PILL (54-270)	153.8 (± 36.7)	84.9 (± 20.8)	< 0.0001
SF-MPQ sensory score (0-33)	10.4 (± 4.8)	0.1 (± 0.3)	< 0.0001
SF-MPQ affective score (0-12)	3.1 (± 1.7)	0.0 (± 0.0)	< 0.0001
PSQI global score (0-21)	10.9 (± 3.4)	3.2 (± 2.0)	< 0.0001

Mean (± SD). FM = fibromyalgia; HC = healthy controls.
SF-MPQ = Short-Form McGill Pain Questionnaire; BDI = Beck Depression Inventory; STAI Y2 = State-Trait Anxiety Inventory (Trait anxiety); PSS = Perceived Stress Scale; CSQ-R = Coping Strategies Questionnaire-Revised; PILL = Pennebaker Inventory of Limbic Languidness; PSQI = Pittsburgh Sleep Quality Index.

† = Independent samples Mann-Whitney U test.

CHAPTER 2: ASSESSMENT OF BRAIN MICRO-STRUCTURAL CHARACTERISTICS OF FIBROMYALGIA PATIENTS USING DIFFUSION TENSOR IMAGING

Introduction

Augmented pain and sensory processing is considered a main feature of fibromyalgia (FM) presentation. At least part of its putative mechanisms likely originate from the central nervous system (CNS) with several lines of evidence supporting this view (Clauw, 2009), including central sensitization mechanisms such as the “wind-up” phenomenon and impaired pain modulatory systems being described in FM patients. Neuroplastic brain changes in chronic pain is well described (Latremoliere and Woolf, 2009; Siddall, 2013), and it is corroborated by neuroimaging studies (Seifert and Maihofner, 2011). Neuroplasticity within the brain is one putative mechanism in FM and concurs with a role for the CNS in its pathophysiology, with functional, neurochemical, and structural brain abnormalities in patients when compared to controls being described (Gracely and Ambrose, 2011).

Recent studies of FM using magnetic resonance imaging (MRI) modalities have focused on macro-structural brain characteristics, with the most common approach being voxel-based morphometry (VBM). Two studies investigated micro-structural features of the brain in FM patients using diffusion MRI (Sundgren et al., 2007; Lutz et al., 2008). Their results only partially overlapped with findings of white matter (WM) abnormalities in the right thalamus. The later study reported several other WM

dissimilarities between FM patients and controls, and attributed these discordant results between both studies to methodological differences (Lutz et al., 2008). These pioneering studies did not benefit from recent methodological improvements in diffusion MRI, including advancements in MR scanners technology, computational methods and availability of dedicated software packages (Hasan et al., 2011; Soares et al., 2013). Recently a study using multi-modal MRI including diffusion reported regional WM abnormalities in FM patients relative to age-matched controls (Ceko et al., 2013)

The main goal of the present study was to determine brain micro-structural characteristics in FM patients, and assess potential WM abnormalities using age-matched controls as reference. Diffusion MRI allows this in a non-invasive manner, by measuring water molecule diffusion within the brain tissues. It is a versatile MRI modality not only for research but also for clinical uses, e.g., detection of acute brain ischemia (Sundgren et al., 2004). Our main focus was to assess micro-structural features of: i. WM tracts using tract-based spatial statistics (TBSS), and ii. Whole brain and pain-related regions of interest (ROI). We hypothesized that FM patients would present both global and regional brain WM abnormalities when compared to matched controls, including pain-related areas of the brain.

Methods

Imaging acquisition parameters

Subjects were accommodated in the MRI scanner as described in chapter 1, methods section. The diffusion weighted imaging (DWI) data acquisition consisted of a single run using an echo-planar imaging sequence (repetition time (TR) ~ 8,000 ms; echo time (TE) = 83 ms; field of view = 256 mm; 2 x 2 x 2 mm^3 voxels; parallel imaging

factor = 2 (GRAPPA)) acquired along 42 non-collinear, non-coplanar directions (b = 1,000 s/mm^2). Two dummy volumes were acquired and discarded to allow the longitudinal magnetization to reach a steady state prior to data acquisition. Seven non-diffusion weighted images (B_0; b = 0 s/mm^2) were acquired at equidistant points throughout the acquisition at a ratio of one B_0 image for every seven diffusion weighted images – within the range of suggested optimum ratios for assumptions of isotropic and anisotropic tensors (Jones et al., 1999; Alexander and Barker, 2005). A total of 68 slices oriented to the axial plane (no gap) were collected to ensure whole brain coverage (from vertex to second cervical spinal process). The image sequence was synchronized to the subject's cardiac cycle via a pulse oximeter signal with no delay (cardiac gating), avoiding data acquisition when the brain is susceptible to cardiac pulsatility which can severely corrupt diffusion weighted data (Jones and Leemans, 2011). We also acquired fieldmap images (TR = 800 ms; TE1 = 4.92 ms, TE2 = 7.38 ms; field of view = 256 mm; 4 x 4 x 2 mm^3 voxels; 68 slices) immediately prior to the DWI data acquisition, in order to correct for geometric distortions secondary to magnetic field inhomogeneities (Jezzard, 2012).

Diffusion tensor imaging, tensor model and related metrics

Diffusion is a physical process, where molecules present a constant random thermal motion at temperatures above absolute zero. This was described by Robert Brown in 1828 (Jones, 2009), thus this is also known as "Brownian motion". Despite its trajectory being a "random walk" in 3D space, Einstein showed in 1905 that one characteristic of diffusion could be characterized if a large enough number of molecules are free to diffuse: the diffusion coefficient D (in units of mm^2/s) is proportional to the

mean square displacement of all molecules, $\langle \Delta r^2 \rangle$, divided by the number of dimensions, n, and the diffusion time, t (Alexander et al., 2007; Jones, 2009):

- $D = \frac{<\Delta r^2>}{6n\Delta t}$

At body temperature (37 Cº) a cube of water of an approximate volume of 2.5 mm^3 present a diffusion coefficient of 3 x 10^{-3} mm^2/s, thus following an observation time of 30 ms water molecules would have displaced approximately 25 μm in all directions on average (Jones, 2009). In the brain, however, water molecules are not free to diffuse as there are many barriers including cellular membranes, myelin sheaths and cytoskeleton macromolecules. Therefore diffusion within brain tissues is approximately four times smaller compared to “free” diffusion, and it is thus called apparent diffusion coefficient (ADC) (Jones, 2009).

Diffusion has contrasting features in gray matter (GM) and WM. In the former diffusion occurs in all directions due to a convoluted tissue orientation (isotropic), while in the latter there is a high directionality component of tissue orientation from the bundling of axonal fibers, i.e., anisotropy. Thus the diffusion magnitude within the brain WM as measured by the ADC will depend on the direction used for measurement, making a single ADC measurement insufficient to fully characterize water diffusion in WM. Where diffusion is isotropic (GM, cerebral spinal fluid (CSF)), the probability of the mean displacement of water molecules can be represented by a diffusion sphere; for anisotropic diffusion however, when diffusion has a preferential main direction such as within WM, this is better described by a diffusion ellipsoid (Figure 2.1 A).

In diffusion MRI magnetic gradients are applied in multiple directions to allow the characterization of diffusion within the brain parenchyma. Using a diffusion weighting

factor (b-value), a brain image composed of several volume elements (voxels) can be acquired by imposing magnetic gradients on a particular direction. Non-diffusion weighted images where the b-value is zero are also acquired. By measuring the water displacement in multiple directions from the diffusion-weighted and non-diffusion weighted images the diffusion can be quantified in a voxelwise manner.

In order to adequately represent diffusion in an anisotropic medium such as WM, data from diffusion MRI can be modeled in a voxel-by-voxel basis using a diffusion tensor (Basser et al., 1994a; Basser et al., 1994b), i.e., diffusion tensor imaging (DTI). The diffusion tensor **D** is a 3 x 3 symmetric matrix, where the diagonal elements represent diffusivities along three orthogonal axes (D_{xx}, D_{yy}, and D_{zz}) and correlations between those are represented by the symmetric off-diagonal elements ($D_{xy} = D_{yx}$, $D_{xz} = D_{zx}$, and $D_{yz} = D_{zy}$):

$$\mathbf{D} = \begin{bmatrix} D_{xx} & D_{xy} & D_{xz} \\ D_{yx} & D_{yy} & D_{yz} \\ D_{zx} & D_{zy} & D_{zz} \end{bmatrix}$$

The diffusion ellipsoid can be described by applying a mathematical procedure to the diffusion tensor matrix, i.e., diagonalization, so that its internal frame of reference (x', y', z') matches the principal axes of the measurement frame (x, y, z). In such case, all off-diagonal elements are zero and the orientation of the ellipsoid main axes is given by eigenvectors (ε_1, ε_2, ε_3), with the orientation of the tensor depicted by the principal eigenvector (ε_1) – its direction is assumed to be parallel to the dominant fiber orientation within the voxel being measured. The degree of diffusion along the eigenvectors is given by the respective eigenvalues: λ_1, λ_2, λ_3 (corresponding to D_{xx}, D_{yy}, and D_{zz}); thus

the displacement within the ellipsoid in each axis is scaled to the square root of the corresponding eigenvalue (according to Einstein's formula) (Winston, 2012). The eigenvalues are, by definition, sorted according to their magnitude, i.e., $\lambda_1 > \lambda_2 > \lambda_3$ (Figure 2.1 A).

From the eigenvalues determined from the tensor model it is possible to derive scalar measurements that allow simplification of the diffusion data (as opposed to have brain images where each voxel contains a 3 x 3 matrix). These quantitative parameters were originally proposed by Basser and Pierpaoli in 1996 (Basser and Pierpaoli, 1996), and they include:

- **Trace**, which measures the magnitude of diffusion:
  - Sum of the three eigenvalues: $\lambda_1 + \lambda_2 + \lambda_3$
- **Mean diffusivity (MD)**, the mean diffusion across all three axes:
  - Average of the three eigenvalues :$(\lambda_1 + \lambda_2 + \lambda_3) / 3$
- **Fractional anisotropy (FA)** is an anisotropy index, that measures the fraction of the tensor that can be attributed to anisotropy parallel to the orientation of the main fiber tract (in the formula, L = λ):
  - FA = $\sqrt{\frac{3}{2}} \frac{\sqrt{(L1-MD)^2+(L2-MD)^2+(L3-MD)^2}}{\sqrt{L1^2+L2^2+L3^2}}$

Both trace and MD have units of mm^2/s, while FA is dimensionless and normalized so that its values range from 0 (isotropic diffusion) to 1 (anisotropic diffusion, i.e., constrained along one axis).

MD is known to have remarkably similar values across GM and WM (similarly to the ADC) - around 7×10^{-4} mm^2/s (Winston, 2012) - and show increased values in areas with local inflammation / edema (Alexander et al., 2007) while increased cellularity

(Gauvain et al., 2001) and cellular swelling (Benveniste et al., 1992) reduces MD. FA values for healthy WM have a peak close to 0.3 (Alexander et al., 2007), with values around 0.2 for cortical GM, 0.2-0.4 in deep GM and a wider range in WM (circa 0.45 in subcortical WM to about 0.8 in the corpus callosum) (Beaulieu, 2009). Given such variability for FA values across the brain it becomes clear that only similar brain regions can be compared using this measure, i.e., comparing the FA from area "X" to area "Y" is meaningless to infer underlying micro-structural differences such as axonal density or degree of myelination (Beaulieu, 2009). It has been reported that the parallel disposition of WM bundles is key for diffusion anisotropy (Alexander et al., 2007), due to the presence of axonal membranes. Myelination has a secondary modulatory role for FA, as unmyelinated fibers also present anisotropic diffusion and animal models of dysmyelination (failure to form normal myelin) showed an average FA reduction of only 15% (range 0-32%) (Beaulieu, 2009). Hence several factors can impact the FA value measured within a voxel including axonal count and density, myelination, fiber organization, and crossing fibers (Winston, 2012).

It is important to note that FA does not describe the tensor shape or distribution in its entirety, as different eigenvalue combinations can result in similar FA values. Thus studies have used the eigenvalues separately or in combination to provide a more specific understanding of WM micro-structure (Alexander et al., 2007; Winston, 2012):

- **Axial diffusivity (AD)** is the diffusivity parallel (longitudinal) to the main axis of diffusion:
    - Represented by λ_1

- **Radial diffusivity (RD)** is the diffusivity perpendicular (orthogonal) to the main axis of diffusion:
    - Average of the two eigenvalues orthogonal to λ_1: $(\lambda_2 + \lambda_3) / 2$

These two measures, as they are derived from the eigenvalues directly, also have units of mm^2/s. AD is considered a marker for axonal damage (reduced AD ≈ axonal degeneration), while increases in RD reflects myelin degradation (Alexander et al., 2007; Winston, 2012).

Lastly, the **mode (MO)** of anisotropy can specify the geometric shape of the ellipsoid (Ennis and Kindlmann, 2006) (in the formula, L = λ):

- MO = $\frac{L1\ x\ L2\ x\ L3}{\left(\sqrt{(L1-MD)^2+(L2-MD)^2+(L3-MD)^2}\right)^3}$

Its values range from -1 to +1 (dimensionless), describing a tensor that is disc-shaped (planar anisotropy) to one that is a tubular (linear anisotropy) respectively (Smith and Kindlmann, 2009; Winston, 2012). MO values closer to -1, indicating a disc-shaped (oblate) tensor where $\lambda_1 \approx \lambda_2$, is suggestive of crossing fibers while values closer to +1 (prolate tensor) indicates primarily a single dominant fiber ($\lambda_2 \approx \lambda_3$) (Fig. 2.1 B). MO is orthogonal (mathematically independent) to FA, and it can provide important additional information about diffusion within the brain. This importance can be appreciated when assessing FA measurements, as brain areas with crossing WM tracts (lower MO values) will present lower FA values in the absence of any WM abnormality (Alexander et al., 2007).

DWI preprocessing steps

All processing steps for diffusion weighted images were done using the Oxford Centre for Functional Magnetic Resonance Imaging of the Brain (FMRIB) software

library (FSL v. 5.0.5) (Smith et al., 2004; Jenkinson et al., 2012) (http://fsl.fmrib.ox.ac.uk/fsl/fslwiki). DWI and fieldmap images were reoriented to the Montreal Neurological Institute (MNI) brain template using the FSL tool "fslreorient2std", and then loaded into the visualization tool "FSLview" to be visually checked for any obvious artifacts. Eddy current and motion artifact correction was done using the FMRIB Diffusion Toolbox (FDT), followed by application of the rotational component of the transformation for each volume to the gradient direction encoding vectors. The resulting eddy current and motion corrected DWI images were visually inspected. Individual brain masks were derived from the first B_0 image using the Brain Extraction Tool (BET) (Smith, 2002). Fieldmap images were processed using the FSL tool "fsl_prepare_fieldmap", and then used to correct geometric distortions in the DWI images as implemented by FSL's FUGUE, and the resulting output was visually inspected for artifacts.

Finally, a diffusion tensor model was estimated from the undistorted DWI images using weighted linear least-squares regression as implemented by FDT (Behrens et al., 2003). An image of the sum of squared error was also produced by FDT and it was visually checked for artifacts, as well as the calculated FA, MD, AD and MO parametric maps. RD images were calculated as the average of the maps for the two radial vectors eigenvalues (λ_2, λ_3) using the FSL tool "fslmaths".

Tract-based spatial statistics

Tract-Based Spatial Statistics (TBSS) (Smith et al., 2006) were used to carry out voxelwise analysis of the FA data for FM patients and controls. TBSS processing steps include: 1) non-linear registration of the FA maps to a 1 x 1 x 1 mm^3 standard space FA image as target (FMRIB58_FA: high-resolution average of 58 FA maps from healthy

male and female subjects aged between 20-50 (http://fsl.fmrib.ox.ac.uk/fsl/fslwiki/FMRIB58_FA)); 2) a mean FA image derived from all subjects was created, then thinned to represent the center of the major WM tracts common to all subjects, i.e., a mean WM skeleton image; 3) the mean FA skeleton was thresholded at 0.2 to include FA values with acceptable cross-subject variability, then each individual's normalized FA map was projected into the skeleton resulting in a 4D image file containing the skeletonized FA data for all subjects.

Non-FA images of the additional DTI metrics (AD, MD, RD, MO) were also processed using TBSS. Each of the non-FA images was registered into standard space by applying the non-linear registration calculated for FA images, then projected onto the original mean FA skeleton. Therefore for each non-FA DTI metric a 4D skeletonized image was generated, where voxels in the same spatial location contain each of those metrics values respectively.

Statistical analyses

TBSS analysis (voxelwise)

A between-group permutation-based nonparametric t-test (Nichols and Holmes, 2002) using age as a covariate of no interest was done, using the 4D skeletonized mean FA image as input for the FSL tool "randomise" with 5,000 permutations and using the threshold-free cluster enhancement option. This option allows the detection of cluster-like formation(s) of significant voxels with no arbitrary thresholding while controlling for family-wise error rate across space, therefore correcting for multiple comparisons (Smith and Nichols, 2009). This way, voxelwise statistics reported here were tested for significance at p-value < 0.05, corrected.

The WM skeleton is thin (few voxels wide) thus hard to visualize when overlaid onto a brain image, therefore we used the FSL tool “tbss_fill” to thicken the skeleton areas with significant group differences for enhanced visualization. Location of significant differences between groups were identified using FSLview and the built-in anatomical atlases (http://fsl.fmrib.ox.ac.uk/fsl/fslwiki/Atlases), as well as a MRI-based atlas of human WM (Oishi and Crain, 2011).

Whole brain, WM skeleton and pain-related region of interest analyses

To perform between-group comparisons for the whole brain and WM skeleton, each DTI parametric map was averaged across the whole brain and across all voxels within the WM skeleton for each subject.

Additionally, a region of interest (ROI) analysis was done based on *a priori* brain anatomical regions that are commonly activated following noxious stimulation (Peyron et al., 2000; Apkarian et al., 2005), including a subcortical structure (thalamus) as well as cortical areas including the primary (SI) and secondary (SII) somatosensory cortices, the insula, and the anterior cingulate cortex (ACC). The inferior parietal lobule (IPL) was also included, which is a cortical area that integrates somatosensory and visual inputs and was activated following noxious pressure stimulus to the thumbnail during stimulus-evoked functional MRI in the participating FM patients and controls (unpublished data). A binary mask image was generated for each of those ROIs using three probabilistic atlases available in FSL (http://fsl.fmrib.ox.ac.uk/fsl/fslwiki/Atlases): the Harvard-Oxford cortical and subcortical atlases (Desikan et al., 2006) and the Jülich histological atlas (Eickhoff et al., 2006). From the Harvard-Oxford atlases ROI masks for right and left thalamus and insula were derived, while the ACC mask was built as a single region;

right and left SI, SII, and IPL were derived from the Jülich atlas. Since the cortical ROIs were constructed from probabilistic atlases moderately thresholded at p = 0.25, they encompassed voxels beyond the cortical mantle and included WM voxels within it, a method used previously for DTI measurements (Stein et al., 2012). These WM voxels preferentially include afferent/efferent fibers associated with the cortical region proximal to it (Salat et al., 2009a). We extracted the mean for each DTI metric across all voxels within each ROI, as well from the WM skeleton voxels within it (Figure 2.2).

Between-group differences were assessed using analyses of covariance with age as a covariate of no interest. All statistical tests were done using SPSS v. 18, with significance thresholding of $p < 0.05$.

We also assessed associations of DTI metrics measured in the whole brain and ROIs with subject's clinical measures and psychosocial questionnaire scores using the Pearson's correlation coefficient "r". Correlations with p-value < 0.01 were considered significant.

Results

Subjects demographics characteristics, clinical measures and questionnaires

A full description of the FM patients and controls is presented in chapter 1, results section.

TBSS analysis (voxelwise)

Between-group WM skeleton-based comparisons, corrected for age, identified several clusters where FM patients had lower FA compared to controls (Table 2.1; Figures 2.3 to 2.6). The largest cluster (2,305 voxels) included the right corticospinal tract and WM adjacent to the right SI and the primary motor cortex (M1), and several

clusters summing 2,729 voxels were localized within the corpus callosum, including the genu, body and splenium. Two clusters were localized in the anterior limbs of the internal capsule (IC) and anterior corona radiata, one on the left (709 voxels) and another on the right (431 voxels) side. The left corticospinal tract, and WM adjacent to the left SI and M1 were part of another cluster with 568 voxels. Other clusters were localized in the inferior fronto-occiptal, inferior longitudinal and superior longitudinal fasciculi (1,984 voxels), while 140 voxels were localized deep within WM. No significant cluster was found for FM having increased FA compared to controls.

Group differences for other DTI metrics included significant increases of RD (10,356 voxels) and MD (10,805 voxels) for the patient group, while MO showed reductions for patients in a limited spatial distribution (1,526 voxels) – see description below. No group differences for AD were found in either direction.

Figures 2.3 to 2.6 show the spatial distribution of significant clusters in which FM patients had lower FA values compared to controls (left panel), and where FM patients had greater RD values (right top panel) and greater MD values (right bottom panel) (green = WM skeleton; red = FA, blue = RD, purple = MD, yellow = overlap between FA and RD / MD in the right-sided panels). Figure 2.3 and 2.4 show sagittal and axial views respectively of significant FA differences in the corpus callosum (left panel); overlap of FA and RD are noticeable in the genu and body, and also anterior limbs of IC (right top panel) while MD mostly overlaps FA in the genu and right anterior limb of IC (right bottom panel). Corticospinal tracts had significant reduction of FA in patients bilaterally (Figure 2.5, left panel), with MD differences overlapping both sides while RD showed a similar pattern however slightly less distributed (right bottom and top panels,

respectively). WM tracts close to SI and M1 with reduced FA in patients are shown in Figure 2.6 left panel, with the tracts showing overlap of RD and MD differences depicted on the right top and bottom panels respectively.

Significantly reduced MO in patients as compared to controls was spatially limited compared to the other DTI metrics' parametric maps, with differences mostly over the genu, body and splenium of corpus callosum (765 voxels), and parts of the corona radiata (761 voxels) (data not shown). No increases of MO for patients compared to controls were significant.

Whole brain, WM skeleton and pain-related region of interest analyses

Comparing DTI metrics across the whole brain showed no group differences for FA ($p = 0.32$), however AD and MD were significantly reduced for FM patients compared to controls ($p = 0.023$ and $p = 0.037$ respectively) while RD approached significance ($p = 0.051$) (Figure 2.7). For measures within the WM skeleton no significant differences were found, although FA reduction in patients compared to controls was close to significance ($p = 0.065$).

ROI analyses revealed an interesting pattern (Table 2.2 and 2.3). When comparing DTI metrics across all voxels within each ROI (non-skeletonised), no significant differences were found for FA ($0.093 < p < 0.984$) but the left and right SI in FM patients had significantly reduced AD ($p = 0.034$ and $p = 0.004$ respectively), RD ($p = 0.045$; $p = 0.005$) and MD ($p = 0.041$; $p = 0.004$) compared to controls. The right inferior parietal lobule also showed a similar reduction for patients but did not reach significance (p-value for AD = 0.052; RD = 0.066; MD = 0.06) (Table 2.2).

Assessing metrics for WM skeleton voxels within each ROI showed more varied differences (Table 2.3). For WM skeleton FA and RD, both left and right SI showed significant differences in patients compared to controls (reduced FA in left and right SI: $p = 0.002$ and $p = 0.001$ respectively; increased RD: $p = 0.004$ and $p = 0.011$) while for MD only left SI showed a significant increase ($p = 0.016$). Compared to controls, FM patients showed significant reductions in AD, RD and MD in the left insula (all at $p < 0.001$).

Association of DTI metrics with clinical and psychosocial measures

When assessed in the whole brain (non-skeletonised), DTI metrics showed significant correlations with age in FM patients (r for FA = -0.54, AD = 0.49, RD = 0.56; MD = 0.54) and controls (AD = 0.65; RD = 0.68; MD = 0.67), indicating that increased age is associated with reduced FA and increased AD, RD, and MD. Within the WM skeleton, negative correlations between age and FA ($r = -0.47$) and between BMI and AD, RD, and MD were found only for patients ($-0.68 < r < -0.47$) (Table 2.4), thus increased BMI in patients is correlated with decreases in AD, RD and MD. No associations for DTI metrics and pain characteristics were found, and no psychosocial measures were significantly correlated with DTI metrics for either group at $p < 0.01$.

For FM patients, non-skeletonised ROIs showed significant negative associations with age and FA in several ROIs except left SII, ACC and left IPL ($-0.62 < r < -0.38$), while AD, RD, and MD were positively associated with age in most ROIs except SI bilaterally and ACC ($0.48 < r < 0.68$) (Table 2.5). Controls showed no significant associations of age and FA, however AD, RD, and MD were positively associated with age in all ROIs but left and right thalamus and left insula ($0.45 < r < 0.66$) (Table 2.5).

For correlations of DTI metrics within the WM skeleton, FM patients showed negative associations for age and FA ($-0.63 < r < -0.54$) and positive associations for other metrics (AD, RD, MD; $0.47 < r < 0.60$) in the left and right thalamus (Table 2.6). Controls showed only negative correlation between age and left IPL FA ($r = -0.47$). In FM patients only, significant negative correlations of BMI were found in the right thalamus and AD ($r = -0.50$); right SI and left SII and AD, RD, and MD ($-0.73 < r < -0.48$); and left IPL for AD ($r = -0.52$) and both IPL for RD and MD ($-0.60 < -0.48$) (Table 2.6).

Discussion

Global and regional WM abnormalities in the brain of FM patients, as compared to age- and sex-matched healthy controls, are suggested based on the results reported here. Supporting a role for the CNS in FM pathophysiology, global abnormalities were found by reductions of diffusion anisotropy and increased radial and mean diffusivity along WM tracts associated with multiple functional roles including sensory, motor, visual, auditory and inter-hemispheric connectivity. Regional differences of diffusion patterns were also revealed in pain-related brain locations, further supporting CNS micro-structural abnormalities as a putative mechanism in FM.

WM skeleton abnormalities in TBSS

WM tracts are the “information highways” in the CNS, and have been traditionally divided in three groups according to their connectivity (Jellison et al., 2004; Wycoco et al., 2013):

1. **Projection fibers** connect cortical areas with subcortical (deep nuclei) structures, brainstem, cerebellum and spinal cord, and can be subdivided

in corticofugal (efferent) and corticopetal (afferent). They include corticospinal, corticobulbar, and corticopontine tracts, thalamic radiations and geniculocalcarine tracts (optic radiations).

2. **Association fibers** connect cortical areas within the same hemisphere. These fibers can be short range such as the subcortical U fibers connecting adjacent gyri, or long range including cingulum, superior and inferior fronto-occiptal fasciculi, uncinate fasciculus, superior longitudinal (arcuate) fasciculus and inferior longitudinal (occipto-temporal) fasciculus.
3. **Commissural fibers** provide interconnection of similar cortical areas between the two hemispheres, and they include the corpus callosum and the anterior commissure.

All the above WM tracts are typically identifiable in DTI color maps, and other tracts that are occasionally seen include optic tract, fornix, tapetum, and several fibers within the brainstem and cerebellum.

Mean FA reductions in patients were localized within projection (corticospinal tracts, WM adjacent to SI / M1), association (inferior fronto-occiptal, inferior longitudinal and superior longitudinal fasciculi), and commissural (along all corpus callosum (genu, body, splenium)) fibers. Reduction in anisotropy, signaling potential WM abnormalities, within WM tracts that connect brain regions subserving different functional roles is in agreement with typical FM clinical symptoms, such as widespread pain, fatigue, and impaired cognition (Clauw, 2009). Projection fibers identified here with FA reductions potentially include corticospinal (motor control for body), corticobulbar (motor control for cranial nerves), and corticopontine (arises from precentral and postcentral gyri, with

contributory fibers from premotor, supplementary motor, posterior parietal, prefrontal and temporal cortices and project to pontine nuclei) tracts, as these fiber bundles run together and cannot be discriminated from each other via DTI data (Jellison et al., 2004). As these projection fibers project to their targets they contribute to form the internal capsule and its subdivisions (anterior limb, genu, posterior limb) in a somatotopic manner (Schuenke et al., 2007; Wycoco et al., 2013). Not surprising, significant differences in DTI metrics (reduced FA, increased RD and MD) in FM patients relative to controls have been found within the internal capsule as well. Intra-hemispherical connections served by long association fibers might also be affected in patients, as reduction in FA has been found within several fasciculi (inferior fronto-occiptal, inferior longitudinal and superior longitudinal). Functional roles of these fasciculi include integration of auditory and visual cortices to the prefrontal cortex, visual emotion and memory, and integration of auditory and speech nuclei (Wycoco et al., 2013). Finally, sensorimotor impairments and auditory hypersensitivity reported in FM might be a consequence of disturbed inter-hemispheric connectivity through the corpus callosum, as evidenced by overlapping altered DTI metrics values in patients relative to controls within this major WM bundle. In sum, several WM tracts that transmit information to and from different cortical areas show signs of WM abnormalities in FM and can potentially explain many symptoms that characterize the clinical presentation of affected patients.

Of the 126,241 WM skeleton voxels tested for DTI metric differences between patients and controls, 7% showed reduced FA, while 8.2% and 8.5% showed increased RD and MD respectively with several tracts presenting superimposition of these metrics. Anisotropy within WM is a result of micro-structural barriers to water diffusion, including

axonal diameter and packing density, membrane permeability, and levels of myelination (Jones et al., 2013). The most commonly used anisotropy index is FA (Sundgren, 2009), and its value can be impacted by all those factors as well as the main fiber directionality (-ies) within a given voxel, .i.e., more than one main fiber orientation tends to reduce the FA measured in that voxel. For this reason, we also measured the mode (MO) of anisotropy as it provides insight into fiber orientations within a voxel. Despite finding significant reductions of MO for patients relative to controls over the corpus callosum and corona radiata, they represented only 17.2% of voxels showing FA reductions (1.2% of WM skeleton voxels). Therefore it seems unlikely that crossing fibers can fully explain the FA reductions in FM patients reported here.

From the above, it follows that presence of micro-structural WM abnormalities in the brains of FM patients must be considered. Animal models of dysmyelination showed an increase in RD but no effects on AD (Song et al., 2002), thus in those WM tracts of FM patients presenting reduced FA and increased RD (but no AD changes) a process of myelin degradation could be in place. Increases in diffusivity as shown by MD in similar spatial locations further support this possibility, as myelin modulates the amount of anisotropy – but increased MD could also be a consequence of local inflammation and edema (Alexander et al., 2007).

Global and regional differences of DTI metrics in the whole brain and WM skeleton

Whole brain analysis for FA showed no significant differences between FM patients and controls however reduced AD and MD was found for patients; none of those differences were present for WM skeleton comparisons. Assessment of diffusion across all voxels within pain-related ROIs (including both GM and WM) showed a

reduction of MD within left and right SI. Both RD and AD were also reduced within SI bilaterally, but not FA – highlighting the importance of evaluating all DTI metrics for a more detailed understanding of WM micro-structure. Reduction of MD within SI is a curious finding, as apparent diffusion (which is proportional to MD) is usually stable across subjects and even mammalian species (Basser and Jones, 2002; Winston, 2012), and as mentioned previously MD increases are usually interpreted as a sign of local water increase secondary to inflammation (Alexander et al., 2007), and decreases of this metric have been related to increased tumor cellularity (Gauvain et al., 2001) and to neuronal swelling evoked by excitotoxins including glutamate (Benveniste et al., 1992).

An abrupt local reduction change in apparent diffusion is a marker of a brain ischemic event (Moseley et al., 1990) with animal models showing 30-50% decrease in diffusion within the affected brain area in the acute phase, which is attributed mainly to cytotoxic edema (Le Bihan, 2003; Fung et al., 2011). Then a gradual increase of diffusion to baseline levels within 1-2 weeks (pseudonormalization) takes place, followed by a marked increased in the chronic stage as tissue disintegration ensues (Alexander et al., 2007). A similar time course for DTI metrics have been reported for the acute (↑ FA, ↓ MD), subacute (↓ FA, ↓ MD), and chronic (↓ FA, ↑ MD) stages (Fung et al., 2011). In the acute phase cytotoxic edema dominates with a consequent shift of water from the extra- to the intracellular space, with the consequent contraction of the former and restricted diffusion space in the latter supporting increased anisotropy. During the subacute period vasogenic edema develops thus increasing extracellular water content while persistent cytotoxic edema keeps intracellular water levels relatively

unchanged, reducing anisotropy but keeping mean diffusivity low. Chronic stage characteristic vasogenic edema persistence, gliosis and neuronal loss results in still reduce FA and an increase of MD (Fung et al., 2011).

Reductions of MD within SI brain parenchyma reported here are much less intense compared to those in brain ischemia (left SI = 5.1%; right = 7%) and they represent group averages instead of individual brain changes. With these caveats in mind, one could hypothesize that the mechanisms underlying decreased MD in acute brain ischemic event may play a role for those findings within SI. WM and GM show different responses to ischemic injury, with WM presenting greater reductions in FA (Fung et al., 2011) since even minimal eigenvalue changes during ischemia within GM will lead to increases in FA due to the relative isotropic diffusion found in healthy GM. Our findings match this situation, where parenchymal SI presents with unchanged FA and reduced MD while the WM skeleton shows reduced anisotropy and increased MD supporting diffusion pattern changes in both GM and WM of SI. As cytotoxic edema arises from almost any brain insult including hypoxia, toxic or metabolic perturbations (Liang et al., 2007), it is tempting to speculate that blood hypoperfusion to SI may lead to a local, chronic ischemia able to trigger cytotoxic edema - thus reducing MD – but not severe enough to exceed cellular compensatory mechanisms (ionic pumps within plasma membrane) that prevents cell death. This hypothetical mechanism needs to be investigated using animal models of localized hypoperfusion in the brain. An alternative explanation would be local accumulation of excitotoxins such as glutamate within the SI region. It has been shown that a high interstitial concentration of glutamate is necessary to evoke cytotoxicity, in order to counterbalance uptake mechanisms that continuously

remove this neurotransmitter (Benveniste et al., 1992). Such scenario is supported by evidence that FM patients present abnormalities of “windup” phenomenon (Staud, 2006), which involves NDMA receptor mechanisms and glutamate is one of its main ligands. Glutamate is involved in neurotransmission in different levels across the somatosensory pathways (Broman, 1994), which includes mediation of SI neuronal responses to noxious stimulation (Pollard, 2000). Thus it is possible that a toxic accumulation of glutamate within SI parenchyma secondary to sustained input from peripheral tissues may lead to the present findings of reduced MD in this brain region.

The left insula of patients showed reduced AD, RD, and MD within the WM skeleton (but not FA) relative to controls while no significant changes were found for its parenchymal mean values. The insula is an important brain region involved in a multitude of functions including nociception and pain processing (Craig, 2009), with functional MRI studies showing a role for it in both sensory-discriminative and affective-emotional pain dimensions (Apkarian et al., 2005). Our findings point to reduced diffusion in all directions including along the dominant fiber direction (AD). The number of WM skeleton voxels captured by the mask representing the insula is relatively small, and these results may be an artifact despite the highly significant differences between the two groups. This finding must be investigated further in future studies.

Correlational analyses found negative associations for DTI metrics and age, a well known effect reported by other groups in healthy subjects (Hsu et al., 2010; Lebel et al., 2012; Zhang et al., 2014). The mean BMI for FM patients was at the far end of the “overweight” classification but still not obese, however it was significantly different compared to the mean BMI for controls. Increased BMI in patients was associated with

reduced mean diffusivity in right SI, left SII and IPL bilaterally. Studies using diffusion MRI found reduced MD values in otherwise healthy obese adults compared to non-obese (Karlsson et al., 2013), and other recent studies also reported reductions of DTI metrics in obese subjects compared to non-obese (Stanek et al., 2011; Xu et al., 2013). Given our findings, future studies using diffusion MRI in FM patients may benefit from including a matching procedure for BMI for subjects across groups.

Only three previous studies have used diffusion MRI in a sample of FM patients and controls. The pioneering study by Sundgren and colleagues reported a FA reduction in the right thalamus in patients relative to controls but no other differences were found in other pain-related ROIs or whole brain diffusivity (Sundgren et al., 2007). This result was replicated by a subsequent study, however it showed a much more complex pattern of differences between FM patients and controls that included both increase and decreases in FA in patients across ROIs (Lutz et al., 2008). Those results are not in agreements with the findings presented here. We used *a priori* defined anatomical ROIs instead of manually drawn ones, higher magnetic fields (3 vs. 1.5 Tesla), and validated software packages for DTI data processing and analysis – all these are recent methodological advances that those studies did not benefit from, and a direct comparison of results must be done with caution. Recently a study using multiple MRI modalities including diffusion MRI found no differences for whole brain comparisons between younger and older FM patients and age-matched controls; ROI analyses based on clusters found in concurrent VBM analysis on the other hand detected decreased FA for older FM patients in the corpus callosum adjacent to the posterior cingulate cortex and marginally increased FA for younger patients in WM

medial to the left putamen (Ceko et al., 2013). None of these studies reported use of two techniques regarded as useful in minimizing data corruption that were part of the processing pipeline for the present study, namely cardiac-gated data acquisition and fieldmap-based geometric distortion correction, which may explain in part the discrepant findings.

Other chronic pain conditions have been recently studied using DTI, including temporomandibular disorders (Moayedi et al., 2012; Wilcox et al., 2013), trigeminal neuralgia / neuropathy (Wilcox et al., 2013; Desouza et al., 2014) and chronic back pain (Mansour et al., 2013). This last study is noteworthy, as it followed recent onset back pain patients over time and found that a distinct pattern of WM abnormalities at baseline was predictive of pain persistence over one year. This study highlights the potential of using diffusion MRI to assess brain structural predisposition for developing chronic pain.

In conclusion, FM patients presented abnormalities in several WM tracts compared to controls. The affected areas serve as connectivity pathways for several cortical areas serving diverse roles including sensorimotor and cognitive functions. Although a causal pathway cannot be inferred from this cross-sectional data, it provides further evidence for CNS involvement in FM pathophysiology.

Figures

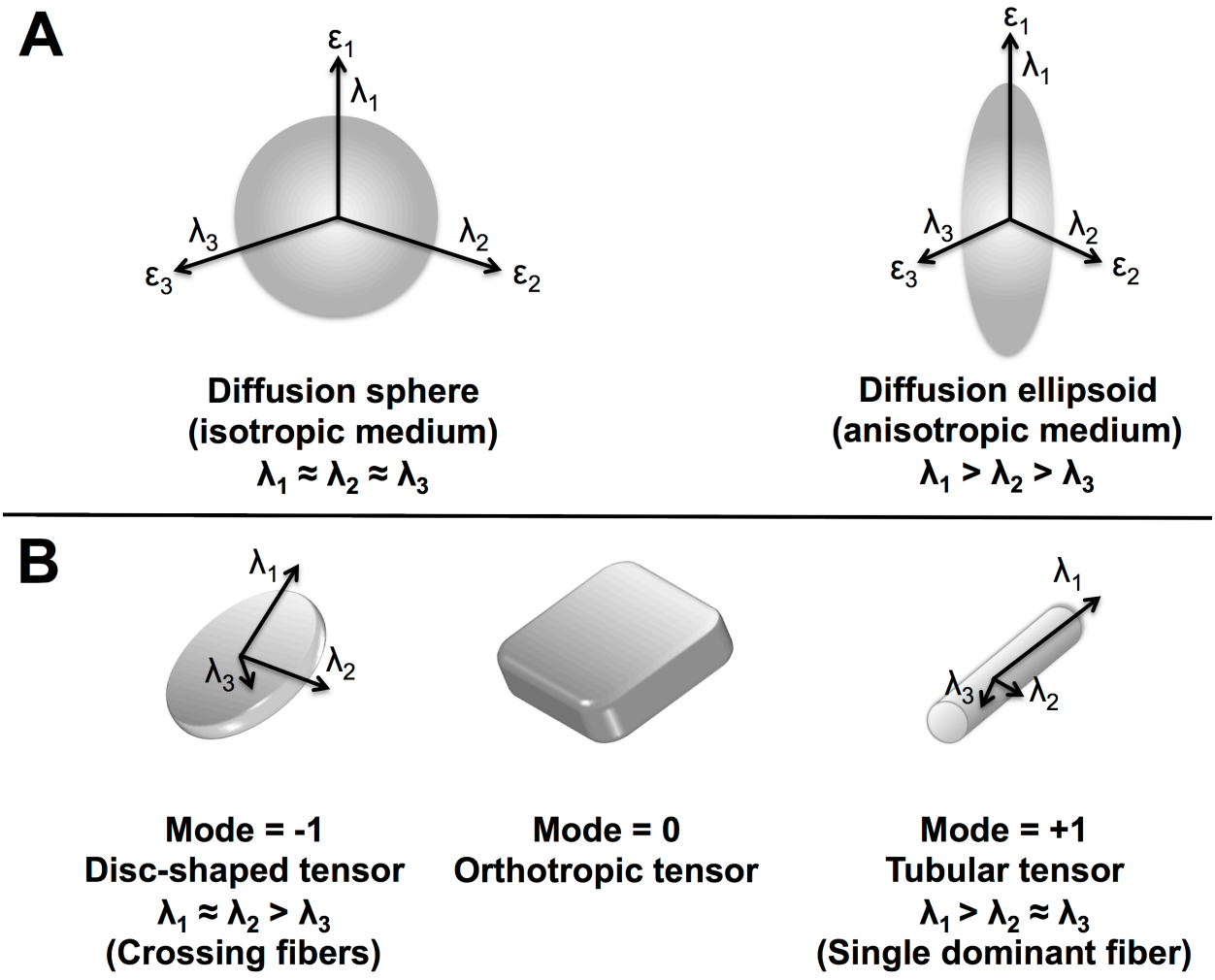

Figure 2.1. Diffusion tensor model and associated measures. A: Depiction of diffusion sphere and diffusion ellipsoid, with its respective eigenvectors and eigenvalues; B: Mode of anisotropy and its relation to the geometric shape of the tensor.

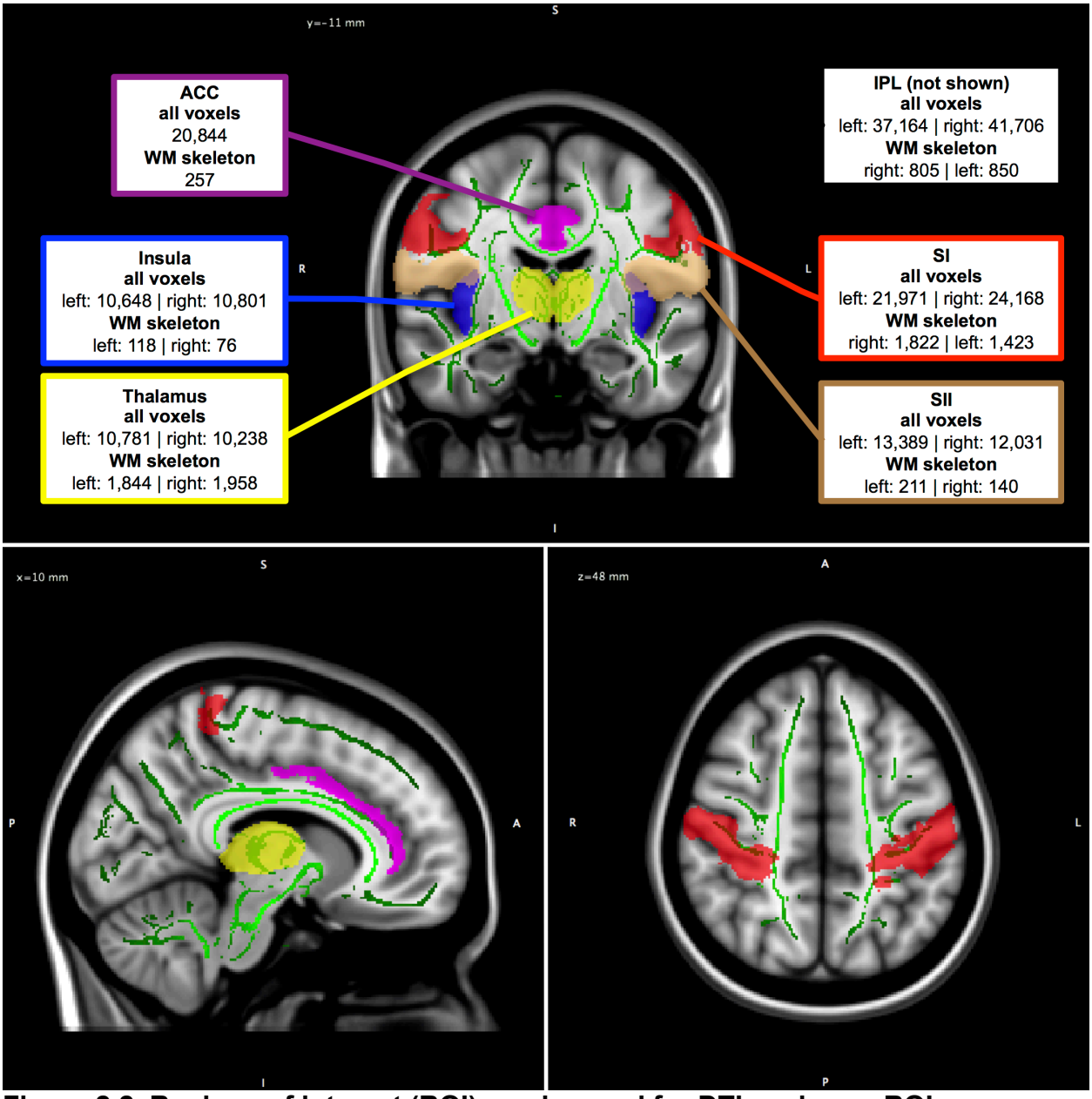

Figure 2.2. Regions of interest (ROI) masks used for DTI analyses. ROIs are shown in coronal view with their respective total and white matter skeleton only sizes (in voxels) (top panel). Sagittal view (bottom left) shows the thalamus (yellow), SI (red) and ACC (purple), while an axial view (bottom right) shows SI bilaterally (red). WM skeleton is represented by green lines. Voxel size = 1 mm^3.

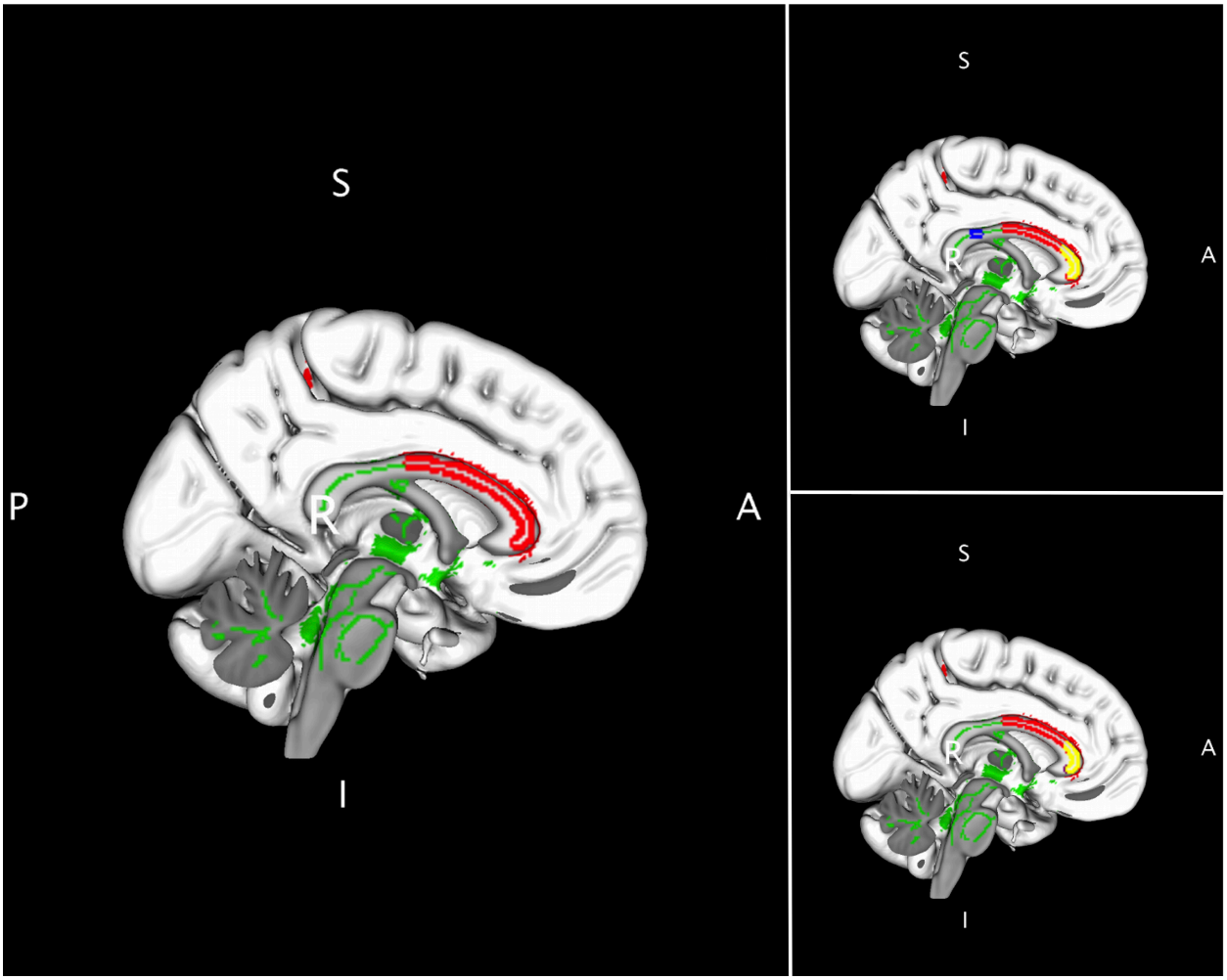

Figure 2.3. TBSS voxelwise results for between-group differences overlaid in 3D MNI brain template shown in sagittal view, highlighting the corpus callosum. Relative to controls, left panel shows FA reduction for patients (red); top right panel shows RD increase for patients (blue); bottom right panel shows MD increase for patients (purple). Right panels also show the FA maps (red), and overlap between FA and RD or MD in the respective panels is represented in yellow. WM skeleton is represented by green lines. A = anterior, P = posterior, S = superior, I = inferior, R = right.

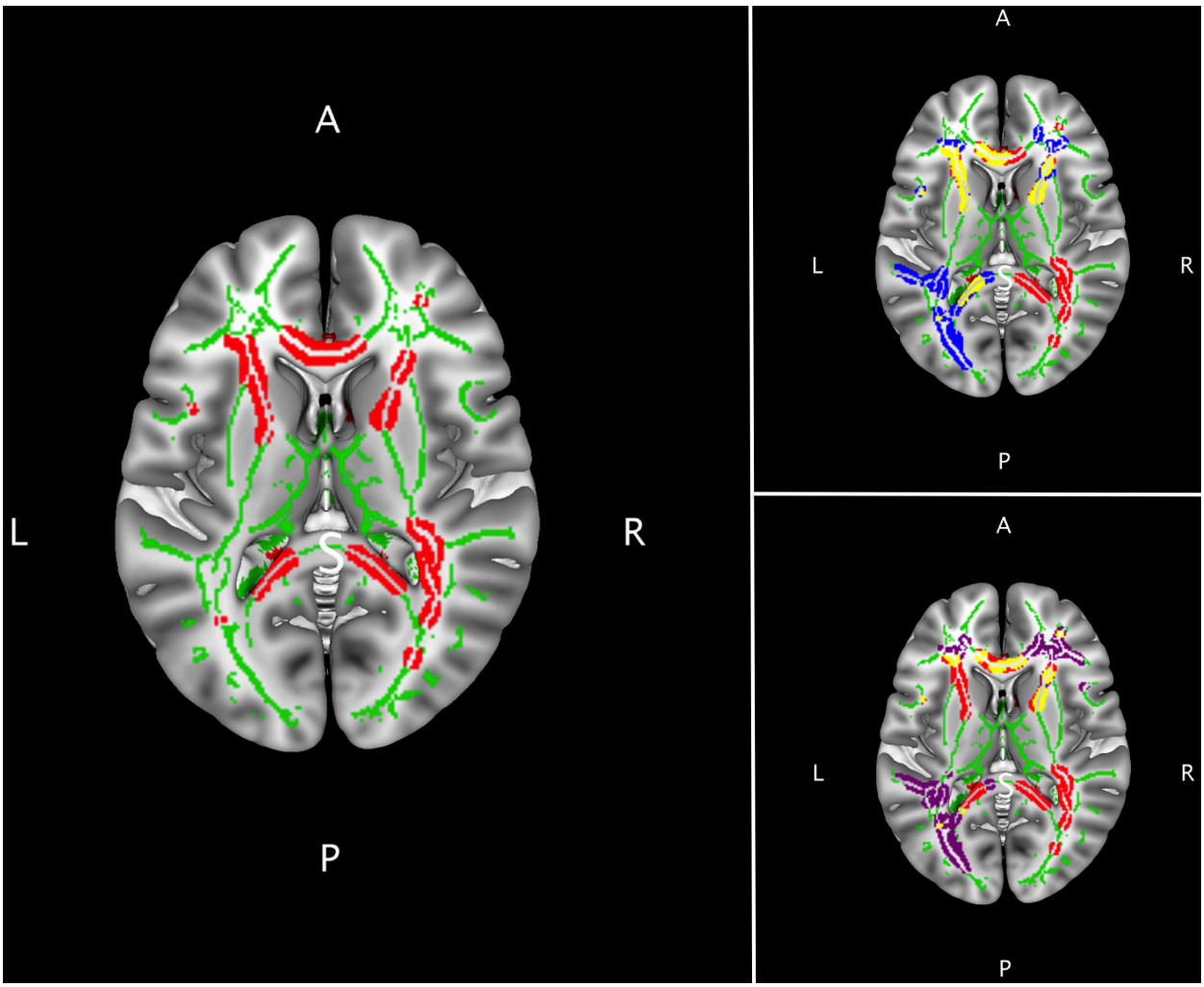

Figure 2.4. TBSS voxelwise results for between-group differences overlaid in 3D MNI brain template shown in axial view, highlighting the corpus callosum and internal capsule. Relative to controls, left panel shows FA reduction for patients (red); top right panel shows RD increase for patients (blue); bottom right panel shows MD increase for patients (purple). Right panels also show the FA maps (red), and overlap between FA and RD or MD in the respective panels is represented in yellow. WM skeleton is represented by green lines. A = anterior, P = posterior, L = left, R = right.

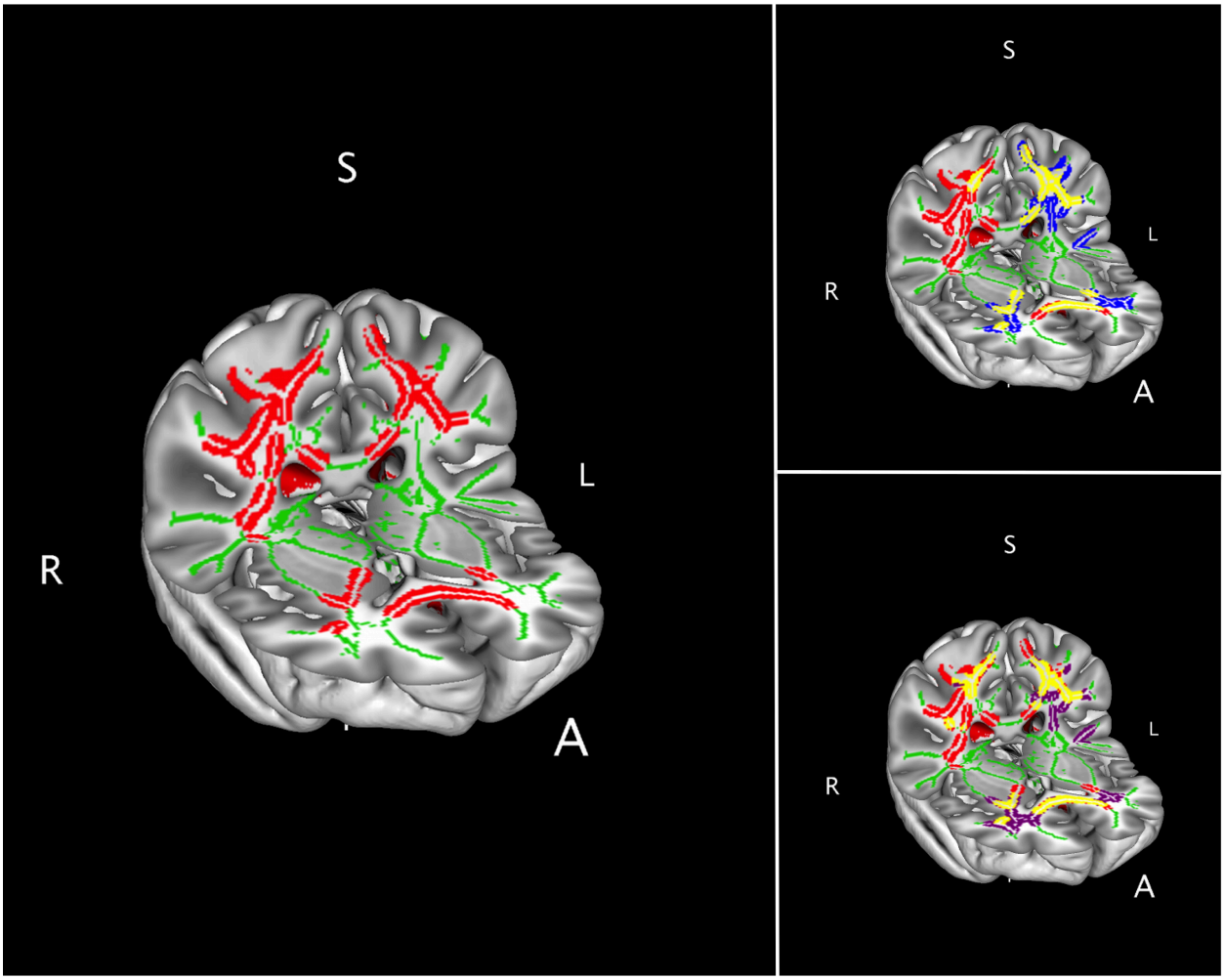

Figure 2.5. TBSS voxelwise results for between-group differences overlaid in 3D MNI brain template shown in axio-coronal view, highlighting the corticospinal tracts. Relative to controls, left panel shows FA reduction for patients (red); top right panel shows RD increase for patients (blue); bottom right panel shows MD increase for patients (purple). Right panels also show the FA maps (red), and overlap between FA and RD or MD in the respective panels is represented in yellow. WM skeleton is represented by green lines. A = anterior, S = superior, L = left, R = right.

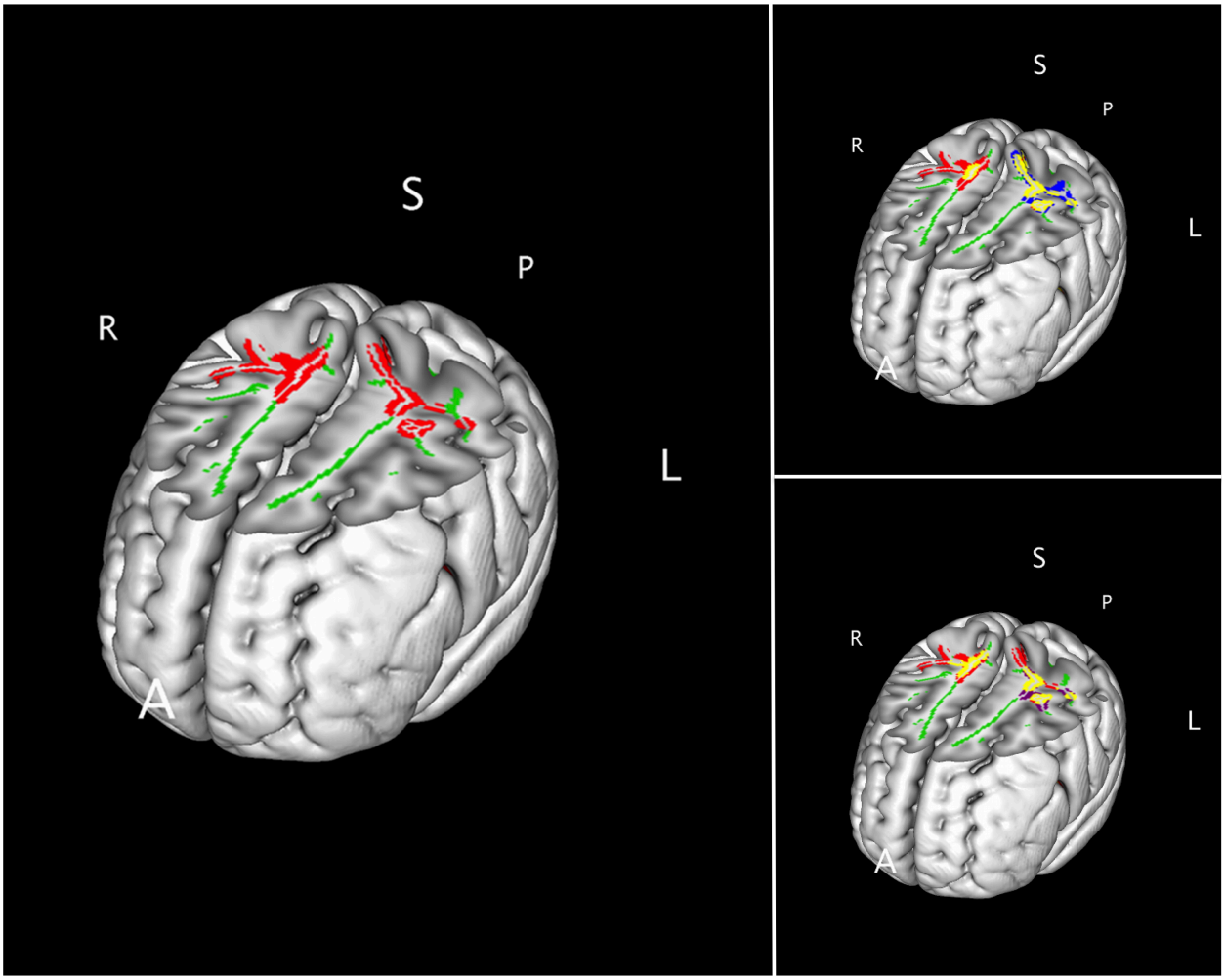

Figure 2.6. TBSS voxelwise results for between-group differences overlaid in 3D MNI brain template shown in axio-coronal view, highlighting the white matter adjacent to SI and M1. Relative to controls, left panel shows FA reduction for patients (red); top right panel shows RD increase for patients (blue); bottom right panel shows MD increase for patients (purple). Right panels also show the FA maps (red), and overlap between FA and RD or MD in the respective panels is represented in yellow. WM skeleton is represented by green lines. A = anterior, P = posterior, S = superior, L = left, R = right.

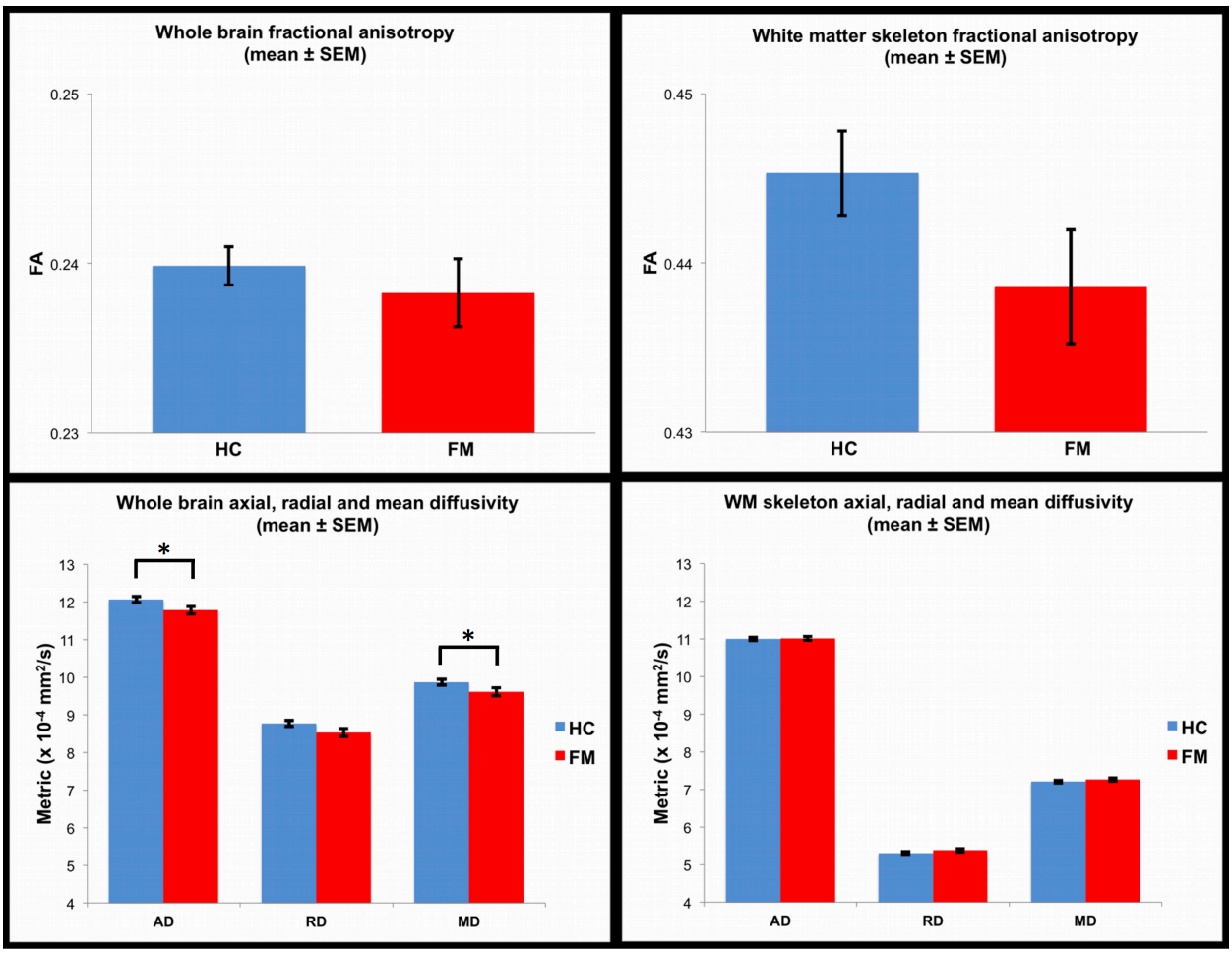

Figure 2.7. DTI metrics mean values for whole brain and WM skeleton voxels. Left panel shows whole brain FA (top) and AD, RD, and MD values (bottom). Mean values for WM skeleton voxels are depicted on the right panels for FA (top) and AD, RD, and MD (bottom). * = $p < 0.05$.

Tables

Table 2.1. Locations with lower fractional anisotropy in FM patients compared to controls.

Location	Cluster(s) size (voxels sum)	T statistic	MNI coordinates (mm) X	Y	Z
Corticospinal tract right	2,305	4.55	20	-30	49
SI / M1 right	-	-	20	-34	53
CC splenium	2,729	3.81	17	-46	19
genu	-	-	-4	28	0
body	-	-	-10	2	28
Anterior IC / CR left	709	4.25	-21	11	14
right	431	4.86	14	9	5
Corticospinal tract left	568	4.05	-23	-33	44
SI / M1 left	-	-	-15	-29	55
Inferior fronto-occiptal, inferior longitudinal, superior longitudinal fasciculi	1,984	3.96	37	-50	-4
	-	-	-44	0	21
	-	-	37	-36	6
Scattered	140	3.81	-34	11	21

MNI = Montreal Neurological Institute.
SI / M1 = white matter adjacent to primary somatosensory (SI) and motor (M1) cortices.
CC = corpus callosum; IC = internal capsule; CR = corona radiata. Scattered = voxels deep within white matter.

All clusters reported are significant at p-value < 0.05, voxelwise, corrected. Voxel size = 1 mm^3. T-statistic and coordinates reported for peak voxel within cluster; if a location is included in more than one cluster, the cluster with lower p-value is considered for peak voxel.

Table 2.2. DTI metrics mean values for non-skeletonised pain-related regions of interest.

		FA					AD (x 10^{-4} mm^2/s)					RD (x 10^{-4} mm^2/s)					MD (x 10^{-4} mm^2/s)				
		FM		HC			FM		HC			FM		HC			FM		HC		
ROI	Side	Mean	SD	Mean	SD	p-value†	Mean	SD	Mean	SD	p-value†	Mean	SD	Mean	SD	p-value†	Mean	SD	Mean	SD	p-value†
Thalamus	Left	0.272	0.019	0.272	0.010	n.s.	11.97	1.43	12.24	0.82	n.s.	8.38	1.41	8.59	0.78	n.s.	9.58	1.41	9.80	0.79	n.s.
	Right	0.274	0.018	0.272	0.010	n.s.	11.56	1.17	11.95	0.87	n.s.	7.94	1.15	8.28	0.82	n.s.	9.15	1.15	9.50	0.84	n.s.
SI	Left	0.221	0.011	0.224	0.008	n.s.	11.59	1.04	12.13	0.88	0.034*	8.76	0.99	9.24	0.82	0.045*	9.71	1.01	10.21	0.84	0.041*
	Right	0.216	0.012	0.220	0.007	n.s.	11.64	1.00	12.37	0.91	0.003*	8.78	0.98	9.43	0.81	0.005*	9.73	0.98	10.41	0.84	0.004*
SII	Left	0.147	0.010	0.146	0.007	n.s.	11.14	1.38	11.05	0.82	n.s.	9.26	1.32	9.23	0.80	n.s.	9.89	1.34	9.83	0.81	n.s.
	Right	0.144	0.009	0.146	0.007	n.s.	11.22	1.03	11.33	0.75	n.s.	9.30	0.98	9.38	0.71	n.s.	9.94	0.99	10.03	0.72	n.s.
Insula	Left	0.166	0.011	0.165	0.008	n.s.	11.94	0.96	12.07	0.75	n.s.	9.62	0.98	9.73	0.73	n.s.	10.40	0.97	10.51	0.74	n.s.
	Right	0.165	0.010	0.164	0.006	n.s.	11.66	0.80	11.84	0.64	n.s.	9.35	0.82	9.50	0.63	n.s.	10.12	0.81	10.28	0.63	n.s.
ACC	-	0.218	0.009	0.220	0.008	n.s.	11.91	0.65	12.10	0.58	n.s.	8.62	0.62	8.75	0.51	n.s.	9.72	0.62	9.87	0.53	n.s.
IPL	Left	0.166	0.008	0.166	0.005	n.s.	10.69	0.75	10.91	0.61	n.s.	8.52	0.73	8.72	0.59	n.s.	9.24	0.74	9.45	0.59	n.s.
	Right	0.162	0.009	0.163	0.005	n.s.	10.19	0.67	10.47	0.43	0.052	8.15	0.66	8.41	0.41	0.066	8.83	0.66	9.10	0.41	0.060

FM = fibromyalgia patients; HC = healthy controls. ROI = region of interest. Non-skeletonised ROI value is the mean of all voxels within the ROI.
FA = fractional anisotropy; AD = axial diffusivity; RD = radial diffusivity; MD = mean diffusivity.
SI = primary somatosensory cortex; SII = secondary somatosensory cortex; ACC = anterior cingulate cortex; IPL = inferior parietal lobule.

† = Analises of covariance, with age as a covariate of no interest. * = p-values < 0.05 considered significant. n.s. = not significant p-values. Results close to significance are also shown (0.05 ≤ p-values ≤ 0.075).

Table 2.3. DTI metrics mean values for white matter skeletonised pain-related regions of interest.

		FA					AD (x 10^{-4} mm^2/s)					RD (x 10^{-4} mm^2/s)					MD (x 10^{-4} mm^2/s)				
		FM		HC			FM		HC			FM		HC			FM		HC		
ROI	**Side**	**Mean**	**SD**	**Mean**	**SD**	**p-value†**	**Mean**	**SD**	**Mean**	**SD**	**p-value†**	**Mean**	**SD**	**Mean**	**SD**	**p-value†**	**Mean**	**SD**	**Mean**	**SD**	**p-value†**
Thalamus	Left	0.351	0.019	0.352	0.010	n.s.	10.74	0.54	10.82	0.32	n.s.	6.39	0.58	6.40	0.29	n.s.	7.84	0.55	7.87	0.29	n.s.
	Right	0.345	0.019	0.345	0.010	n.s.	10.91	0.49	11.08	0.40	n.s.	6.51	0.52	6.61	0.30	n.s.	7.98	0.50	8.10	0.33	n.s.
SI	Left	0.408	0.024	0.427	0.021	0.002*	10.31	0.30	10.24	0.26	n.s.	5.48	0.28	5.28	0.25	0.004*	7.09	0.24	6.93	0.24	0.016*
	Right	0.398	0.021	0.416	0.018	0.001*	10.80	0.32	10.82	0.32	n.s.	5.84	0.25	5.68	0.22	0.011*	7.49	0.23	7.39	0.23	n.s.
SII	Left	0.327	0.019	0.329	0.016	n.s.	9.27	0.40	9.24	0.31	n.s.	5.63	0.28	5.64	0.23	n.s.	6.84	0.30	6.84	0.23	n.s.
	Right	0.269	0.019	0.275	0.020	n.s.	9.66	0.35	9.57	0.46	n.s.	6.53	0.27	6.41	0.35	n.s.	7.57	0.27	7.47	0.36	n.s.
Insula	Left	0.240	0.016	0.231	0.024	n.s.	10.17	0.40	10.63	0.48	0.0003*	7.09	0.34	7.51	0.47	0.0003*	8.12	0.34	8.55	0.45	0.0001*
	Right	0.250	0.023	0.241	0.017	n.s.	10.41	0.48	10.59	0.52	n.s.	7.14	0.33	7.34	0.46	0.067	8.23	0.34	8.42	0.47	n.s.
ACC	-	0.482	0.036	0.488	0.035	n.s.	12.20	0.61	11.93	0.55	n.s.	5.43	0.38	5.26	0.38	n.s.	7.69	0.35	7.49	0.35	0.032*
IPL	Left	0.346	0.019	0.342	0.020	n.s.	10.03	0.33	9.87	0.35	n.s.	5.90	0.27	5.90	0.29	n.s.	7.27	0.27	7.22	0.29	n.s.
	Right	0.330	0.020	0.338	0.019	n.s.	9.79	0.36	9.77	0.37	n.s.	5.93	0.27	5.87	0.31	n.s.	7.22	0.26	7.17	0.32	n..s.

FM = fibromyalgia patients; HC = healthy controls. ROI = region of interest. White matter skeletonised ROI value is the mean of WM skeleton voxels only within the ROI.
FA = fractional anisotropy; AD = axial diffusivity; RD = radial diffusivity; MD = mean diffusivity.
SI = primary somatosensory cortex; SII = secondary somatosensory cortex; ACC = anterior cingulate cortex; IPL = inferior parietal lobule.

† = Analises of covariance, with age as a covariate of no interest. * = p-values < 0.05 considered significant. n.s. = not significant p-values. Results close to significance are also shown (0.05 ≤ p-values ≤ 0.075).

Table 2.4. Correlations for DTI metrics in the whole brain and white matter skeleton voxels.

		Age (years)		BMI (kg / m^2)	
Location	**Metric**	**FM**	**HC**	**FM**	**HC**
Whole brain	FA	-0.539*	n.s.	n.s.	n.s.
	AD	0.494*	0.648*	n.s.	n.s.
	RD	0.558*	0.678*	n.s.	n.s.
	MD	0.539*	0.671*	n.s.	n.s.
WM skeleton	FA	-0.465	n.s.	n.s.	n.s.
	AD	n.s.	n.s.	-0.677*	n.s.
	RD	n.s.	n.s.	-0.470*	n.s.
	MD	n.s.	n.s.	-0.607*	n.s.

FM = fibromyalgia; HC = healthy controls.
FA = fractional anisotropy; AD = axial diffusivity; RD = radial diffusivity; MD = mean diffusivity.
Correlations as measured by Pearson's correlation coefficient.
* = p-value < 0.01. n.s. = not significant p-values. Correlations close to significance are also shown (0.01 ≤ p-value ≤ 0.015).

Table 2.5. Correlations for DTI metrics for non-skeletonised pain-related regions of interest.

		Age (years)							
		FM				HC			
ROI	Side	FA	AD	RD	MD	FA	AD	RD	MD
Thalamus	Left	−	+	+	+	x	x	x	x
	Right	−	+	+	+	x	x	x	x
SI	Left	−	x	x	x	x	+	+	+
	Right	−	x	x	x	x	+	+	+
SII	Left	x	+	+	+	x	+	+	+
	Right	−	+	+	+	x	+	+	+
Insula	Left	−	+	+	+	x	x	+	+
	Right	−	+	+	+	x	+	+	+
ACC	-	x	x	x	x	x	+	+	+
IPL	Left	x	+	+	+	x	+	+	+
	Right	−	+	+	+	x	+	+	+

FM = fibromyalgia; HC = healthy controls.
FA = fractional anisotropy; AD = axial diffusivity; RD = radial diffusivity; MD = mean diffusivity.
SI = primary somatosensory cortex; SII = secondary somatosensory cortex; ACC = anterior cingulate cortex; IPL = inferior parietal lobule.
Correlations as measured by Pearson's correlation coefficient.
Plus (+) or minus (-) signs indicate positive or negative correlations at p-value < 0.01. Not significant correlations are marked by "x".

Table 2.6. Correlations for DTI metrics in FM patients only for white matter skeletonised pain-related regions of interest.

		FM							
		Age (years)				BMI (kg / m^2)			
ROI	Side	FA	AD	RD	MD	FA	AD	RD	MD
Thalamus	Left	-	+	+	+	x	x	x	x
	Right	-	+	+	+	x	-	x	x
SI	Left	x	-	x	x	x	x	x	x
	Right	x	x	x	x	x	-	-	-
SII	Left	x	x	x	x	x	-	-	-
	Right	x	x	x	x	x	x	x	x
Insula	Left	x	x	x	x	x	x	x	x
	Right	x	x	x	x	x	x	x	x
ACC	-	x	x	x	x	x	x	x	x
IPL	Left	x	x	x	x	x	-	-	-
	Right	x	x	x	x	x	x	-	-

FA = fractional anisotropy; AD = axial diffusivity; RD = radial diffusivity; MD = mean diffusivity.
SI = primary somatosensory cortex; SII = secondary somatosensory cortex; ACC = anterior cingulate cortex; IPL = inferior parietal lobule.
Correlations as measured by Pearson's correlation coefficient.
Plus (+) or minus (-) signs indicate positive or negative correlations at p-value < 0.01. Not significant correlations are marked by "x".

CHAPTER 3: ASSESSMENT OF BRAIN MACRO-STRUCTURAL CHARACTERISTICS IN FIBROMYALGIA USING HIGH-RESOLUTION T1-WEIGHTED ANATOMICAL IMAGING

Introduction

The brain is a relatively dynamic organ that can present functional and / or structural modifications in response to its various demands, so-called neuroplasticity. One such demand is persistent or chronic pain, where frequent nociceptive input can drive structural changes in the brain (May, 2008; Schmidt-Wilcke, 2008). Several studies using neuroimaging methods have provided evidence for these changes in different chronic pain conditions (Seifert and Maihofner, 2011; Smallwood et al., 2013). Based on these findings it has been proposed that chronic pain is not only a clinical symptom but a disease in its own right (Tracey and Bushnell, 2009), an opinion that has been embraced by many investigators (Doleys, 2010; Davis, 2013) but not all (Sullivan et al., 2013).

Fibromyalgia (FM) is one such chronic pain condition, for which diverse lines of investigation support central nervous system (CNS) alterations that potentially contribute to its clinical presentation (Schweinhardt et al., 2008). Studies of brain macro-structural characteristics in FM patients are relatively numerous, with the majority focusing on gray matter (GM) assessment using voxel-based morphometry (VBM) (May, 2011) and a few others reporting other measures including brain volume estimates, cortical thickness and subcortical structures shape and volumetric analyses. The results

across VBM studies show discordant findings regarding location of GM differences and even the direction of change. Possible explanations for this include small sample sizes and differences in methodology for imaging data acquisition and processing.

Our goal was to perform a comprehensive assessment of macro-structural brain features in a single, well characterized large sample of FM patients and age- and sex-matched controls. We used high-resolution anatomical MRI images to investigate different structural aspects of the brain, including volume estimates for different tissue types, GM density and volume, subcortical structures volumes, and cortical and subcortical characteristics.

Methods

Imaging acquisition parameters

Subjects were accommodated in the MRI scanner as described in chapter 1, methods section. A high-resolution T1-weighted anatomical image was acquired for each subject using a magnetization prepared rapid gradient echo (MP-RAGE) sequence (repetition time (TR) = 1,820 ms; echo time (TE) = 3.74 ms; inversion time (TI) = 900 ms; flip angle = 8º; field of view = 256 mm; 1 x1 x 1 mm^3 voxels; 160 slices acquired axially parallel to the anterior commissure-posterior commissure line; parallel imaging factor = 2 (GRAPPA)).

Imaging data processing pipelines

Processing steps for high-resolution T1-weighted anatomical images were done using two freely available neuroimaging software packages: 1) the Oxford Centre for Functional Magnetic Resonance Imaging of the Brain (FMRIB) software library (FSL v. 5.0.5) (Smith et al., 2004; Jenkinson et al., 2012) (http://fsl.fmrib.ox.ac.uk/fsl/fslwiki); and

2) Freesurfer image analysis suite v. 5.3.0 (http://surfer.nmr.mgh.harvard.edu/). Each analysis was processed using the necessary tool(s) from each software package, and are detailed below.

Anatomical images were reoriented to match the MNI brain template orientation using the FSL tool “fslreorient2std” (with exception of the input images for subcortical structure segmentation (FSL’s SIENAX) and cortical surface reconstruction (Freesurfer)). Before any further processing, all anatomical images were loaded into FSLview and visually checked for any obvious artifacts.

Brain tissue volumes estimation

Brain tissue volumes, normalized for individual head size, were estimated using the FSL tool SIENAX (Smith et al., 2002). SIENAX uses as input the reoriented high-resolution T1-weighted anatomical image and process it in a series of steps: 1) brain and skull images are extracted using the Brain Extraction Tool (BET) (Smith, 2002); 2) the brain image is affine-registered to the MNI152 standard brain template (available in FSL; http://fsl.fmrib.ox.ac.uk/fsl/fslwiki/Atlases), using the skull image to determine the registration scaling. This step calculates a volumetric scaling factor, that is used for head size normalization; 3) tissue-type segmentation with partial volume estimation is carried out (Zhang et al., 2001) to calculate total volume of brain tissue. In addition, gray matter (GM), white matter (WM), peripheral GM and ventricular cerebrospinal fluid (CSF) estimates of volumes were also computed.

Output files from SIENAX were visually checked for any problems. Volume estimates for each subject in mm^3, normalized for head size, were used for statistical testing.

Gray matter assessment via voxel-based morphometry

We used voxel-based morphometry (VBM) to assess the relative concentration of gray matter at the voxel level. This was accomplished using the validated FSL-VBM pipeline (Douaud et al., 2007) that applies an optimized VBM protocol (Good et al., 2001). The reoriented anatomical images had non-brain tissue extracted using BET, then were GM segmented prior to non-linear registration to the MNI152 standard brain template. The resulting images were averaged and flipped along the x-axis to create a left-right symmetric, study-specific GM template. Subsequently, subject's GM images were non-linearly registered to this study-specific template and "modulated" to correct for local expansion / contraction due to the non-linear component of the spatial transformation. The modulated GM images were concatenated into a 4D multi-subject image then smoothed with an isotropic Gaussian kernel with a sigma = 3 (full width at half maximum (FWHM) = 6.9 mm). The modulated, smoothed 4D multi-subject GM image was the input image for voxelwise and ROI analyses.

For voxelwise analysis, a between-group permutation-based nonparametric t-test (Nichols and Holmes, 2002) using age as a covariate of no interest was done. This test was implemented via the FSL tool "randomise" with 5,000 permutations and using the threshold-free cluster enhancement option. This option allows the detection of clusters of significant voxels with no arbitrary thresholding while controlling for family-wise error rate across space, therefore correcting for multiple comparisons (Smith and Nichols, 2009). This way, voxelwise statistics reported here were tested for significance at p-value < 0.05, corrected.

For whole brain and ROI analysis, *a priori* defined anatomical brain regions were used that are commonly activated following noxious stimulation (Peyron et al., 2000; Apkarian et al., 2005), including the thalamus, primary (SI) and secondary (SII) somatosensory cortices, the insula, and the anterior cingulate cortex (ACC) (left / right separately except ACC). The inferior parietal lobule (IPL) was also included, which is a cortical area that integrates somatosensory and visual inputs and was activated following noxious pressure stimulus to the thumbnail during stimulus-evoked BOLD fMRI in the participating FM patients and controls (unpublished data). A binary mask image was generated for each of those ROIs using three probabilistic atlases available in FSL (http://fsl.fmrib.ox.ac.uk/fsl/fslwiki/Atlases), the Harvard-Oxford cortical and subcortical atlases (Desikan et al., 2006) and the Jülich histological atlas (Eickhoff et al., 2006). From the Harvard-Oxford atlases we derived the ROI masks for right and left thalamus and insula, while the ACC mask was built as a single region; right and left SI, SII, and IPL were derived from the Jülich atlas.

For each subject, the GM density was extracted for the whole brain and ROIs and then multiplied it by the volume of each region to calculate the GM volume in mm^3.

Subcortical structures segmentation and volumetric analysis

Original anatomical images were processed using a FSL tool named “fsl_anat” (http://fsl.fmrib.ox.ac.uk/fsl/fslwiki/fsl_anat), a fully automated processing pipeline with the goal of obtaining segmentation of subcortical structures. Relevant steps for our goal included reorienting original anatomical images to the MNI brain template orientation, automatic cropping of the image, bias-field correction, linear and non-linear registration to the MNI standard brain template, non-brain tissue extraction, and finally subcortical

structure segmentation. This final step used FIRST, a FSL tool that incorporates prior anatomical information from manually segmented images from 336 data sets that includes healthy and pathological (including cases of schizophrenia and Alzheimer's disease) brains with an age range of 4-87 years (Patenaude et al., 2011). From this data, a 3D mesh model is created for each structure and fitted to the subject's image, followed by a boundary correction to convert from a mesh-based to a volumetric representation. Fifteen different subcortical structures were segmented: brainstem (includes 4^{th} ventricle), amygdala, caudate nucleus, hippocampus, nucleus accumbens, putamen, globus pallidus and thalamus (left/right separately except brainstem). Quality assessment for the processed data was done through visual check of the output images from the registration and segmentation steps.

Volume measures in mm^3 for all subcortical structures for each subject were determined and used for statistical testing.

Assessment of brain cortical and subcortical characteristics

Freesurfer image analysis suite was used to perform automated cortical surface reconstruction and volumetric segmentation of the original anatomical images for all subjects. Details of the procedures performed were previously described (Dale et al., 1999; Fischl et al., 1999a; Fischl et al., 1999b; Fischl and Dale, 2000; Fischl et al., 2001). In short, preprocessing included motion correction, intensity normalization (bias field correction), non-brain tissue removal, segmentation of subcortical WM, and separation of cerebral hemispheres. Gray / white matter and gray / CSF boundaries were identified and modeled as white matter and pial surfaces, respectively. Finally, automated topology correction and surface deformation following intensity gradients

took place to obtain cortical surface models (=mesh models from a non-uniform grid of triangles). Further processing included registration to a spherical atlas for cross-subject cortical geometry matching, and cortical parcellation into units based on the gyri / sulci structure for automated labeling (Fischl et al., 2004; Desikan et al., 2006).

The triangles forming the mesh for the cortical surface model intersect at a vertex, which has an X, Y, Z index and it is assigned a value. Distance between vertices is approximately 1 mm. Cortical measurements included thickness (vertex by vertex distance between the white and pial surfaces), area (relative to the WM surface), and volume. Gyral WM volumetric measurement was determined by using curvature landmarks and WM surface information to assign to the underlying WM the same label as the cortical parcellation unit above it, using a distance constraint of 5 mm for label expansion (Salat et al., 2009a).

For vertexwise analysis, we did between-group comparison of cortical thickness, area and volume using all subjects' cortical models sampled to a common space surface ("fsaverage"; average of nondemented 40 brains (http://freesurfer.net/fswiki/Buckner40Testing)), and smoothed on the surface with a 10 mm FWHM kernel. We used a Freesurfer tool (Qdec) to run a general linear model for group differences on each those measures using age as a covariate of no interest.

ROI analyses used cortical parcellation units that were in approximately similar spatial locations as *a priori* anatomical pain-related regions (left / right separately except ACC): postcentral gyrus (SI+SII), insula, ACC (rostral+caudal ACC), and supramarginal gyrus (IPL) (Figure 3.4 and 3.5). Measures of cortical thickness (mm), area (mm^2), and

volume (mm^3) as well as gyral WM volume (mm^3) for each ROI were used for statistical testing.

Statistical analyses

Unless otherwise noted, between-group differences were assessed using analysis of covariance with age as a covariate of no interest, with group status as independent variable and output measures of each of the aforementioned analysis pipelines as dependent variables. All statistical tests were done using SPSS v. 18, with significance thresholding of $p < 0.05$.

We also assessed associations for each of the aforementioned dependent variables with subject's clinical measures and psychosocial questionnaire scores using the Pearson's correlation coefficient "r". Correlations with p-value < 0.01 were deemed significant.

Results

Subjects demographics characteristics, clinical measures and questionnaires

A full description of the FM patients and controls is presented in chapter 1, results section.

Brain tissue volumes estimation

We assessed volumes for total brain, GM only, WM only, peripheral GM (excluding subcortical (deep) GM structures such as the basal ganglia and brainstem) and ventricular CSF (Fig. 3.1) with age as a covariate. No statistical significant differences for between-group comparisons were found (Table 3.1).

Correlations between volumes estimates and clinical variables for both groups were significant for age and GM (r for FM patients = -0.52; controls' r = -0.53) and

peripheral GM (patients' r = -0.54; controls' r = -0.59) volumes, and ventricular CSF volume was positively associated with age for patients only (r = 0.56). This implies that increased age is associated with decreases in GM and peripheral GM volumes and to increased ventricular CSF volume. BMI had a negative association with total brain volume in FM patients only (r = -0.47), and the association with GM volume was close to significance (r = -0.46; p = 0.011) but not for WM volume (r = -0.39; p = 0.34). No significant correlations for volumes estimates and psychosocial variables were found at p = 0.01.

Gray matter assessment via voxel-based morphometry

GM density was estimated in a voxel-by-voxel fashion for the subjects included in this study (Fig 3.2, top panel). Voxelwise comparison found no significant between-group differences at $p < 0.05$, corrected. The voxel with the lowest p-value (0.076) was located over the right cerebellar lobule V. We also estimated GM volume for the whole brain and for pain-related ROIs (Fig. 3.2, bottom panel). Similarly, no significant between-group differences were found (Table 3.2).

Correlational analyses showed that age was negatively correlated with GM volume in the whole brain, left SI, left SII, and in both insula and IPL bilaterally for FM patients ($-0.65 < r < -0.41$) and for controls (except left insula and left IPL) ($-0.66 < r < -0.39$). Pain duration in FM patients was negatively associated with GM volume in the left IPL (r = -0.51). Thus increased age is associated with reduced GM in both groups, while pain duration in patients is only associated with reductions of GM volume in the left IPL. No significant correlations were found between GM volume and psychosocial measures.

Subcortical structures segmentation and volumetric analyses

Following the segmentation of subcortical structures, we estimated their volumes (Table 3.3). Between-group comparisons, corrected for age, showed significant volumetric increase in the right amygdala (p-value = 0.021) while the left amygdala volume difference approached significance (p = 0.064) (Fig. 3.3).

When assessing correlations, age was negatively associated with volume of left and right thalamus (r = -0.48 and r = -0.44 respectively) and caudate nucleus (r = -0.52, r = -0.47) for FM patients. No clinical pain measures showed significant associations with subcortical structures volumes. Of the psychosocial measures, only PILL score showed a significant negative correlation with the left globus pallidus (r = -0.61; p < 0.001) and right amygdala (r = -0.47; p = 0.008) for patients. This implies that increased somatic awareness is associated with reductions in volume for these structures.

Assessment of brain cortical and subcortical characteristics

Vextexwise analysis, corrected for age, found no significant group differences for cortical thickness, area or volume in neither of the cerebral hemispheres (data not shown).

Likewise, no cortical measurements were significant for the ROI analyses (Table 3.4), with an increase of left insula area for FM patients relative to controls close to significance (p = 0.057). For gyral WM volume measurements (Table 3.5), significant volume increases in the patient group were found for the ACC (p = 0.030) and the left insula (p = 0.019, Fig. 3.6) relative to controls.

Negative correlations for age and cortical thickness were significant in the ACC, insula and supramarginal gyrus bilaterally in patients (-0.59 < r < -0.48) and controls (-

0.60 < r < -0.37) (Table 3.6). Age and cortical volume were significantly associated for FM patients only in the left insula (r = -0.47), and supramarginal gyri (left = -0.61, right = -0.47). Of the psychosocial measures, only CSQ-R ignoring pain score for patients was positively correlated with left postcentral gyrus thickness (r = 0.58) implying that patients with greater scores for this coping strategy present with increased cortical thickness in brain regions associated with somatosensory processing.

No significant associations for gyral WM volumes and demographic characteristics or clinical measures were found for either group. Somatic awareness, as measured by PILL scores, was negatively associated with bilateral supramarginal gyrus (left = -0.47, right = -0.48; both $p < 0.01$), right postcentral gyrus (r = -0.44; p = 0.015) and ACC (r = -0.47; p = 0.009) gyral WM volume (Fig. 3.7). Trait anxiety was negatively correlated with gyral WM volume in the left supramarginal gyrus (r = -0.48; p = 0.009) and right insula (r = -0.45; p = 0.012) (Fig. 3.7).

Discussion

Our findings provide an overall view of macro-structural brain features in FM patients. In line with findings described by previous studies, some of the measurements showed no significant differences compared to controls while others provide initial evidence of structural abnormalities that can help explain the symptomatology described for this condition.

Volumes estimates for total brain, total GM, total WM, peripheral GM or ventricular CSF was no different between FM patients and controls, replicating findings from others (Burgmer et al., 2009; Ceko et al., 2013; Fallon et al., 2013). Two studies reported reduced total brain and GM volumes for patients compared to controls, one

with a relatively small sample size (Kuchinad 2007) and another that used a different methodology for volumes estimation (Jensen, 2013).

VBM analysis of GM also showed no differences between groups for global GM density or pain-related ROIs. This is the most often used approach for brain structural assessment in FM, and the results reported are not always in agreement. Whole brain comparisons showed decrease of GM density / volume in several areas for FM patients as compared to controls including left thalamus, parahippocampal gyri, anterior and posterior cingulate cortices, insula, prefrontal cortical areas, left supplementary motor area and right premotor cortex (Kuchinad et al., 2007; Schmidt-Wilcke et al., 2007; Wood et al., 2009; Puri et al., 2010; Ceko et al., 2013). One study reported increases in GM for patients in the left orbitofrontal cortex, left cerebellum and striatum bilaterally (Schmidt-Wilcke et al., 2007) while another detected no group differences (Hsu et al., 2009). When assessing GM differences within ROIs, FM patients showed reduced GM volumes in bilateral hippocampus, ACC, inferior frontal gyrus, left amygdala and left insula (Lutz et al., 2008; Burgmer et al., 2009; Robinson et al., 2011) – the latter difference was shown to be present for FM patients with depression but not for those without (Hsu et al., 2009). Each of these studies reported a different set of brain regions with altered GM volume, and the most concordant finding across most of them seems to be a decrease in GM in the ACC. Recently one study showed that, by splitting FM patients into younger and older cohorts, there is restricted directionality for the GM volumes differences: only increases for the younger FM cohort and only decreases for the older cohort were found when compared to age-matched controls respectively (Ceko et al., 2013). Interestingly, GM alterations have also been shown in healthy

controls lacking habituation to noxious stimulus (Stankewitz et al., 2013) and increased pain ratings are associated with decreases in GM density (Emerson et al., 2014). Therefore interpretation of GM density / volume differences or the lack thereof between patients and controls must be made with caution.

Of the subcortical structures measured for total volume in the present study, only the amygdalae presented increased whole volume for FM patients compared to controls. A recent study using similar methodology found differences for brainstem volume but not for the amygdala (Fallon et al., 2013). One study reported a significant reduction of volume related to GM in the left amygdala (Burgmer et al., 2009) and another described a bilateral reduction for GM-related amygdala volume that did not survive multiple comparisons correction (Lutz et al., 2008). The amygdala is part of the limbic system, and it has been associated with emotions processing (Schulkin, 2006). While it is difficult to explain the discrepancies between our results and that of others, the emotional burden related to FM supported by our findings of psychosocial measures may induce neuroplastic changes in this region.

Similarly to VBM analysis of GM volume, no significant differences were found for cortical thickness, area or volume for both vertexwise and ROI analyses. This is in contrast to the results of Jensen and colleagues, who reported reduced cortical thickness for FM patients in the left rostral ACC, and gyri within the frontal and temporal lobes (Jensen et al., 2013), while younger FM patients presented increased thickness (left insula, left SII, left premotor cortex, right superior temporal and right posterior parietal cortices) and older patients reduced thickness (right premotor /SII / M1 cortices, and posterior cingulate cortex and precuneus) compared to age-matched controls

(Ceko et al., 2013). This inconsistency relative to cortical thickness measurements reflects the inconsistent findings for GM volume analysis using VBM, and it is possible that these analyses are not sufficiently sensitive to detect potential differences in the cortical mantle of FM patients.

Regional WM volumes comparisons showed increased volume for gyral WM adjacent to the ACC and left insula, and as mentioned before we found no differences for total WM volume between patients and controls. It has been suggested that WM volume loss can have specific patterns across brain space and over time in degenerative processes (Salat et al., 2009a). Our results showed increased volumes, while degenerative diseases affecting WM usually are related to volume reduction. One possible explanation is that a local inflammatory edema within these WM regions could cause a volumetric increase, and our findings of WM skeleton abnormalities within these regions may support this possibility (see chapter 2).

Correlations of an inverse association of age and several GM volume measures were not surprising, as they are widely reported in the literature (Good et al., 2001). BMI negative association with total brain volume reinforces the need to match this parameter across groups in future studies. The inverse relationship of somatic awareness and amygdala volume for FM patients is curious, especially with our finding of increased volume of this structure in patients. Replication of these findings by future studies may help clarify this paradoxical situation. Finally, somatic awareness and trait anxiety were negatively associated with the WM gyral volume associated with several pain-related brain regions. This provides initial evidence that affective symptoms of FM impact not only cortical areas but also their associated WM.

In conclusion, brain macro-structural abnormalities in FM patients seem to be unrelated to global volumetric measures of GM or WM or cortical characteristics. Regional differences for amygdala volume and gyral WM adjacent to the ACC and left insula suggest that more localized changes may be involved in this condition's pathophysiology. Future studies should investigate this possibility by using *a priori* defined anatomical regions, as well as functional ROIs derived from fMRI studies that are not restricted by anatomical boundaries.

Figures

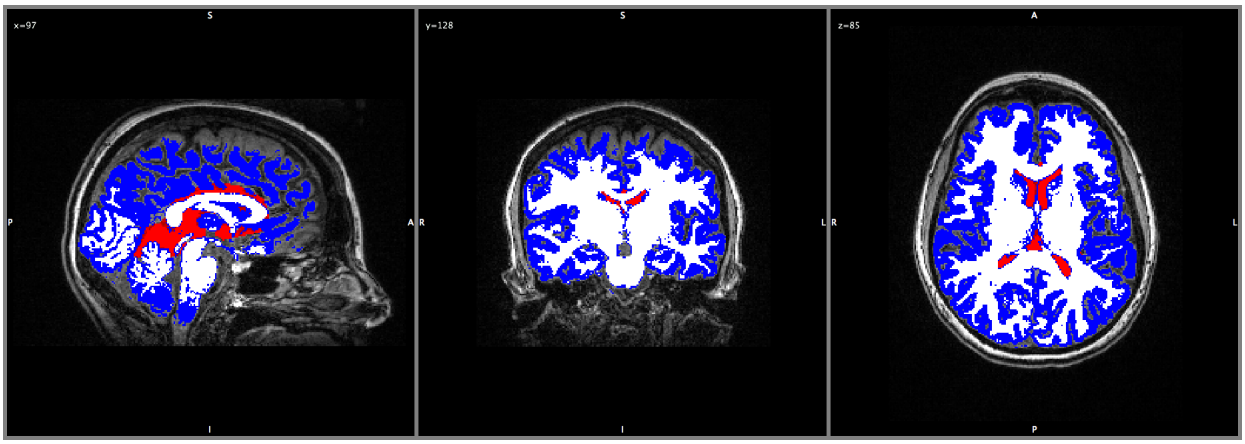

Figure 3.1. Brain segmentation for volumes estimates. GM is shown in blue, WM in white and ventricular CSF in red.

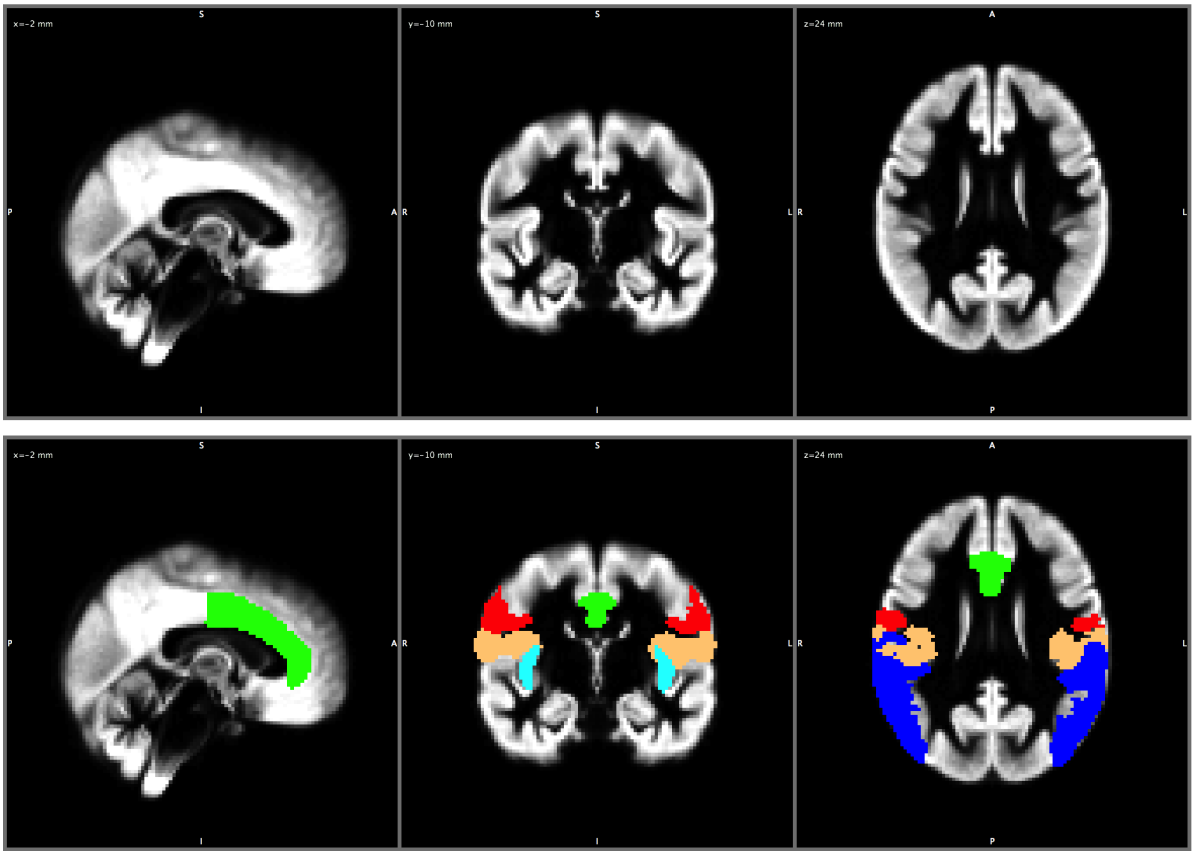

Figure 3.2. Study-specific gray matter (GM) template and regions of interest (ROI). The GM template was used for registration (top). Masks used to extract GM volume for each ROI (bottom): SI = red, SII = brown, Insula = light blue, ACC = green, IPL = dark blue.

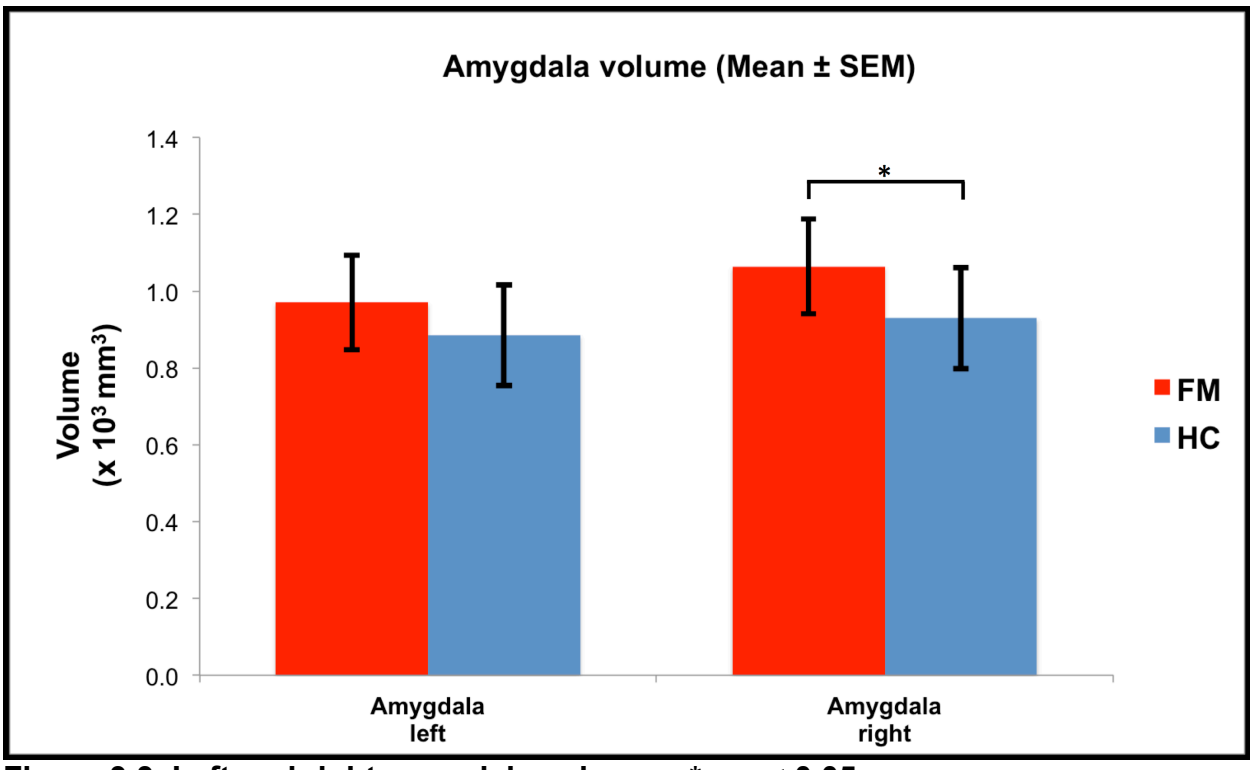

Figure 3.3. Left and right amygdala volumes. * = p < 0.05.

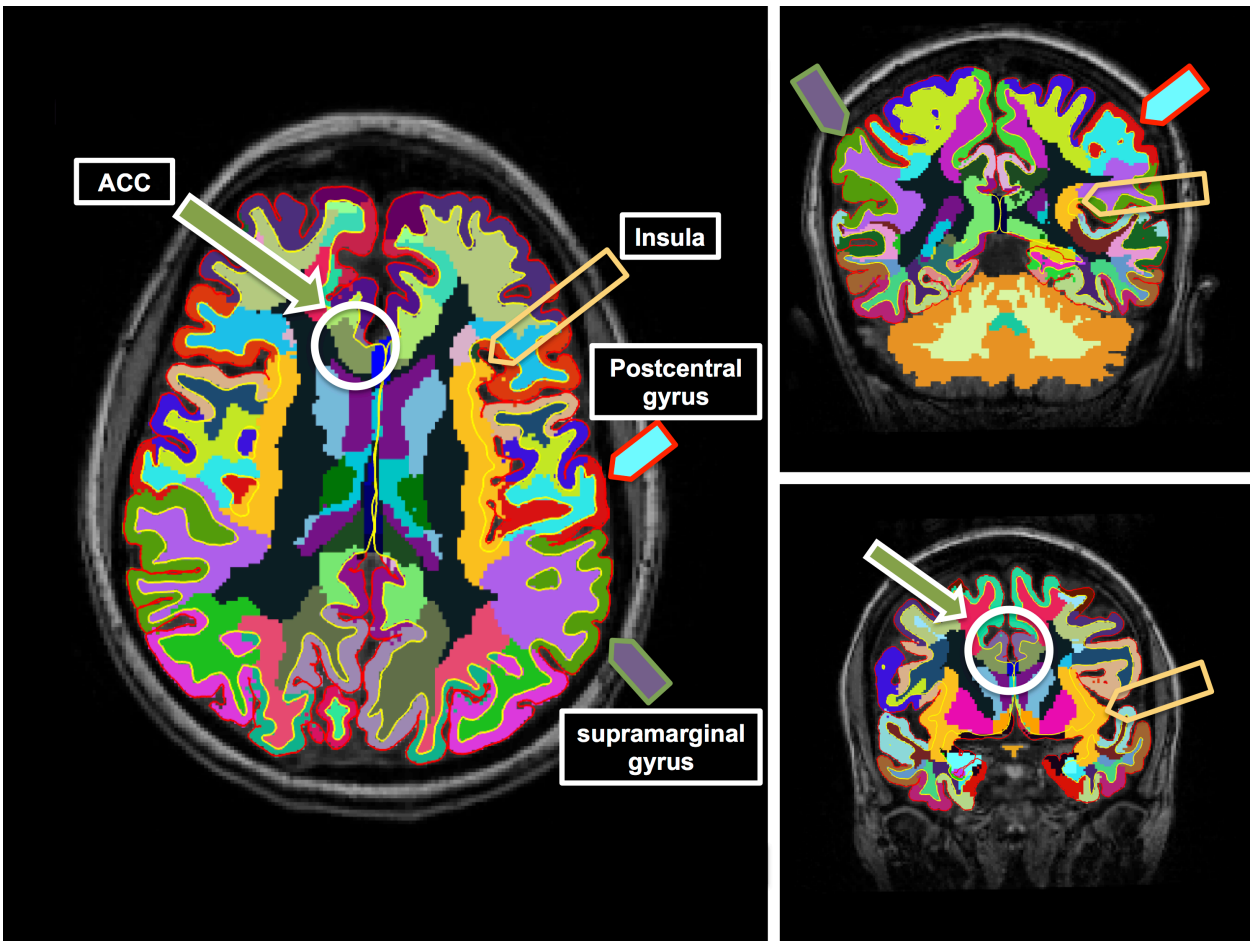

Figure 3.4. Brain cortical parcellations and subcortical regions used for region of interest (ROI) analyses in 2D view. Left panel (axial view): The outer red line corresponds to the pial surface (GM / CSF boundary) and the internal yellow line corresponds to the WM / GM boundary. Right panels show same ROIs in coronal view. Arrows used to indicate each ROI use outer / inner colors corresponding to the GM and WM portions of the ROI respectively.

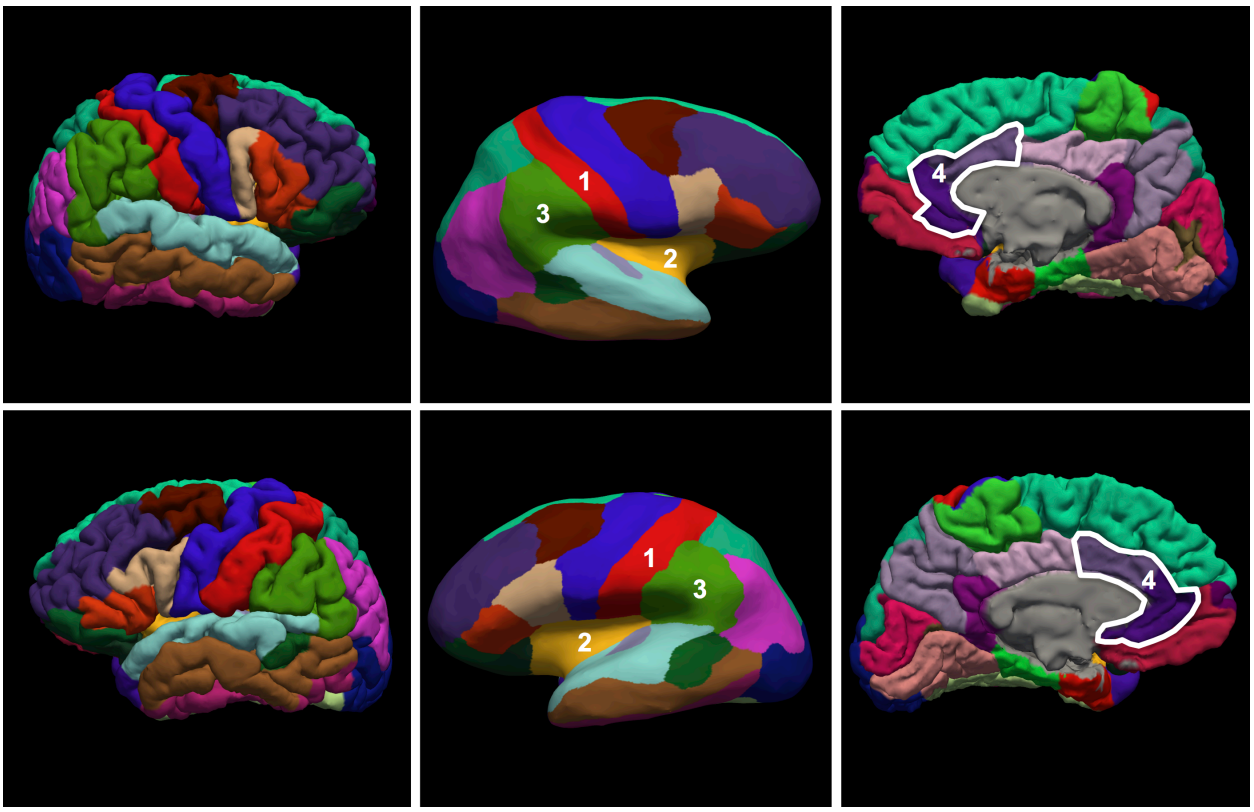

Figure 3.5. Brain cortical parcellations used for region of interest (ROI) analyses in 3D view. Left (top) and right (bottom) hemispheres are shown. Pial surface is shown in the outer panels, and the middle panel shows inflated surfaces. Numbers represent the ROIs: postcentral gyrus = 1, insula = 2; supramarginal gyrus = 3; ACC = 4.

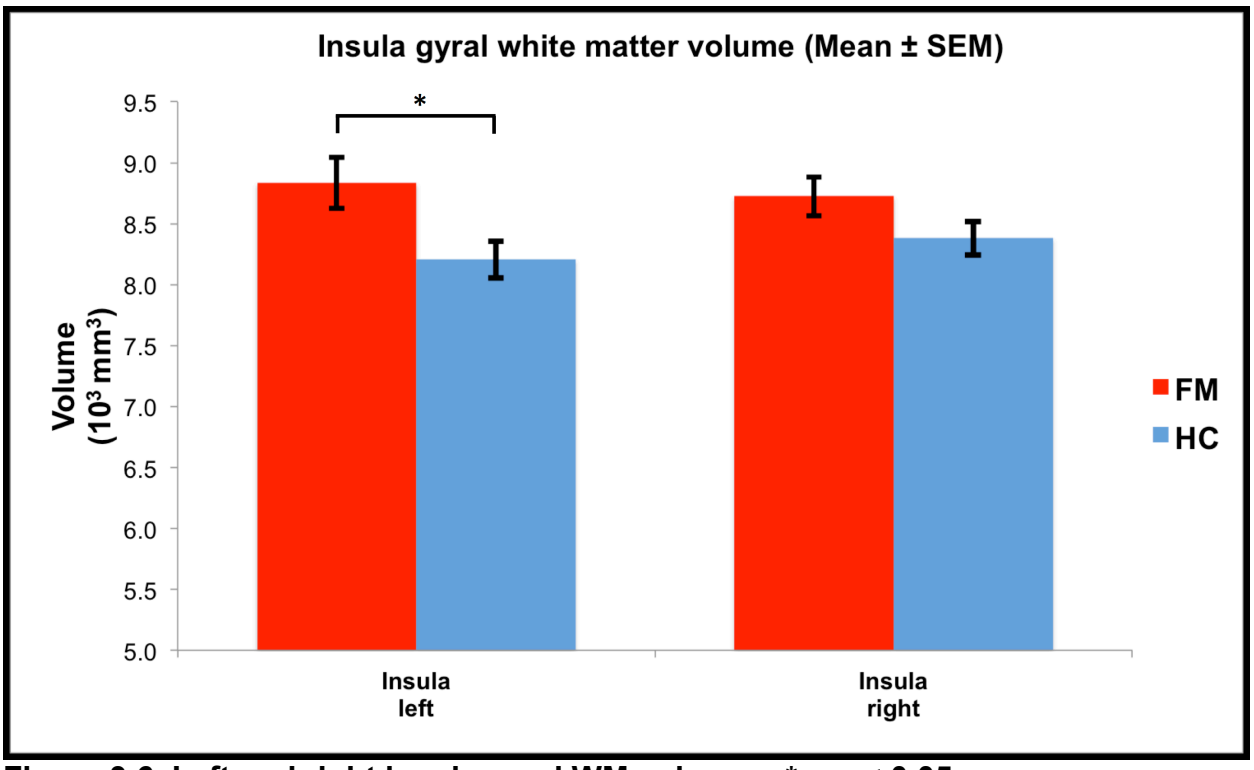

Figure 3.6. Left and right insula gyral WM volumes. * = p < 0.05.

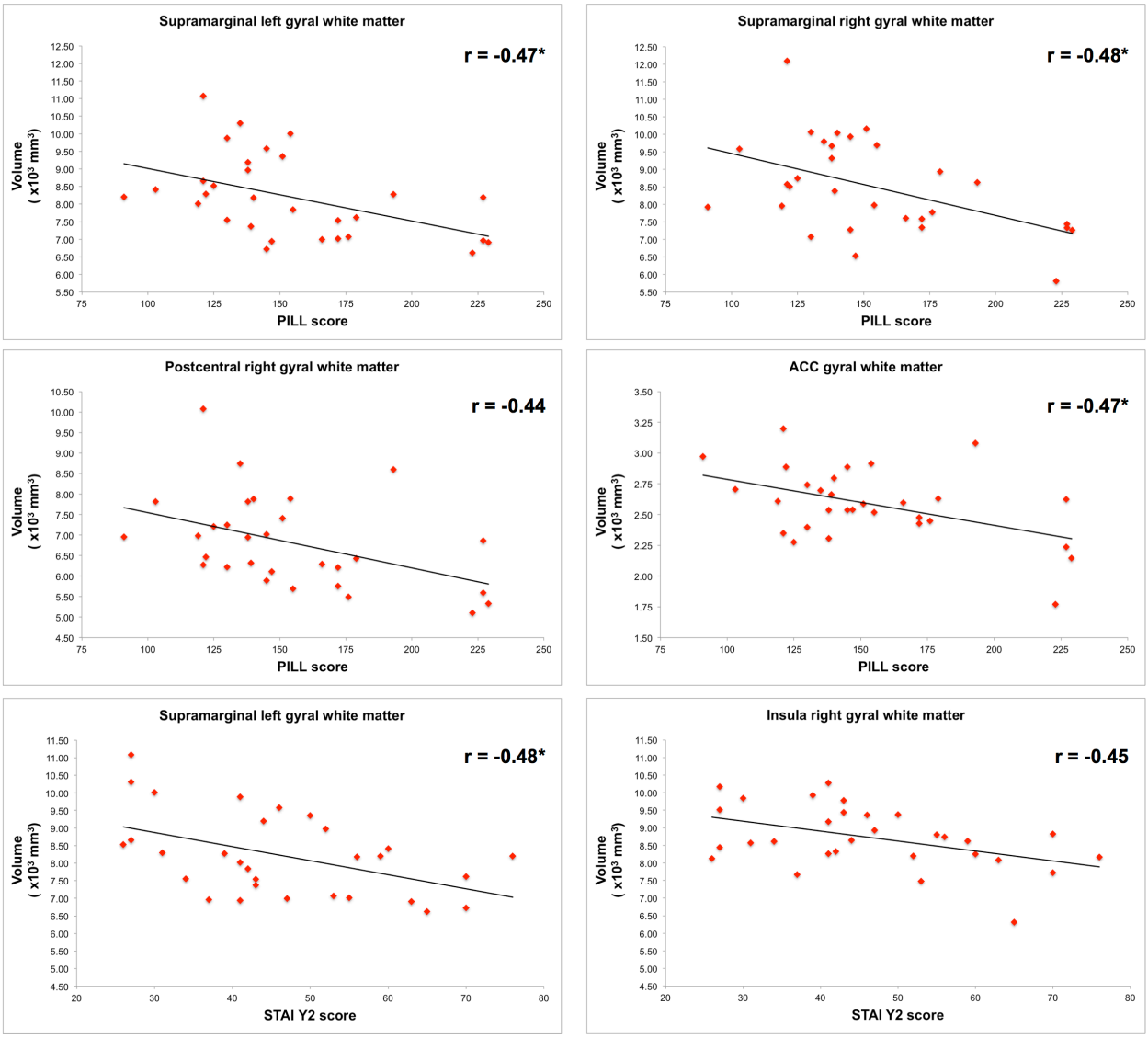

Figure 3.7. Correlations for gyral white matter volumes and questionnaire scores. * = p < 0.01. Correlations close to significance are also shown (0.01 ≤ p ≤ 0.015).

Tables

Table 3.1. Brain tissue volumes estimates.

	FM	HC	
	(x 10^3 mm^3)		p-value†
Total brain	1,489.8 (± 72.1)	1,487.9 (± 66.1)	0.916
Gray matter	767.2 (± 43.8)	774.6 (± 40.5)	0.497
White matter	722.6 (± 34.9)	713.2 (± 35.8)	0.311
Peripheral gray matter	627.4 (± 37.3)	631.7 (± 33.8)	0.637
Ventricular CSF	30.2 (± 12.2)	32.5 (± 8.8)	0.407

Mean (± SD). FM = fibromyalgia; HC = healthy controls.
Volume estimates normalised to a reference skull size (Montreal Neurological Institute brain template of 152 averaged brains).
Peripheral gray matter excludes subcortical gray matter structures.
CSF = Cerebrospinal Fluid.

†=Analises of covariance, with age as a covariate of no interest.

Table 3.2. Gray matter volume as measured by voxel-based morphometry.

		FM	HC	
		(x 10^3 mm^3)		p-value†
Whole brain		720.2 (± 29.30)	720.3 (± 28.40)	0.980
Thalamus	Left	1.9 (± 0.21)	1.9 (± 0.20)	0.529
	Righ	1.6 (± 0.16)	1.6 (± 0.18)	0.527
SI	Left	9.3 (± 0.69)	9.5 (± 0.86)	0.321
	Righ	10.1 (± 0.82)	10.3 (± 0.82)	0.416
SII	Left	6.9 (± 0.86)	6.9 (± 0.65)	0.892
	Righ	5.7 (± 0.72)	5.8 (± 0.70)	0.792
Insula	Left	5.2 (± 0.44)	5.3 (± 0.32)	0.223
	Righ	5.6 (± 0.50)	5.7 (± 0.36)	0.433
ACC	-	10.7 (± 1.52)	10.2 (± 1.23)	0.159
IPL	Left	18.7 (± 1.63)	18.8 (± 1.94)	0.945
	Righ	19.2 (± 2.05)	19.6 (± 1.96)	0.382

Mean (± SD). FM = fibromyalgia; HC = healthy controls.
SI = Primary Somatosensory Cortex; SII = Secondary Somatosensory Cortex; ACC = Anterior Cingulate Cortex; IPL = Inferior Parietal Lobule.

†=Analises of covariance, with age as a covariate of no interest.

Table 3.3. Subcortical structures volume estimates.

		FM	HC	
		(x 10^3 mm^3)		p-value†
Nucleus accumbens	Left	0.43 (± 0.12)	0.43 (± 0.10)	n.s.
	Right	0.36 (± 0.10)	0.35 (± 0.12)	n.s.
Amygdala	Left	0.97 (± 0.18)	0.89 (± 0.19)	0.064
	Right	1.06 (± 0.23)	0.93 (± 0.21)	0.021*
Globus pallidus	Left	1.73 (± 0.17)	1.70 (± 0.17)	n.s.
	Right	1.70 (± 0.18)	1.66 (± 0.17)	n.s.
Hippocampus	Left	3.13 (± 0.33)	3.15 (± 0.38)	n.s.
	Right	3.22 (± 0.32)	3.19 (± 0.42)	n.s.
Caudate nucleus	Left	3.26 (± 0.48)	3.24 (± 0.51)	n.s.
	Right	3.43 (± 0.52)	3.37 (± 0.54)	n.s.
Putamen	Left	4.67 (± 0.68)	4.63 (± 0.56)	n.s.
	Right	4.62 (± 0.57)	4.40 (± 0.57)	n.s.
Thalamus	Left	7.58 (± 0.67)	7.46 (± 0.72)	n.s.
	Right	7.41 (± 0.63)	7.22 (± 0.71)	n.s.
Brainstem	-	20.76 (± 1.98)	20.03 (± 2.38)	n.s.

Mean (± SD). FM = fibromyalgia; HC = healthy controls.

† = Analises of covariance, with age as a covariate of no interest.
* = p-values < 0.05 considered significant. n.s. = not significant p-values.
Results close to significance are also shown (0.05 ≤ p-values ≤ 0.075).

Table 3.4. Cortical thickness, area, and volume measurements.

		Thickness (mm)					Area (x10^3 mm^2)					Volume (x10^3 mm^3)				
		FM		HC			FM		HC			FM		HC		
ROI	Side	Mean	SD	Mean	SD	p-value†	Mean	SD	Mean	SD	p-value†	Mean	SD	Mean	SD	p-value†
Postcentral gyrus	Left	2.09	0.12	2.10	0.12	n.s.	3.77	0.42	3.78	0.42	n.s.	8.93	1.14	9.05	1.19	n.s.
	Right	2.06	0.11	2.07	0.12	n.s.	3.67	0.50	3.68	0.44	n.s.	8.48	1.24	8.66	1.18	n.s.
Insula	Left	2.97	0.16	3.01	0.15	n.s.	2.20	0.30	2.07	0.21	0.057	6.50	0.93	6.26	0.64	n.s.
	Right	2.95	0.20	2.99	0.18	n.s.	2.16	0.21	2.10	0.24	n.s.	6.28	0.66	6.28	0.63	n.s.
ACC	-	5.51	0.37	5.57	0.35	n.s.	1.44	0.21	1.36	0.17	n.s.	4.30	0.67	4.12	0.56	n.s.
Supramarginal gyrus	Left	2.53	0.14	2.52	0.13	n.s.	3.57	0.50	3.48	0.44	n.s.	9.92	1.51	9.64	1.37	n.s.
	Right	2.50	0.15	2.52	0.13	n.s.	3.49	0.53	3.36	0.43	n.s.	9.42	1.66	9.14	1.30	n.s.

FM = fibromyalgia patients; HC = healthy controls. ROI = region of interest. ACC = anterior cingulate cortex.

† = Analises of covariance, with age as a covariate of no interest. n.s. = not significant p-values. Results close to significance are shown (0.05 ≤ p-values ≤ 0.075).

Table 3.5. Gyral white matter volume measurements.

ROI	Side	FM ($x10^3$ mm^3)	HC ($x10^3$ mm^3)	p-value†
Postcentral gyrus	Left	6.84 (± 0.93)	6.80 (± 1.02)	n.s.
	Right	6.82 (± 1.12)	6.85 (± 0.09)	n.s.
Insula	Left	8.84 (± 1.16)	8.20 (± 0.82)	0.019
	Right	8.72 (± 0.87)	8.38 (± 0.76)	n.s.
ACC	-	5.17 (± 0.58)	4.84 (± 0.53)	0.030
Supramarginal gyrus	Left	8.21 (± 1.17)	7.98 (± 1.00)	n.s.
	Right	8.50 (± 1.34)	8.20 (± 1.21)	n.s.

FM = fibromyalgia patients; HC = healthy controls. ROI = region of interest. ACC = anterior cingulate cortex.

† = Analises of covariance, with age as a covariate of no interest. n.s. = not significant p-values.

Table 3.6. Correlations between cortical measures and age.

ROI	Side	Age (years)					
		FM			HC		
		thickness (mm)	area (mm^2)	volume (mm^3)	thickness (mm)	area (mm^2)	volume (mm^3)
Postcentral gyrus	Left	n.s.	n.s.	n.s.	n.s.	n.s.	n.s.
	Right	n.s.	n.s.	n.s.	n.s.	n.s.	n.s.
Insula	Left	-0.486*	n.s.	-0.466*	-0.597*	n.s.	n.s.
	Right	-0.532*	n.s.	-0.453	-0.398	n.s.	n.s.
ACC	-	-0.585*	n.s.	n.s.	-0.484*	n.s.	n.s.
Supramarginal gyrus	Left	-0.483*	-0.455	-0.611*	-0.557*	n.s.	-0.443
	Right	-0.535*	n.s.	-0.468*	-0.368	n.s.	n.s.

FM = fibromyalgia; HC = healthy controls.
ACC = anterior cingulate cortex.
Correlations as measured by Pearson's correlation coefficient.
* = p-value < 0.01. n.s. = not significant p-values. Correlations close to significance are also shown (0.01 ≤ p-value ≤ 0.015).

CHAPTER 4: OVERALL IMPLICATIONS OF PRESENT FINDINGS AND FUTURE DIRECTIONS

Present findings overview

This dissertation describes a comprehensive investigation of structural brain features of a well characterized sample of FM patients, using the data from age- and sex-matched healthy controls as a reference. Our findings support the view that FM pathophysiology is related to brain abnormalities, not only due to functional impairment as reported in the literature but also secondary to its structural features. One strength of this project is the use of multimodal MRI with several quality measures to assess brain structure at both micro- and macro-scales.

Cerebral tissue microscopic spatial arrangement can be probed using diffusion MRI, a non-invasive imaging technique that integrates microscopic displacement of water molecules within the brain parenchyma into a single parameter at a millimetric (voxel) resolution: the apparent diffusion coefficient (Le Bihan, 2003). Further mathematical modeling can provide even more information about diffusion directionality according to the main fibers orientation, and these can help us infer features of white matter (WM) tracts such as axonal and myelination status as well as perform *in vivo* tractography to better understand brain anatomical connectivity. We presented evidence that FM patients have abnormalities within major WM tracts connecting cortical areas that serve several functional roles, supporting an association between WM abnormalities and the multitude of symptoms commonly reported by these patients.

Recent studies show the potential of diffusion MRI to predict the transition to pain chronicity (Mansour et al., 2013), and this imaging technique can potentially help us understand brain-related risk factors for FM (see below) that might contribute to the wide variation of the clinical presentation of these patients, the so-called “fibromyalgia spectrum” (Wolfe et al., 2011).

High-resolution brain anatomical imaging provides information on the macro-structural level of the different cerebral tissues. This has been mostly used to assess gray matter (GM) volume / density in FM patients using voxel-based morphometry (VBM) with varying results. Our analyses investigated different characteristics of GM (brain volume estimates, VBM, cortical characteristics of thickness, area, and volume) and showed no significant differences between patients and controls. Our main findings were an increased volume in the amygdalae and for WM volumes adjacent to the ACC and left insula. Based on the incongruity of results for macro-structural brain abnormalities in FM reported in the literature and the present findings, it is possible that neuroplastic changes in the brains of FM patients have a more subtle and localized pattern within subcortical structures and WM.

Our findings also support a view that brain structural abnormalities in FM are better detected at the micro-scale as previously suggested (Lutz et al., 2008), at least with the available present MRI technology. Diffusion MRI is a rapidly developing imaging technique, not only related to technological advancements in data acquisition but also the mathematical modeling of diffusion and the knowledge about the biological correlates of the different diffusion-related metrics. Future research of brain structural properties in FM will greatly benefit from these developments, and likely will help further

our understanding of central pathophysiological mechanisms underlying this complex condition.

Future directions

Neuroimaging has contributed largely to our current understanding of FM (Schweinhardt et al., 2008), and will likely play an expanding role in progressing it further. Refinement of experimental designs, disease classification systems and neuroimaging tools might allow the latter to play a role in the taxonomy of functional somatic syndromes (Browning et al., 2011). Use of neuroimaging to assess specific characteristics of pain syndromes may help bridge the gap between the genetic background to the presenting phenotype of a patient (Tracey, 2011). Collection of multi-modal brain data from the same individual by means of neuroimaging techniques that provide complementary information is becoming a standard (Soares et al., 2013), an approach that we used in this study to some extent. Multi-modal brain neuroimaging provides a global overview of brain structure and function, and for complex conditions as FM this may be a fruitful way to improve the understanding of its pathophysiology. Other investigators have also realized that and successfully implemented such an approach (Ceko et al., 2013).

FM usually presents in patients with one or more comorbid conditions – the so-called functional somatic syndromes (FSS). It has been implied that this polysyndromic presentation arises from mechanisms that are common to these conditions (Yunus, 2007). However, there are also differential characteristics between these comorbid conditions that seems specific to each of them (White, 2010). Given this dichotomous situation – FSSs can be both heterogeneous and associated with each other – an

interesting strategy has been proposed: for mechanisms that are believe to be shared among different FSSs, patients presenting with two or more FSS should be included in the subject sample; on the other hand if the interest is to understand what differentiates one FSS (e.g., FM) from others, a more “clean” subject sample presenting with FM only should be sought (Warren et al., 2013). Although attractive, this approach may be difficult to implement as FM patients most commonly present with one or more comorbid FSS than not – thus making the investigation of mechanisms unique to FM problematic.

In order to investigate risk factors for a condition that might be related to its causal pathway, a longitudinal design is necessary (Grimes and Schulz, 2002). However this is difficult in rare conditions or those that do not have a clear onset such as FM. A longitudinal study with FM-free participants followed over time to detect those that develop the condition would be prohibitively expensive and taxing to the participants. An alternative approach can be suggested based on the acknowledged wide variation of FM clinical symptoms (“fibromyalgianess” (Wolfe et al., 2011)). Many studies looking to assess some type of characteristic across the lifespan do not usually follow individuals for years or decades but rather recruit a large sample of subjects representative of the age range of interest (Salat et al., 2009a; Salat et al., 2009b; Lebel et al., 2012). This strategy could be adapted to FM where a large sample of patients could be recruited across the spectrum of clinical symptomatology, i.e., from patients that fits diagnostic criteria yet have little or no comorbid conditions and are functional, to those patients that present with a plethora of symptoms and comorbidities and are functionally incapacitated. This “fibromyalgia spectrum span” approach could improve our understanding on the mechanisms that makes the burden of FM greater for a

subset of patients but not for others. Future investigations of FM using neuroimaging or other methods may benefit from such approach, with the ultimate goal of increasing our understanding of this puzzling and complex condition that deeply affects the lives of its sufferers.

REFERENCES

1. Aaron, L. A. and Buchwald, D. (2001). "A review of the evidence for overlap among unexplained clinical conditions." Ann Intern Med 134(9 Pt 2): 868-81.

2. Abbi, B. and Natelson, B. H. (2013). "Is chronic fatigue syndrome the same illness as fibromyalgia: evaluating the 'single syndrome' hypothesis." QJM 106(1): 3-9.

3. Abeles, A. M., Pillinger, M. H., Solitar, B. M. and Abeles, M. (2007). "Narrative review: the pathophysiology of fibromyalgia." Ann Intern Med 146(10): 726-34.

4. Ablin, J. N., Buskila, D., Van Houdenhove, B., Luyten, P., Atzeni, F. and Sarzi-Puttini, P. (2012). "Is fibromyalgia a discrete entity?" Autoimmun Rev 11(8): 585-8.

5. Ablin, J. N., Cohen, H. and Buskila, D. (2006). "Mechanisms of Disease: genetics of fibromyalgia." Nat Clin Pract Rheumatol 2(12): 671-8.

6. Alexander, A. L., Lee, J. E., Lazar, M. and Field, A. S. (2007). "Diffusion tensor imaging of the brain." Neurotherapeutics 4(3): 316-29.

7. Alexander, D. C. and Barker, G. J. (2005). "Optimal imaging parameters for fiber-orientation estimation in diffusion MRI." Neuroimage 27(2): 357-67.

8. Anderson, R. J., McCrae, C. S., Staud, R., Berry, R. B. and Robinson, M. E. (2012). "Predictors of clinical pain in fibromyalgia: examining the role of sleep." J Pain 13(4): 350-8.

9. Apkarian, A. V., Baliki, M. N. and Farmer, M. A. (2013). "Predicting transition to chronic pain." Curr Opin Neurol 26(4): 360-7.

10. Apkarian, A. V., Bushnell, M. C., Treede, R. D. and Zubieta, J. K. (2005). "Human brain mechanisms of pain perception and regulation in health and disease." Eur J Pain 9(4): 463-84.

11. Barsky, A. J. and Borus, J. F. (1999). "Functional somatic syndromes." Ann Intern Med 130(11): 910-21.

12. Basser, P. J. and Jones, D. K. (2002). "Diffusion-tensor MRI: theory, experimental design and data analysis - a technical review." NMR Biomed 15(7-8): 456-67.

13. Basser, P. J., Mattiello, J. and LeBihan, D. (1994a). "MR diffusion tensor spectroscopy and imaging." Biophys J 66(1): 259-67.

14. Basser, P. J., Mattiello, J. and LeBihan, D. (1994b). "Estimation of the effective self-diffusion tensor from the NMR spin echo." J Magn Reson B 103(3): 247-54.

15. Basser, P. J. and Pierpaoli, C. (1996). "Microstructural and physiological features of tissues elucidated by quantitative-diffusion-tensor MRI." J Magn Reson B 111(3): 209-19.

16. Beaulieu, C. (2009). The Biological Basis of Diffusion Anisotropy. In Diffusion MRI. Johansen-Berg, H. and Behrens, T. London, Academic Press (Elsevier)**:** 105-26.

17. Beck, A. T., Steer, R. A. and Carbin, M. G. (1988). "Psychometric properties of the Beck Depression Inventory: Twenty-five years of evaluation." Clinical Psychology Review 8(1): 77-100.

18. Beck, A. T., Ward, C. H., Mendelson, M., Mock, J. and Erbaugh, J. (1961). "An inventory for measuring depression." Arch Gen Psychiatry 4: 561-71.

19. Behrens, T. E., Woolrich, M. W., Jenkinson, M., Johansen-Berg, H., Nunes, R. G., Clare, S., Matthews, P. M., Brady, J. M. and Smith, S. M. (2003). "Characterization and propagation of uncertainty in diffusion-weighted MR imaging." Magn Reson Med 50(5): 1077-88.

20. Benveniste, H., Hedlund, L. W. and Johnson, G. A. (1992). "Mechanism of detection of acute cerebral ischemia in rats by diffusion-weighted magnetic resonance microscopy." Stroke 23(5): 746-54.

21. Berger, A., Dukes, E., Martin, S., Edelsberg, J. and Oster, G. (2007). "Characteristics and healthcare costs of patients with fibromyalgia syndrome." Int J Clin Pract 61(9): 1498-508.

22. Broman, J. (1994). "Neurotransmitters in subcortical somatosensory pathways." Anat Embryol (Berl) 189(3): 181-214.

23. Browning, M., Fletcher, P. and Sharpe, M. (2011). "Can neuroimaging help us to understand and classify somatoform disorders? A systematic and critical review." Psychosom Med 73(2): 173-84.

24. Burgmer, M., Gaubitz, M., Konrad, C., Wrenger, M., Hilgart, S., Heuft, G. and Pfleiderer, B. (2009). "Decreased gray matter volumes in the cingulo-frontal cortex and the amygdala in patients with fibromyalgia." Psychosom Med 71(5): 566-73.

25. Burgmer, M., Petzke, F., Giesecke, T., Gaubitz, M., Heuft, G. and Pfleiderer, B. (2011). "Cerebral activation and catastrophizing during pain anticipation in patients with fibromyalgia." Psychosom Med 73(9): 751-9.

26. Busch, A. J., Webber, S. C., Brachaniec, M., Bidonde, J., Bello-Haas, V. D., Danyliw, A. D., Overend, T. J., Richards, R. S., Sawant, A. and Schachter, C. L. (2011). "Exercise therapy for fibromyalgia." Curr Pain Headache Rep 15(5): 358-67.

27. Buskila, D. and Neumann, L. (2005). "Genetics of fibromyalgia." Curr Pain Headache Rep 9(5): 313-5.

28. Buysse, D. J., Reynolds, C. F., 3rd, Monk, T. H., Berman, S. R. and Kupfer, D. J. (1989). "The Pittsburgh Sleep Quality Index: a new instrument for psychiatric practice and research." Psychiatry Res 28(2): 193-213.

29. Casale, R., Cazzola, M., Arioli, G., Gracely, R. H., Ceccherelli, F., Atzeni, F., Stisi, S., Cassisi, G., Altomonte, L., Alciati, A., Leardini, G., Gorla, R., Marsico, A., Torta, R., Giamberardino, M. A., Buskila, D., Spath, M., Marinangeli, F., Bazzichi, L., Di Franco, M., Biasi, G., Salaffi, F., Carignola, R. and Sarzi-Puttini, P. (2008). "Non pharmacological treatments in fibromyalgia." Reumatismo 60 Suppl 1: 59-69.

30. Ceko, M., Bushnell, M. C., Fitzcharles, M. A. and Schweinhardt, P. (2013). "Fibromyalgia interacts with age to change the brain." Neuroimage Clin 3: 249-60.

31. Cervero, F. (2009). Pain Theories. In Science of Pain. Basbaum, A. I. and Bushnell, M. C. Amsterdam; Boston, Elsevier: 5-10.

32. Cervero, F. and Laird, J. (1991). "One pain or many pains?" Physiology 6(6): 268-273.

33. Chapman, L. J. and Chapman, J. P. (1987). "The measurement of handedness." Brain Cogn 6(2): 175-83.

34. Clauw, D. J. (2009). "Fibromyalgia: an overview." Am J Med 122(12 Suppl): S3-S13.

35. Cohen, S., Kamarck, T. and Mermelstein, R. (1983). "A global measure of perceived stress." J Health Soc Behav 24(4): 385-96.

36. Cook, D. B., Lange, G., Ciccone, D. S., Liu, W. C., Steffener, J. and Natelson, B. H. (2004). "Functional imaging of pain in patients with primary fibromyalgia." J Rheumatol 31(2): 364-78.

37. Cook, D. B., Stegner, A. J. and McLoughlin, M. J. (2007). "Imaging pain of fibromyalgia." Curr Pain Headache Rep 11(3): 190-200.

38. Craig, A. D. (2009). "How do you feel--now? The anterior insula and human awareness." Nat Rev Neurosci 10(1): 59-70.

39. Croft, P., Dunn, K. M. and Von Korff, M. (2007). "Chronic pain syndromes: you can't have one without another." Pain 131(3): 237-8.

40. Dale, A. M., Fischl, B. and Sereno, M. I. (1999). "Cortical surface-based analysis. I. Segmentation and surface reconstruction." Neuroimage 9(2): 179-94.

41. Davis, K. D. (2011). "Neuroimaging of pain: what does it tell us?" Curr Opin Support Palliat Care 5(2): 116-21.

42. Davis, K. D. (2013). "Is chronic pain a disease? Evaluating pain and nociception through self-report and neuroimaging." J Pain 14(4): 332-3.

43. Desikan, R. S., Segonne, F., Fischl, B., Quinn, B. T., Dickerson, B. C., Blacker, D., Buckner, R. L., Dale, A. M., Maguire, R. P., Hyman, B. T., Albert, M. S. and Killiany, R. J. (2006). "An automated labeling system for subdividing the human

cerebral cortex on MRI scans into gyral based regions of interest." Neuroimage 31(3): 968-80.

44. Desouza, D. D., Hodaie, M. and Davis, K. D. (2014). "Abnormal trigeminal nerve microstructure and brain white matter in idiopathic trigeminal neuralgia." Pain 155(1): 37-44.

45. Doleys, D. M. (2010). "How neuroimaging studies have challenged us to rethink: is chronic pain a disease?" J Pain 11(4): 399-400.

46. Douaud, G., Smith, S., Jenkinson, M., Behrens, T., Johansen-Berg, H., Vickers, J., James, S., Voets, N., Watkins, K., Matthews, P. M. and James, A. (2007). "Anatomically related grey and white matter abnormalities in adolescent-onset schizophrenia." Brain 130(Pt 9): 2375-86.

47. Ehrlich, G. E. (2003). "Fibromyalgia, a virtual disease." Clin Rheumatol 22(1): 8-11.

48. Eickhoff, S. B., Heim, S., Zilles, K. and Amunts, K. (2006). "Testing anatomically specified hypotheses in functional imaging using cytoarchitectonic maps." Neuroimage 32(2): 570-82.

49. Emerson, N. M., Zeidan, F., Lobanov, O. V., Hadsel, M. S., Martucci, K. T., Quevedo, A. S., Starr, C. J., Nahman-Averbuch, H., Weissman-Fogel, I., Granovsky, Y., Yarnitsky, D. and Coghill, R. C. (2014). "Pain sensitivity is inversely related to regional grey matter density in the brain." Pain 155(3): 566-73.

50. Ennis, D. B. and Kindlmann, G. (2006). "Orthogonal tensor invariants and the analysis of diffusion tensor magnetic resonance images." Magn Reson Med 55(1): 136-46.

51. Fallon, N., Alghamdi, J., Chiu, Y., Sluming, V., Nurmikko, T. and Stancak, A. (2013). "Structural alterations in brainstem of fibromyalgia syndrome patients correlate with sensitivity to mechanical pressure." Neuroimage Clin 3: 163-70.

52. Fischl, B. and Dale, A. M. (2000). "Measuring the thickness of the human cerebral cortex from magnetic resonance images." Proc Natl Acad Sci U S A 97(20): 11050-5.

53. Fischl, B., Liu, A. and Dale, A. M. (2001). "Automated manifold surgery: constructing geometrically accurate and topologically correct models of the human cerebral cortex." IEEE Trans Med Imaging 20(1): 70-80.

54. Fischl, B., Sereno, M. I. and Dale, A. M. (1999a). "Cortical surface-based analysis. II: Inflation, flattening, and a surface-based coordinate system." Neuroimage 9(2): 195-207.

55. Fischl, B., Sereno, M. I., Tootell, R. B. and Dale, A. M. (1999b). "High-resolution intersubject averaging and a coordinate system for the cortical surface." Hum Brain Mapp 8(4): 272-84.

56. Fischl, B., van der Kouwe, A., Destrieux, C., Halgren, E., Segonne, F., Salat, D. H., Busa, E., Seidman, L. J., Goldstein, J., Kennedy, D., Caviness, V., Makris, N., Rosen, B. and Dale, A. M. (2004). "Automatically parcellating the human cerebral cortex." Cereb Cortex 14(1): 11-22.

57. Fung, S. H., Roccatagliata, L., Gonzalez, R. G. and Schaefer, P. W. (2011). "MR diffusion imaging in ischemic stroke." Neuroimaging Clin N Am 21(2): 345-77, xi.

58. Gauvain, K. M., McKinstry, R. C., Mukherjee, P., Perry, A., Neil, J. J., Kaufman, B. A. and Hayashi, R. J. (2001). "Evaluating pediatric brain tumor cellularity with diffusion-tensor imaging." AJR Am J Roentgenol 177(2): 449-54.

59. Giesecke, T., Gracely, R. H., Williams, D. A., Geisser, M. E., Petzke, F. W. and Clauw, D. J. (2005). "The relationship between depression, clinical pain, and experimental pain in a chronic pain cohort." Arthritis Rheum 52(5): 1577-84.

60. Good, C. D., Johnsrude, I. S., Ashburner, J., Henson, R. N., Friston, K. J. and Frackowiak, R. S. (2001). "A voxel-based morphometric study of ageing in 465 normal adult human brains." Neuroimage 14(1 Pt 1): 21-36.

61. Gowers, W. R. (1904). "A Lecture on Lumbago: Its Lessons and Analogues: Delivered at the National Hospital for the Paralysed and Epileptic." Br Med J 1(2246): 117-21.

62. Gracely, R. H. and Ambrose, K. R. (2011). "Neuroimaging of fibromyalgia." Best Pract Res Clin Rheumatol 25(2): 271-84.

63. Gracely, R. H., Geisser, M. E., Giesecke, T., Grant, M. A., Petzke, F., Williams, D. A. and Clauw, D. J. (2004). "Pain catastrophizing and neural responses to pain among persons with fibromyalgia." Brain 127(Pt 4): 835-43.

64. Gracely, R. H., McGrath, F. and Dubner, R. (1978). "Ratio scales of sensory and affective verbal pain descriptors." Pain 5(1): 5-18.

65. Gracely, R. H., Petzke, F., Wolf, J. M. and Clauw, D. J. (2002). "Functional magnetic resonance imaging evidence of augmented pain processing in fibromyalgia." Arthritis Rheum 46(5): 1333-43.

66. Graham, W. (1953). "The fibrosits syndrome." Bull Rheum Dis 3(8): 33-4.

67. Grimes, D. A. and Schulz, K. F. (2002). "An overview of clinical research: the lay of the land." Lancet 359(9300): 57-61.

68. Gwilym, S. E., Filippini, N., Douaud, G., Carr, A. J. and Tracey, I. (2010). "Thalamic atrophy associated with painful osteoarthritis of the hip is reversible after arthroplasty: a longitudinal voxel-based morphometric study." Arthritis Rheum 62(10): 2930-40.

69. Hannonen, P. (2013). "Fibromyalgia-worth a diagnosis?" Ann Med 45(1): 1-3.

70. Harris, R. E. and Clauw, D. J. (2006). "How do we know that the pain in fibromyalgia is "real"?" Curr Pain Headache Rep 10(6): 403-7.

71. Hasan, K. M., Walimuni, I. S., Abid, H. and Hahn, K. R. (2011). "A review of diffusion tensor magnetic resonance imaging computational methods and software tools." Comput Biol Med 41(12): 1062-72.

72. Hsu, E. S. (2011). "Acute and chronic pain management in fibromyalgia: updates on pharmacotherapy." Am J Ther 18(6): 487-509.

73. Hsu, J. L., Van Hecke, W., Bai, C. H., Lee, C. H., Tsai, Y. F., Chiu, H. C., Jaw, F. S., Hsu, C. Y., Leu, J. G., Chen, W. H. and Leemans, A. (2010). "Microstructural white matter changes in normal aging: a diffusion tensor imaging study with higher-order polynomial regression models." Neuroimage 49(1): 32-43.

74. Hsu, M. C., Harris, R. E., Sundgren, P. C., Welsh, R. C., Fernandes, C. R., Clauw, D. J. and Williams, D. A. (2009). "No consistent difference in gray matter volume between individuals with fibromyalgia and age-matched healthy subjects when controlling for affective disorder." Pain 143(3): 262-7.

75. Jellison, B. J., Field, A. S., Medow, J., Lazar, M., Salamat, M. S. and Alexander, A. L. (2004). "Diffusion tensor imaging of cerebral white matter: a pictorial review of physics, fiber tract anatomy, and tumor imaging patterns." AJNR Am J Neuroradiol 25(3): 356-69.

76. Jenkinson, M., Beckmann, C. F., Behrens, T. E., Woolrich, M. W. and Smith, S. M. (2012). "Fsl." Neuroimage 62(2): 782-90.

77. Jensen, K. B., Kosek, E., Petzke, F., Carville, S., Fransson, P., Marcus, H., Williams, S. C., Choy, E., Giesecke, T., Mainguy, Y., Gracely, R. and Ingvar, M. (2009). "Evidence of dysfunctional pain inhibition in Fibromyalgia reflected in rACC during provoked pain." Pain 144(1-2): 95-100.

78. Jensen, K. B., Petzke, F., Carville, S., Fransson, P., Marcus, H., Williams, S. C., Choy, E., Mainguy, Y., Gracely, R., Ingvar, M. and Kosek, E. (2010). "Anxiety and depressive symptoms in fibromyalgia are related to poor perception of health but not to pain sensitivity or cerebral processing of pain." Arthritis Rheum 62(11): 3488-95.

79. Jensen, K. B., Srinivasan, P., Spaeth, R., Tan, Y., Kosek, E., Petzke, F., Carville, S., Fransson, P., Marcus, H., Williams, S. C., Choy, E., Vitton, O., Gracely, R., Ingvar, M. and Kong, J. (2013). "Overlapping structural and functional brain changes in patients with long-term exposure to fibromyalgia pain." Arthritis Rheum 65(12): 3293-303.

80. Jezzard, P. (2012). "Correction of geometric distortion in fMRI data." Neuroimage 62(2): 648-51.

81. Jones, D. K. (2009). Gaussian Modeling of the Diffusion Signal. In Diffusion MRI. Johansen-Berg, H. and Behrens, T. London, Academic Press (Elsevier): 37-54.

82. Jones, D. K., Horsfield, M. A. and Simmons, A. (1999). "Optimal strategies for measuring diffusion in anisotropic systems by magnetic resonance imaging." Magn Reson Med 42(3): 515-25.

83. Jones, D. K., Knosche, T. R. and Turner, R. (2013). "White matter integrity, fiber count, and other fallacies: the do's and don'ts of diffusion MRI." Neuroimage 73: 239-54.

84. Jones, D. K. and Leemans, A. (2011). "Diffusion tensor imaging." Methods Mol Biol 711: 127-44.

85. Jorge, L. L. and Amaro, E., Jr. (2012). "Brain imaging in fibromyalgia." Curr Pain Headache Rep 16(5): 388-98.

86. Karlsson, H. K., Tuulari, J. J., Hirvonen, J., Lepomaki, V., Parkkola, R., Hiltunen, J., Hannukainen, J. C., Soinio, M., Pham, T., Salminen, P., Nuutila, P. and Nummenmaa, L. (2013). "Obesity is associated with white matter atrophy: a combined diffusion tensor imaging and voxel-based morphometric study." Obesity (Silver Spring) 21(12): 2530-7.

87. Kuchinad, A., Schweinhardt, P., Seminowicz, D. A., Wood, P. B., Chizh, B. A. and Bushnell, M. C. (2007). "Accelerated brain gray matter loss in fibromyalgia patients: premature aging of the brain?" J Neurosci 27(15): 4004-7.

88. Lachaine, J., Beauchemin, C. and Landry, P. A. (2010). "Clinical and economic characteristics of patients with fibromyalgia syndrome." Clin J Pain 26(4): 284-90.

89. Latremoliere, A. and Woolf, C. J. (2009). "Central sensitization: a generator of pain hypersensitivity by central neural plasticity." J Pain 10(9): 895-926.

90. Le Bihan, D. (2003). "Looking into the functional architecture of the brain with diffusion MRI." Nat Rev Neurosci 4(6): 469-80.

91. Lebel, C., Gee, M., Camicioli, R., Wieler, M., Martin, W. and Beaulieu, C. (2012). "Diffusion tensor imaging of white matter tract evolution over the lifespan." Neuroimage 60(1): 340-52.

92. Lee, M. C. and Tracey, I. (2013). "Imaging pain: a potent means for investigating pain mechanisms in patients." Br J Anaesth 111(1): 64-72.

93. Lee, Y. H., Choi, S. J., Ji, J. D. and Song, G. G. (2012). "Candidate gene studies of fibromyalgia: a systematic review and meta-analysis." Rheumatol Int 32(2): 417-26.

94. Lerma, C., Martinez, A., Ruiz, N., Vargas, A., Infante, O. and Martinez-Lavin, M. (2011). "Nocturnal heart rate variability parameters as potential fibromyalgia biomarker: correlation with symptoms severity." Arthritis Res Ther 13(6): R185.

95. Liang, D., Bhatta, S., Gerzanich, V. and Simard, J. M. (2007). "Cytotoxic edema: mechanisms of pathological cell swelling." Neurosurg Focus 22(5): E2.

96. Luerding, R., Weigand, T., Bogdahn, U. and Schmidt-Wilcke, T. (2008). "Working memory performance is correlated with local brain morphology in the medial frontal and anterior cingulate cortex in fibromyalgia patients: structural correlates of pain-cognition interaction." Brain 131(Pt 12): 3222-31.

97. Lutz, J., Jager, L., de Quervain, D., Krauseneck, T., Padberg, F., Wichnalek, M., Beyer, A., Stahl, R., Zirngibl, B., Morhard, D., Reiser, M. and Schelling, G. (2008). "White and gray matter abnormalities in the brain of patients with fibromyalgia: a diffusion-tensor and volumetric imaging study." Arthritis Rheum 58(12): 3960-9.

98. Mansour, A. R., Baliki, M. N., Huang, L., Torbey, S., Herrmann, K. M., Schnitzer, T. J. and Apkarian, A. V. (2013). "Brain white matter structural properties predict transition to chronic pain." Pain 154(10): 2160-8.

99. Martinez-Lavin, M. (2007). "Biology and therapy of fibromyalgia. Stress, the stress response system, and fibromyalgia." Arthritis Res Ther 9(4): 216.

100. May, A. (2008). "Chronic pain may change the structure of the brain." Pain 137(1): 7-15.

101. May, A. (2011). "Structural brain imaging: a window into chronic pain." Neuroscientist 17(2): 209-20.

102. McBeth, J. and Mulvey, M. R. (2012). "Fibromyalgia: mechanisms and potential impact of the ACR 2010 classification criteria." Nat Rev Rheumatol 8(2): 108-16.

103. McCain, G. A. and Scudds, R. A. (1988). "The concept of primary fibromyalgia (fibrositis): clinical value, relation and significance to other chronic musculoskeletal pain syndromes." Pain 33(3): 273-87.

104. Melzack, R. (1987). "The short-form McGill Pain Questionnaire." Pain 30(2): 191-7.

105. Merskey, H. and Bogduk, N. (1994). Classification of chronic pain: descriptions of chronic pain syndromes and definitions of pain terms. Seattle, WA, IASP Press.

106. Mifflin, K. A. and Kerr, B. J. (2014). "The transition from acute to chronic pain: understanding how different biological systems interact." Can J Anaesth 61(2): 112-122.

107. Moayedi, M., Weissman-Fogel, I., Salomons, T. V., Crawley, A. P., Goldberg, M. B., Freeman, B. V., Tenenbaum, H. C. and Davis, K. D. (2012). "White matter brain and trigeminal nerve abnormalities in temporomandibular disorder." Pain 153(7): 1467-77.

108. Moldofsky, H. and Scarisbrick, P. (1976). "Induction of neurasthenic musculoskeletal pain syndrome by selective sleep stage deprivation." Psychosom Med 38(1): 35-44.

109. Moldofsky, H., Scarisbrick, P., England, R. and Smythe, H. (1975). "Musculosketal symptoms and non-REM sleep disturbance in patients with "fibrositis syndrome" and healthy subjects." Psychosom Med 37(4): 341-51.

110. Moseley, M. E., Cohen, Y., Mintorovitch, J., Chileuitt, L., Shimizu, H., Kucharczyk, J., Wendland, M. F. and Weinstein, P. R. (1990). "Early detection of regional cerebral ischemia in cats: comparison of diffusion- and T2-weighted MRI and spectroscopy." Magn Reson Med 14(2): 330-46.

111. Munguia-Izquierdo, D. and Legaz-Arrese, A. (2011). "Determinants of sleep quality in middle-aged women with fibromyalgia syndrome." J Sleep Res.

112. Nebel, M. B. and Gracely, R. H. (2009). "Neuroimaging of fibromyalgia." Rheum Dis Clin North Am 35(2): 313-27.

113. Nichols, T. E. and Holmes, A. P. (2002). "Nonparametric permutation tests for functional neuroimaging: a primer with examples." Hum Brain Mapp 15(1): 1-25.

114. Oaklander, A. L., Herzog, Z. D., Downs, H. M. and Klein, M. M. (2013). "Objective evidence that small-fiber polyneuropathy underlies some illnesses currently labeled as fibromyalgia." Pain 154(11): 2310-6.

115. Oishi, K. and Crain, B. J. (2011). MRI atlas of human white matter. Elsevier science & technology books. London, Elsevier,: 1 online resource (vii, 257 p.) ill. (chiefly col.).

116. Osorio, C. D., Gallinaro, A. L., Lorenzi-Filho, G. and Lage, L. V. (2006). "Sleep quality in patients with fibromyalgia using the Pittsburgh Sleep Quality Index." J Rheumatol 33(9): 1863-5.

117. Patenaude, B., Smith, S. M., Kennedy, D. N. and Jenkinson, M. (2011). "A Bayesian model of shape and appearance for subcortical brain segmentation." Neuroimage 56(3): 907-22.

118. Pennebaker, J. W. (1982). The psychology of physical symptoms. New York, NY, Springer-Verlag.

119. Perl, E. R. (2007). "Ideas about pain, a historical view." Nat Rev Neurosci 8(1): 71-80.

120. Petzke, F., Clauw, D. J., Ambrose, K., Khine, A. and Gracely, R. H. (2003). "Increased pain sensitivity in fibromyalgia: effects of stimulus type and mode of presentation." Pain 105(3): 403-13.

121. Petzke, F., Harris, R. E., Williams, D. A., Clauw, D. J. and Gracely, R. H. (2005). "Differences in unpleasantness induced by experimental pressure pain between patients with fibromyalgia and healthy controls." Eur J Pain 9(3): 325-35.

122. Peyron, R., Laurent, B. and Garcia-Larrea, L. (2000). "Functional imaging of brain responses to pain. A review and meta-analysis (2000)." Neurophysiol Clin 30(5): 263-88.

123. Pollard, M. (2000). "Ionotropic glutamate receptor-mediated responses in the rat primary somatosensory cortex evoked by noxious and innocuous cutaneous stimulation in vivo." Exp Brain Res 131(3): 282-92.

124. Prescott, S. A., Ma, Q. and De Koninck, Y. (2014). "Normal and abnormal coding of somatosensory stimuli causing pain." Nat Neurosci 17(2): 183-91.

125. Puri, B. K., Agour, M., Gunatilake, K. D., Fernando, K. A., Gurusinghe, A. I. and Treasaden, I. H. (2010). "Reduction in left supplementary motor area grey matter

in adult female fibromyalgia sufferers with marked fatigue and without affective disorder: a pilot controlled 3-T magnetic resonance imaging voxel-based morphometry study." J Int Med Res 38(4): 1468-72.

126. Queiroz, L. P. (2013). "Worldwide epidemiology of fibromyalgia." Curr Pain Headache Rep 17(8): 356.

127. Robinson, M. E., Craggs, J. G., Price, D. D., Perlstein, W. M. and Staud, R. (2011). "Gray matter volumes of pain-related brain areas are decreased in fibromyalgia syndrome." J Pain 12(4): 436-43.

128. Rodriguez-Raecke, R., Niemeier, A., Ihle, K., Ruether, W. and May, A. (2009). "Brain gray matter decrease in chronic pain is the consequence and not the cause of pain." J Neurosci 29(44): 13746-50.

129. Rosenstiel, A. K. and Keefe, F. J. (1983). "The use of coping strategies in chronic low back pain patients: relationship to patient characteristics and current adjustment." Pain 17(1): 33-44.

130. Ruscheweyh, R., Deppe, M., Lohmann, H., Stehling, C., Floel, A., Ringelstein, E. B. and Knecht, S. (2011). "Pain is associated with regional grey matter reduction in the general population." Pain 152(4): 904-11.

131. Salat, D. H., Greve, D. N., Pacheco, J. L., Quinn, B. T., Helmer, K. G., Buckner, R. L. and Fischl, B. (2009a). "Regional white matter volume differences in nondemented aging and Alzheimer's disease." Neuroimage 44(4): 1247-58.

132. Salat, D. H., Lee, S. Y., van der Kouwe, A. J., Greve, D. N., Fischl, B. and Rosas, H. D. (2009b). "Age-associated alterations in cortical gray and white matter signal intensity and gray to white matter contrast." Neuroimage 48(1): 21-8.

133. Schmidt-Wilcke, T. (2008). "Variations in brain volume and regional morphology associated with chronic pain." Curr Rheumatol Rep 10(6): 467-74.

134. Schmidt-Wilcke, T., Luerding, R., Weigand, T., Jurgens, T., Schuierer, G., Leinisch, E. and Bogdahn, U. (2007). "Striatal grey matter increase in patients suffering from fibromyalgia--a voxel-based morphometry study." Pain 132 Suppl 1: S109-16.

135. Schuenke, M., Schulte, E., Schumacher, U., Ross, L., Lamperti, E. and Taub, E. (2007). Head and Neuroanatomy (THIEME Atlas of Anatomy). Stuttgart, Thieme.

136. Schulkin, J. (2006). "Angst and the amygdala." Dialogues Clin Neurosci 8(4): 407-16.

137. Schweinhardt, P., Sauro, K. M. and Bushnell, M. C. (2008). "Fibromyalgia: a disorder of the brain?" Neuroscientist 14(5): 415-21.

138. Seifert, F. and Maihofner, C. (2011). "Functional and structural imaging of pain-induced neuroplasticity." Curr Opin Anaesthesiol 24(5): 515-23.

139. Seminowicz, D. A., Wideman, T. H., Naso, L., Hatami-Khoroushahi, Z., Fallatah, S., Ware, M. A., Jarzem, P., Bushnell, M. C., Shir, Y., Ouellet, J. A. and Stone, L. S. (2011). "Effective treatment of chronic low back pain in humans reverses abnormal brain anatomy and function." J Neurosci 31(20): 7540-50.

140. Shah, M. A., Feinberg, S. and Krishnan, E. (2006). "Sleep-disordered breathing among women with fibromyalgia syndrome." J Clin Rheumatol 12(6): 277-81.

141. Siddall, P. J. (2013). "Neuroplasticity and pain: what does it all mean?" Med J Aust 198(4): 177-8.

142. Smallwood, R. F., Laird, A. R., Ramage, A. E., Parkinson, A. L., Lewis, J., Clauw, D. J., Williams, D. A., Schmidt-Wilcke, T., Farrell, M. J., Eickhoff, S. B. and Robin, D. A. (2013). "Structural Brain Anomalies and Chronic Pain: A Quantitative Meta-Analysis of Gray Matter Volume." J Pain.

143. Smith, S. and Kindlmann, G. (2009). Cross-subject Comparison of Local Diffusion MRI Parameters. In Diffusion MRI. Johansen-Berg, H. and Behrens, T. London, Academic Press (Elsevier)**:** 147-74.

144. Smith, S. M. (2002). "Fast robust automated brain extraction." Hum Brain Mapp 17(3): 143-55.

145. Smith, S. M., Jenkinson, M., Johansen-Berg, H., Rueckert, D., Nichols, T. E., Mackay, C. E., Watkins, K. E., Ciccarelli, O., Cader, M. Z., Matthews, P. M. and Behrens, T. E. (2006). "Tract-based spatial statistics: voxelwise analysis of multi-subject diffusion data." Neuroimage 31(4): 1487-505.

146. Smith, S. M., Jenkinson, M., Woolrich, M. W., Beckmann, C. F., Behrens, T. E., Johansen-Berg, H., Bannister, P. R., De Luca, M., Drobnjak, I., Flitney, D. E., Niazy, R. K., Saunders, J., Vickers, J., Zhang, Y., De Stefano, N., Brady, J. M. and Matthews, P. M. (2004). "Advances in functional and structural MR image analysis and implementation as FSL." Neuroimage 23 Suppl 1: S208-19.

147. Smith, S. M. and Nichols, T. E. (2009). "Threshold-free cluster enhancement: addressing problems of smoothing, threshold dependence and localisation in cluster inference." Neuroimage 44(1): 83-98.

148. Smith, S. M., Zhang, Y., Jenkinson, M., Chen, J., Matthews, P. M., Federico, A. and De Stefano, N. (2002). "Accurate, robust, and automated longitudinal and cross-sectional brain change analysis." Neuroimage 17(1): 479-89.

149. Smythe, H. A. and Moldofsky, H. (1977). "Two contributions to understanding of the "fibrositis" syndrome." Bull Rheum Dis 28(1): 928-31.

150. Soares, J. M., Marques, P., Alves, V. and Sousa, N. (2013). "A hitchhiker's guide to diffusion tensor imaging." Front Neurosci 7: 31.

151. Song, S. K., Sun, S. W., Ramsbottom, M. J., Chang, C., Russell, J. and Cross, A. H. (2002). "Dysmyelination revealed through MRI as increased radial (but unchanged axial) diffusion of water." Neuroimage 17(3): 1429-36.

152. Spielberger, C. D., Gorsuch, R. L., Lushene, R., Vagg, P. R. and Jacobs, G. A. (1983). Manual for the State-Trait Anxiety Inventory (Form Y2). Palo Alto, CA, Consulting Psychologists Press.

153. Stanek, K. M., Grieve, S. M., Brickman, A. M., Korgaonkar, M. S., Paul, R. H., Cohen, R. A. and Gunstad, J. J. (2011). "Obesity is associated with reduced white matter integrity in otherwise healthy adults." Obesity (Silver Spring) 19(3): 500-4.

154. Stankewitz, A., Valet, M., Schulz, E., Woller, A., Sprenger, T., Vogel, D., Zimmer, C., Muhlau, M. and Tolle, T. R. (2013). "Pain sensitisers exhibit grey matter changes after repetitive pain exposure: A longitudinal voxel-based morphometry study." Pain 154(9): 1732-7.

155. Staud, R. (2006). "Biology and therapy of fibromyalgia: pain in fibromyalgia syndrome." Arthritis Res Ther 8(3): 208.

156. Staud, R. (2007). "Treatment of fibromyalgia and its symptoms." Expert Opin Pharmacother 8(11): 1629-42.

157. Staud, R. (2008). "Autonomic dysfunction in fibromyalgia syndrome: postural orthostatic tachycardia." Curr Rheumatol Rep 10(6): 463-6.

158. Staud, R. (2008). "Heart rate variability as a biomarker of fibromyalgia syndrome." Fut Rheumatol 3(5): 475-483.

159. Staud, R. (2011). "Brain imaging in fibromyalgia syndrome." Clin Exp Rheumatol 29(6 Suppl 69): S109-17.

160. Staud, R. and Rodriguez, M. E. (2006). "Mechanisms of disease: pain in fibromyalgia syndrome." Nat Clin Pract Rheumatol 2(2): 90-8.

161. Stein, N., Sprenger, C., Scholz, J., Wiech, K. and Bingel, U. (2012). "White matter integrity of the descending pain modulatory system is associated with interindividual differences in placebo analgesia." Pain 153(11): 2210-7.

162. Sullivan, M. D., Cahana, A., Derbyshire, S. and Loeser, J. D. (2013). "What does it mean to call chronic pain a brain disease?" J Pain 14(4): 317-22.

163. Sundgren, P. C. (2009). "Diffusion tensor imaging and tractography: have they come of age?" J Neuroophthalmol 29(2): 93-5.

164. Sundgren, P. C., Dong, Q., Gomez-Hassan, D., Mukherji, S. K., Maly, P. and Welsh, R. (2004). "Diffusion tensor imaging of the brain: review of clinical applications." Neuroradiology 46(5): 339-50.

165. Sundgren, P. C., Petrou, M., Harris, R. E., Fan, X., Foerster, B., Mehrotra, N., Sen, A., Clauw, D. J. and Welsh, R. C. (2007). "Diffusion-weighted and diffusion tensor imaging in fibromyalgia patients: a prospective study of whole brain diffusivity, apparent diffusion coefficient, and fraction anisotropy in different regions of the brain and correlation with symptom severity." Acad Radiol 14(7): 839-46.

166. Timmerman, G. M., Calfa, N. A. and Stuifbergen, A. K. (2013). "Correlates of body mass index in women with fibromyalgia." Orthop Nurs 32(2): 113-9.

167. Tracey, I. (2011). "Can neuroimaging studies identify pain endophenotypes in humans?" Nat Rev Neurol 7(3): 173-81.

168. Tracey, I. and Bushnell, M. C. (2009). "How neuroimaging studies have challenged us to rethink: is chronic pain a disease?" J Pain 10(11): 1113-20.

169. Treede, R. D., Kenshalo, D. R., Gracely, R. H. and Jones, A. K. (1999). "The cortical representation of pain." Pain 79(2-3): 105-11.

170. Uceyler, N., Hauser, W. and Sommer, C. (2011). "Systematic review with meta-analysis: cytokines in fibromyalgia syndrome." BMC Musculoskelet Disord 12: 245.

171. Uceyler, N. and Sommer, C. (2013). "Objective evidence that small-fiber polyneuropathy underlies some illnesses currently labeled as fibromyalgia." Pain 154(11): 2569.

172. Uceyler, N., Zeller, D., Kahn, A. K., Kewenig, S., Kittel-Schneider, S., Schmid, A., Casanova-Molla, J., Reiners, K. and Sommer, C. (2013). "Small fibre pathology in patients with fibromyalgia syndrome." Brain 136(Pt 6): 1857-67.

173. Ursini, F., Naty, S. and Grembiale, R. D. (2011). "Fibromyalgia and obesity: the hidden link." Rheumatol Int 31(11): 1403-8.

174. Walitt, B., Fitzcharles, M. A., Hassett, A. L., Katz, R. S., Hauser, W. and Wolfe, F. (2011). "The longitudinal outcome of fibromyalgia: a study of 1555 patients." J Rheumatol 38(10): 2238-46.

175. Warren, J. W., Langenberg, P. and Clauw, D. J. (2013). "The number of existing functional somatic syndromes (FSSs) is an important risk factor for new, different FSSs." J Psychosom Res 74(1): 12-7.

176. Wessely, S., Nimnuan, C. and Sharpe, M. (1999). "Functional somatic syndromes: one or many?" Lancet 354(9182): 936-9.

177. White, P. D. (2010). "Chronic fatigue syndrome: Is it one discrete syndrome or many? Implications for the "one vs. many" functional somatic syndromes debate." J Psychosom Res 68(5): 455-9.

178. Wilcox, S. L., Gustin, S. M., Eykman, E. N., Fowler, G., Peck, C. C., Murray, G. M. and Henderson, L. A. (2013). "Trigeminal nerve anatomy in neuropathic and non-neuropathic orofacial pain patients." J Pain 14(8): 865-72.

179. Williams, D. A. and Gracely, R. H. (2006). "Biology and therapy of fibromyalgia. Functional magnetic resonance imaging findings in fibromyalgia." Arthritis Res Ther 8(6): 224.

180. Winston, G. P. (2012). "The physical and biological basis of quantitative parameters derived from diffusion MRI." Quant Imaging Med Surg 2(4): 254-65.

181. Wolfe, F. (2009). "Fibromyalgia wars." J Rheumatol 36(4): 671-8.

182. Wolfe, F., Clauw, D. J., Fitzcharles, M. A., Goldenberg, D. L., Hauser, W., Katz, R. S., Mease, P., Russell, A. S., Russell, I. J. and Winfield, J. B. (2011). "Fibromyalgia criteria and severity scales for clinical and epidemiological studies: a modification of the ACR Preliminary Diagnostic Criteria for Fibromyalgia." J Rheumatol 38(6): 1113-22.

183. Wolfe, F., Clauw, D. J., Fitzcharles, M. A., Goldenberg, D. L., Katz, R. S., Mease, P., Russell, A. S., Russell, I. J., Winfield, J. B. and Yunus, M. B. (2010). "The American College of Rheumatology preliminary diagnostic criteria for fibromyalgia and measurement of symptom severity." Arthritis Care Res (Hoboken) 62(5): 600-10.

184. Wolfe, F. and Hauser, W. (2011). "Fibromyalgia diagnosis and diagnostic criteria." Ann Med 43(7): 495-502.

185. Wolfe, F., Ross, K., Anderson, J., Russell, I. J. and Hebert, L. (1995). "The prevalence and characteristics of fibromyalgia in the general population." Arthritis Rheum 38(1): 19-28.

186. Wolfe, F., Smythe, H. A., Yunus, M. B., Bennett, R. M., Bombardier, C., Goldenberg, D. L., Tugwell, P., Campbell, S. M., Abeles, M., Clark, P. and et al. (1990). "The American College of Rheumatology 1990 Criteria for the Classification of Fibromyalgia. Report of the Multicenter Criteria Committee." Arthritis Rheum 33(2): 160-72.

187. Wood, P. B., Glabus, M. F., Simpson, R. and Patterson, J. C., 2nd (2009). "Changes in gray matter density in fibromyalgia: correlation with dopamine metabolism." J Pain 10(6): 609-18.

188. Wycoco, V., Shroff, M., Sudhakar, S. and Lee, W. (2013). "White matter anatomy: what the radiologist needs to know." Neuroimaging Clin N Am 23(2): 197-216.

189. Xu, J., Li, Y., Lin, H., Sinha, R. and Potenza, M. N. (2013). "Body mass index correlates negatively with white matter integrity in the fornix and corpus callosum: a diffusion tensor imaging study." Hum Brain Mapp 34(5): 1044-52.

190. Yunus, M., Masi, A. T., Calabro, J. J., Miller, K. A. and Feigenbaum, S. L. (1981). "Primary fibromyalgia (fibrositis): clinical study of 50 patients with matched normal controls." Semin Arthritis Rheum 11(1): 151-71.

191. Yunus, M. B. (2007). "Fibromyalgia and overlapping disorders: the unifying concept of central sensitivity syndromes." Semin Arthritis Rheum 36(6): 339-56.

192. Zhang, X., Li, B. and Shan, B. (2014). "Age-related white matter degradation rule of normal human brain: the evidence from diffusion tensor magnetic resonance imaging." Chin Med J (Engl) 127(3): 532-7.

193. Zhang, Y., Brady, M. and Smith, S. (2001). "Segmentation of brain MR images through a hidden Markov random field model and the expectation-maximization algorithm." IEEE Trans Med Imaging 20(1): 45-57.